From the Department of Congenital Heart Disease and Pediatric Cardiology

Director: Prof. Dr. med. Hans-Heiner Kramer

of the Christian-Albrechts-University, Kiel

Cardiovascular Magnetic Resonance Imaging in the Assessment of Myocardial Blood Flow, Viability, and Diffuse Fibrosis in Congenital and Acquired Heart Disease

Dissertation to obtain doctoral honor

from the Medical Faculty

of Christian-Albrechts-University, Kiel

Written by

Hoang Minh Pham

Can Tho, Vietnam

Kiel 2014

1. Berichterstatter: Prof. Dr. med. Carsten Rickers

2. Berichterstatter: Prof. Dr. med. Norbert Frey

Zum Druck genehmigt, Kiel, den 11.Juni 2014

Tag der mündlichen Prüfung: 23.Juni 2014

gez.: Priv.Doz. Dr.med. Inga Voges

(Vorsitzender der Prüfungskommission)

Table of Contents

List of Abbreviations

ALCAPA	Anomalous origin of the left coronary artery from the pulmonary artery
AR	Aortic regurgitation
ASO	Arterial switch operation
BWG	Bland White Garland Syndrome
CAD	Coronary artery disease
CHD	Congenital heart disease
CI	Cardiac index
CMR	Cardiovascular magnetic resonance
CO	Cardiac output
DORV	Double-outlet right ventricle
DMF	Diffuse myocardial fibrosis
ECG	Electrocardiography
ECV	Extracellular volume
EDV	End diastolic volume
EF	Ejection fraction
ESV	End systolic volume
KD	Kawasaki disease
LAD	Left anterior descending artery
LAV	Left atrium volume
LCA	Left coronary artery
LV	Left ventricle
LA	Left ventricle
MBF	Myocardial blood flow
MF	Myocardial fibrosis
MIDCAP	Minimally invasive direct coronary artery bypass
MPR	Myocardial perfusion reserve
MRI	Magnetic resonance imaging
PET	Positron emission tomography
PWV	Pulse wave velocity
RCA	Right coronary artery
RV	Right ventricle
SI	Signal intensity
SPECT	Single photon emission computed tomography
SV	Stroke volume
TGA	Transposition of the great arteries

List of Figures

List of Tables

1. INTRODUCTION

Congenital heart diseases (CHD) are characterized by abnormalities of the heart or great vessel structures that occur before birth. The prevalence of CHD in live newborns varies from 4/1000 to 50/1000 (Hoffman & Kaplan 2002). In patients after surgical correction of CHD involving the coronary arteries, and in patients with CHD including coronary artery anomalies (Angelini 2007; Hauser et al., 2001; Maiers & Hurwitz, 2008; Vogel et al., 1991), or in acquired coronary artery disease, such as Kawasaki syndrome (Daniels et al., 2012), myocardial ischemia, infarction, and sudden cardiac death can occur. Therefore, assessment of myocardial perfusion and viability is important for the long-term follow-up in these patients.

Diagnostic imaging tools play an important role in the detection of myocardial ischemia. Noninvasive methods which can evaluate myocardial perfusion and viability are stress electro- and echocardiography (Krahwinkel et al., 1997; Mulvagh 2004), single photon emission computed tomography (SPECT) and positron emission tomography (PET). More recently, cardiac magnetic resonance (CMR) imaging has emerged as a promising diagnostic tool for the evaluation of myocardial ischemia (Berman et al., 2006; Salerno & Beller, 2009).

CMR imaging has become a clinically useful modality for diagnosis and management of congenital and acquired heart diseases in children. Advanced techniques in both, data acquisition and image analysis, allow reducing scan time, to improve image quality, and to evaluate cardiac morphology including the coronary arteries, cardiac function, myocardial tissue characteristics, and myocardial perfusion. Therefore, CMR has been become a routine method in the clinical practice of pediatric cardiology.

In this thesis, we evaluated myocardial perfusion, viability diffuse fibrosis using CMR in a population of patients with congenital and acquired heart disease.

1.1 The Importance of Myocardial Perfusion in Congenital and Acquired Heart Diseases

1.1.1 Transposition of the Great Arteries (TGA)

TGA is one of the most common cyanotic CHD's occurring in approximately 3 per 10,000 births or in 5% to 7% of all congenital heart defects (Samánek et al., 1989). Males are more

commonly affected than females, with a male-to-female ratio of 2 to 2.3:1 (Bianca et al., 2001; Samánek, 1994). In TGA, the aorta arises from the right ventricle, and the pulmonary artery originates from the left ventricle (Figure 1) and is commonly associated with other defects such as ventricular septal defect, left ventricular outflow tract obstruction, abnormal coronary artery patterns, aortic coarctation or interrupted aortic arch (Kimball 2010). Various origins and distributions of the coronary circulation have been observed (Martins & Castela., 2008; Sim et al., 1994). Unusual coronary artery origins and courses were described and classified by Yacoub et al in 1978 (Figure 2).
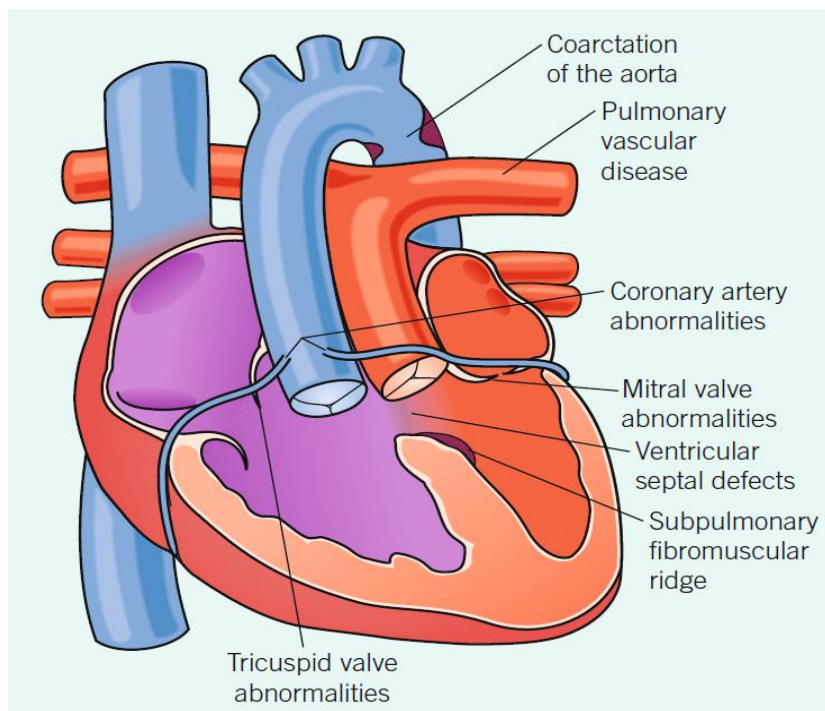
Figure 1. TGA with ventricular septal defect, coronary artery abnormalities, coarctation of the aorta as well as tricuspid and mitral valve abnormalities (Kimball 2010).

Classification of the variations in coronary artery pattern is important for the arterial switch operation (ASO), which has become a common surgical procedure for the anatomical repair of TGA and some forms of double-outlet right ventricle (DORV) (Losay et al., 2001; Pasquali et al., 2002). Transfer of the coronary arteries is one of the most difficult processes during ASO, particularly in cases of various origins and distributions of the coronary artery circulation (Kirklin et al., 1992; Lalezari et al., 2011). Data from several sources have identified coronary events after ASO in TGA patients (Bonhoeffer et al., 1997; Pasquali et al., 2002; Legendre et al., 2003; Raja et al., 2005). Therefore, assessment of myocardial perfusion is important during the follow-up in patients after ASO.
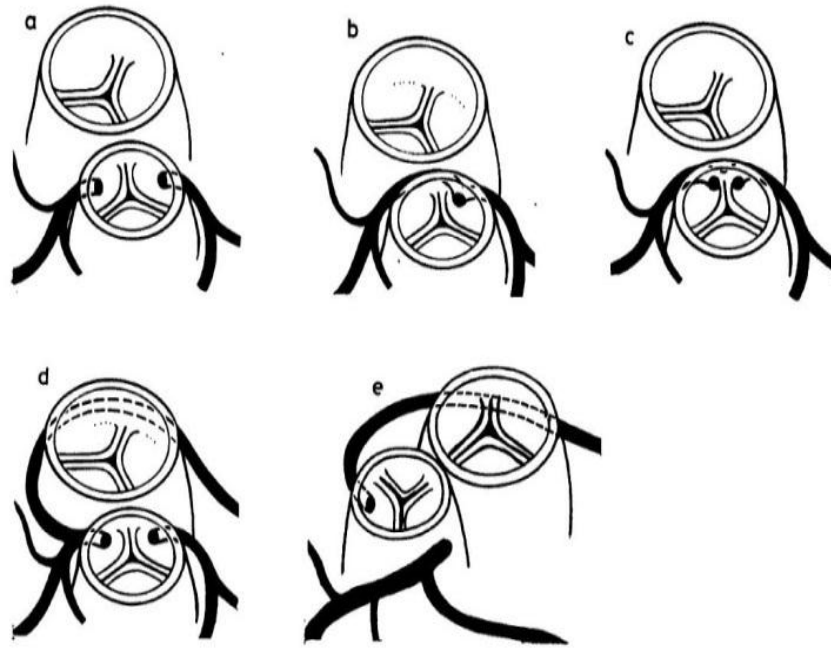
Figure 2. Classification of coronary arterial patterns in TGA by Yacoub & Radley-Smith, 1978. A: Left coronary artery (LCA) takes origin from the left sinus and right coronary artery (RCA) from the right sinus. B: Single coronary artery, LCA and RCA arise from a single ostium. C: Two para-commissural ostia with or without intramural course. D: RCA and circumflex arise from the right ostium, left anterior descending (LAD) alone takes origin from the left ostium. E: RCA and LAD originate from the left from the left posterior sinus, circumflex alone takes origin from the right ostium (Yacoub & Radley-Smith., 1978).

In addition, the successful of the ASO in TGA depends on the elastic function of the transposed aorta. However, several studies have shown evidence, that even after successful anatomical repair, patients may be prone to long term problems. The fate of the aorta and aortic valve has been assessed in previous studies (Losay et al., 2006; Kramer et al., 2003; Langer et al., 2008). The majority of patients show non-progressive dilatation of the aortic root, but only few cases suffer from aortic insufficiency (Görler et al., 2011). In addition, reduced proximal aortic elasticity, structural abnormalities of the arterial walls, and increased carotid artery stiffness have been reported in TGA patients (Niwa et al., 2001; Grotenhuis et al., 2008; Mersich et al., 2006; Murakami et al., 2000). However, data are lacking about the functional status of the entire length of the thoracic aorta as well as its potential change with age after surgical repair, and the impact on left ventricular (LV) function.

1.1.2 Congenital Anomalies of the Coronary Arteries

Normal coronary artery anatomy includes the left and right main coronaries (LCA and RCA). The LCA originates from the left valsava sinus and branches into the LAD and the circumflex artery (CFX). The LAD divides into three branches, such as the left conus, the septal, and the diagonal artery (Figure 3). The RCA arises from the right sinus of valsava and divides into many branches including the sinus node artery, the conal branch, an atrial branch, the right ventricular muscular branches, the posterior descending artery, the atrioventricular node artery, and septal branches (Figure 3) (Driscoll 2006).
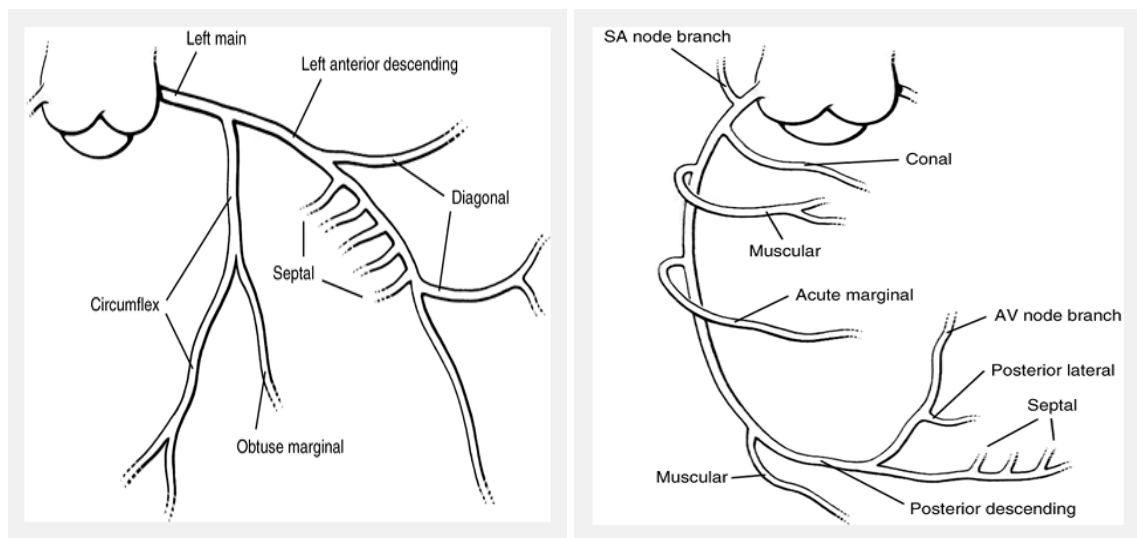
Figure 3. Normal anatomy of the left and right coronary arteries. Based on an illustration in (Driscoll, 2006).

The term congenital anomalies of the coronaries is defined as anomalies of the origin, course, or structure of epicardial coronary arteries (Angelini 2002). They are rare CHD diseases occurring in approximately 0.2-1.4% of the population (Davis et al., 2001). The classification of coronary artery anomalies depends on anatomy and origin of the coronary arteries and has been discussed extensively in the literature (Ogden 1970; Angelini 2002; Fratz et al., 2006; Jacobs & Mavroudis., 2010). Anomalies of the coronary arteries are a high risk factor for myocardial ischemia, the leading cause of myocardial infarction and sudden cardiac death (Alexander & Griffith., 1956). In this thesis, we evaluated patients with different coronary arteries anomalies, such as Bland-White-Garland syndrome, congenital coronary artery fistula, and aberrant main left coronary artery.

a) Bland-White-Garland-Syndrome

Anomalous origin of the LCA from the pulmonary artery (ALCAPA), also known as Bland-White-Garland syndrome (BWG) was described in 1933 by Bland, White, and Garland (Bland et al., 1933). It is a rare congenital coronary artery abnormality and is associated with early infant mortality and also sudden death in adulthood. The incidence of ALCAPA is approximately 1 in 300,000 live births (Davis et al., 2001) and 0.26% of CHD undergoing cardiac catheterization (Askenazi & Nadas., 1975). Patients live into adulthood without treatment in approximately 15% of the reported cases (Perloff 2003). These patients may present with myocardial ischemia, left ventricular dysfunction, myocardial infarction, and as well as sudden cardiac death. In ALCAPA patients, coronary blood flow is supplied mainly by the RCA and coronary collateral vessels from the RCA to the LCA. Patients with a poor collateral circulation may develop myocardial ischemia and infarction. In patients with a well developed coronary collateral system, symptoms may appear later in life (Dodge-Khatami et al., 2002; Wesselhoeft et al., 1968).

Most patients with ALCAPA will undergo surgical treatment early in life. The aim of surgical therapy is to preserve as much myocardium as possible. There are several methods for surgical correction depending on the coronary artery anatomy, such as direct re-implantation, the Tackeuchi procedure, and coronary artery bypass grafting (Perloff 2003). Direct surgical re-implantation of the LCA into the aorta is the most common surgical procedure nowadays. However, there is a high risk of stenosis or occlusion of the LCA after surgical treatment (Kazmierczak et al., 2013; Ramírez et al., 2011). Therefore, it is most important to assess myocardial ischemia in ALCAPA patients before and after surgical treatment.

b) Coronary Fistula

Coronary fistulas are also known as coronary arteriovenous fistula, and were first described by Krause in 1865 (Krause 1865). They are rare anomalies and occur in 0.2 to 0.4% of all CHD (Driscoll 2006) or in 0.3% to 0.87% of patients who undergo coronary angiography (Angelini 2007). In this anatomical condition, the coronary arteries are abnormally connected to the heart chambers or great vessels. In 90% the fistula drains into the cavum of the right ventricle (Perloff 2003). The main therapeutic methods for correction of coronary fistulas are surgical or interventional ligations, which are safe and have good long term results (Urrutia-S et al., 1983). However, several reports showed that myocardial infarction

and cardiac death can occur in the long-term follow up (Valente et al., 2010; Canga et al., 2012).

c) Aberrant LCA

An aberrant LCA is a rare congenital coronary artery anomaly with a reported prevalence of 0.017% - 0.03% (Tuo et al., 2013; Yamanaka & Hobbs, 1990). In this anomaly, the LCA and RCA arise from the same or different anterior sinus of Valsalva (Figure 4). The anomalous LCA from the right sinus was classified into 4 types including the following: **A**: origin at left main trunk from right sinus or right coronary artery; **B**: origin of LAD and CFX from the right coronary sinus; **C**: origin of LAD from right sinus of Valsalva or RCA; **D**: origin of CFX from right sinus or right coronary artery (Roberts et al., 1992). A high incidence of sudden death typically occurs in these patients during or immediately following physical exercise (Cheitlin et al., 2009; Yamanaka & Hobbs, 1990). Particularly in the presence of an inter-arterial course of LCA between the aorta and pulmonary artery, the risk of sudden death is higher. Most patients with such anomalies were treated by surgical therapies, such as bypass, reimplantation, and unroofing. However, myocardial ischemia and sudden death can occur due to development of stenosis or closure of LCA after surgical treatment (Krasuski et al., 2011).
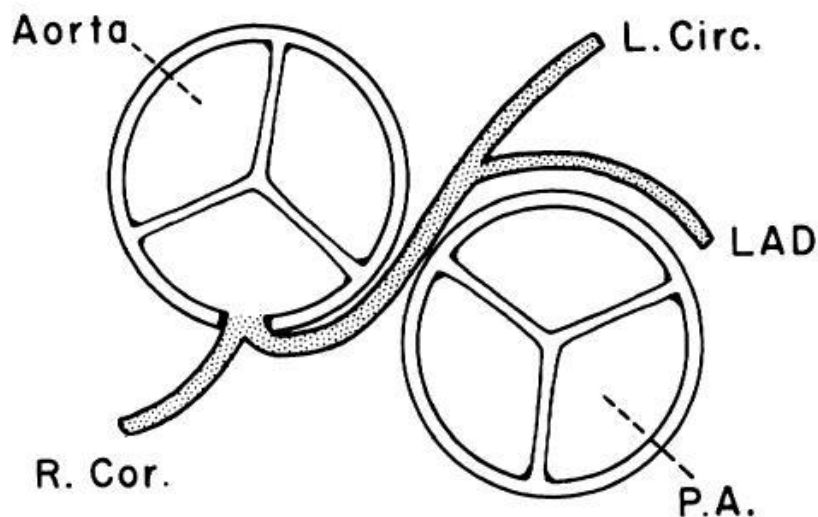
Figure 4. Aberrant main LCA. Main LCA and RCA arise from anterior sinus of Valsalva. The LCA passes obliquely between the aorta and the pulmonary artery; R. Cor: right coronary artery; L. Circ: left coronary artery; LAD: left anterior descending artery; P.A: pulmonary artery. Based on an illustration in (Cheitlin et al., Circulation 1974).

1.1.3 Ross Operation

The Ross procedure is a surgical method which uses the autologous pulmonary valve for replacement of a diseased aortic valve and was first described by Donald Ross in the United Kingdom in 1967 (Ross 1967). It has become a surgical treatment option also in CHD to avoid the use of long-term anticoagulation (Svensson et al., 2003). Other possible advantages of the Ross operation are the following: low risk of endocarditis and thromboembolism, long-term durability, potential growth ability in children, and excellent hemodynamic performance (Charitos et al., 2012).

Coronary artery reimplantation is a part of the operation and can lead to coronary artery stenosis with the risk of myocardial infarction and sudden cardiac death (Somerville et al., 1979). The assessment of myocardial perfusion and ischemia is therefore important during postoperative care.

1.1.4 Heart Transplantation

Heart transplantation was first performed in 1967 by Christian Barnard in South Africa (Barnard et al., 1967). Since then, this technique has been developed and become the treatment of choice for the management of end-stage heart failure in children and adults (Herrington & Tsirka., 2004). The number of cardiac transplantation has been increased, in 2011 more than 100,000 cardiac transplantations were performed worldwide according to the registry of the International Society of Heart and Lung Transplantation (Stehlik et al., 2011). However, there are many factors that have an effect on the results after cardiac transplantation. Coronary allograft vasculopathy is the main factor, limiting the long-term success of the operation and is a recognized cause of myocardial ischemia and sudden cardiac death (Roussel et al., 2008; Nickel et al., 2011).

1.1.5 Kawasaki Syndrome

Kawasaki disease (KD), also known as Kawasaki syndrome or mucocutaneous lymph node syndrome, is an acute systemic vasculitis of unknown etiology and the most important cause of acquired heart disease in childhood in the developed countries. KD was first described in Japan by Tomisaku Kawasaki in 1967 (Kawasaki 1967). Since then, many cases in different countries have been reported. KD occurs most frequently in Japan with an incidence of approximately 188.1 per 100,000 children younger than four years of age, and a male-to-female ratio of 1.5:1 (Kato 2010). KD is associated with the development of coronary artery

aneurysms and stenosis (Figure 5). Acute myocardial infarction can occur in KD patients due to thrombosis of aneurysms or due to developing stenosis of the coronary artery (Dajani et al., 1993). In 1996, Kato et al. reported a follow-up study of 594 KD patients and found coronary artery aneurysms in 25%, myocardial ischemia in 4.7%, myocardial infarction in 1.9% and death due to myocardial infarction in 0.8% of all cases (Kato et al., 1996). Due to this data, assessment of myocardial perfusion and ischemia is of importance in the long-term follow-up of these patients.
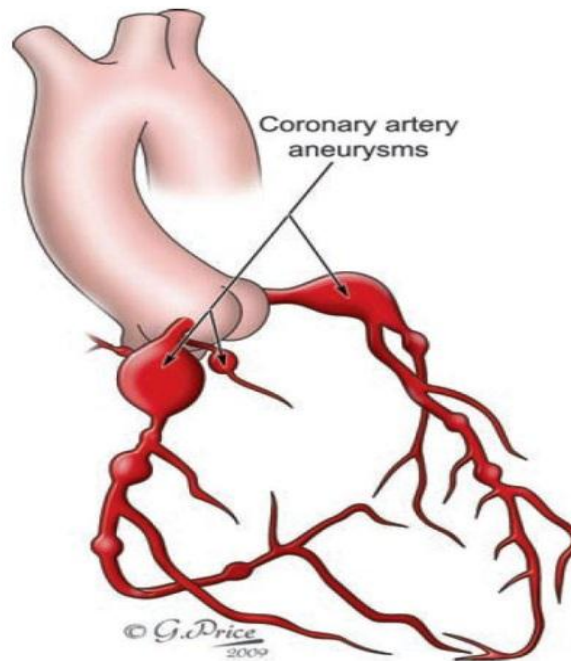
Figure 5. Schematic drawing shows coronary artery aneurysms of KD (Based on an illustration in Sridharan et al., 2010).

1.2 Non-Invasive Diagnostic Imaging for Detection of Myocardial Ischemia

1.2.1 Nuclear Medicine

Nuclear cardiac imaging is the branch of cardiovascular diagnostic imaging that uses radioactive tracers to perform functional images of the heart. SPECT and PET are two types of nuclear imaging which are commonly used in clinical practice. They allow to evaluate cardiac morphology, function, myocardial blood flow and viability (Auerbach et al., 1999; Ghosh et al., 2010; Weindling et al., 1994).

SPECT myocardial perfusion scintigraphy (MPS) is a useful technique for evaluation of ischemic heart disease. Diagnosis of CAD uses a scintillation camera and intravenously injected radiopharmaceuticals, such as thallium-201 and technetium-99m sestamibi, and technetium-99m tetrofosmin, whose distribution in the myocardium is dependent on, and reflects the level of myocardial perfusion. SPECT MPS is normally performed during rest and pharmacological stress. Besides other indications, SPECT MPS is a useful modality for detection of CAD in children with congenital and acquired heart diseases (Sundaram et al., 2009). However, there are some disadvantages: a normal SPECT MPS protocol usually takes 3-4 hours, and uses ionising radiation. In addition, SPECT does not allow exact quantification of myocardial perfusion and perfusion reserve (Bateman 2012; Jadvar et al., 1999).

In contrast, PET provides the ability to quantify absolute myocardial perfusion blood flow and is therefore considered a promising method for the examination of myocardial ischemia. Typical radionuclides used for a PET study are Rubidium-82, Nitrogen-13 (in ammonia) and Oxygen-15 (in water). Blood flow is quantified in units of ml/min/g. The sensitivity and specificity for detection of myocardial ischemia are 87% to 97% and 78% to 100%, respectively (Sampson et al., 2007; Bateman et al., 2006; Grover-McKay et al., 1992). Furthermore, F18-FDG PET allows to differentiate between hibernating or stunned myocardium and to assess myocardial viability in post myocardial infarction patients who benefit significantly from revascularization. However, PET uses ionizing radiation and is expensive (Bateman 2012).

Evaluation of myocardial perfusion and viability by PET offers several potential advantages. Previous studies have demonstrated that PET is superior to SPECT for the detection of myocardial ischemia, because it offers images with a higher resolution and contrast, a better attenuation correction, less scatter, and has the ability to quantify absolute myocardial perfusion (Bateman 2012; Ghosh et al., 2010). For the detection of myocardial ischemia, PET perfusion imaging offers a higher sensitivity and specificity than SPECT (Jaarsma et al., 2012). But there are only few studies using PET and SPECT for the detection of ischemic heart disease in pediatric patients (Sundaram et al., 2009; Singh et al., 2003; Hernandez-Pampaloni et al., 2002; Rickers et al., 2000). Other non-invasive methods for assessing myocardial ischemia without ionizing radiation are often preferred.

1.2.2 Other Cardiac Stress Test

Myocardial contrast echocardiography (MCE) is a diagnostic imaging tool for the assessment of the myocardial microcirculation using microscopic gas-filled bubbles, which can burst by insonation in a myocardial region of interest. Replenishment of this same region with gas-filled bubbles (i.e. myocardial opacification) will provide a measure of myocardial blood flow (Wei et al., 1998; Porter et al., 2001; Kutty et al., 2012) .It can be used to assess myocardial perfusion and viability for detection of myocardial ischemia (Gaibazzi et al., 2012; Kaufmann et al., 2007; Mulvagh, 2004). MCE is non-invasive, does not use ionizing radiation and is easy to perform. However, image quality depends on the acoustic windows.

Exercise stress testing is the most commonly used method to evaluate patients with suspected myocardial ischemia. Treadmill and bicycle ergometer protocols are the most popular stress tests (Rhodes et al., 2010; Morrison et al., 2013). Electrocardiography (ECG) exercise testing can be used for evaluation of cardiac perfusion and function with high yield of diagnostic, prognostic, and functional information (Kashyap et al., 2011). However, in small children ECG exercise testing is difficult to perform.

1.2.3 Cardiovascular Magnetic Resonance Imaging (CMR)

a) History of Magnetic Resonance Imaging and the Development of CMR

In 1946, Felix Bloch and Edward Purcell discovered the nuclear magnetic resonance phenomenon that was a foundation for the development of magnetic resonance imaging (MRI). In 1971, Raymond Damadian could show different tissue MR relaxation times in rats, and the differences of the tissue relaxation times are the basis for good soft tissue contrast in MRI. Peter Mansfield made another fundamental contribution to the development of MRI in 1976 by developing the fast imaging technique known as echo-planar imaging. In 1977, Damadian obtained the first magnetic resonance images of the human (Geva 2006).

The first publication regarding CMR in CHD dates back to 1982 and reported the diagnosis of a ventricular septal defect in lamb hearts (Heneghan et al., 1982). In pediatric cardiology, MRI was applied in the late 1980's by using ECG-triggered spin echo techniques for assessment of cardiac function and blood flow in patients with CHD (Higgins et al., 1988; Chung et al., 1988). Gadolinium-enhanced MRI was first applied in clinical studies in 1984.

Myocardial viability imaging using late gadolinium enhancement was first mentioned in 1988 (Schaefer et al., 1988) and first-pass perfusion imaging is used since 1990 for the detection of myocardial ischemia (Atkinson et al., 1990). Viability assessment by MRI has since then evolved into a "gold-standard" based on the work of Kim et al. (Kim et al., 2000). Since its beginnings data acquisition and image analysis have continuously improved (Earls et al., 2002).

b) Advantages of CMR

CMR imaging has emerged as a promising diagnostic tool for the evaluation of CAD in children. Advantages of cardiac MRI include absence of ionizing radiation, the high spatial resolution, and the ability to assess in one exam morphology, global and regional function, viability, myocardial perfusion, and coronary artery anatomy and patency. A number of studies showed that first-pass perfusion CMR at rest and during pharmacologic stress allows to assess myocardial ischemia, and that LGE can detect scar tissue (Klein et al., 2002; Prakash et al., 2004). First pass perfusion MRI can be analyzed qualitatively, by semi-quantitative analysis, and by absolute quantification of myocardial blood flow (MBF) (Jerosch-Herold et al., 2002).

X-ray coronary angiography is known as the reference standard for detection of CAD (White et al., 1984; Scanlon et al., 1999). However, especially in pediatric patients its invasive nature, and the use of ionizing radiation are important limitations. It has been shown that PET and cardiac MRI have the highest diagnostic accuracy for detection myocardial perfusion abnormalities (Greenwood et al., 2012; Morton et al., 2012). However, CMR has a higher resolution than PET (Jaarsma et al., 2012). The majority of available CMR studies, were performed in adult patients and there are only few examinations in children, in part due to the lack of expertise, access to CMR scanners in pediatric cardiology departments, perhaps also due to need to sedate young patients.

c) CMR Imaging For Detection of Ischemia Heart Disease

➤ First-Pass Perfusion CMR Imaging

First-pass myocardial perfusion MRI is used to monitor the changes in myocardial signal intensity after intravenous injection of a contrast agent by using T1-weighted imaging. In CMR perfusion imaging, the myocardial wash-in of contrast during the first pass of a contrast bolus forms the basis for assessing myocardial perfusion. The T1-weighted signal

intensity is directly related to the concentration of the contrast agent, and its temporal variation in the myocardium can be used to assess regional myocardial perfusion. In ischemic regions the supply of blood and thus contrast enhancement is decreased. As a consequence the signal intensity change is lower in ischemic regions, relative to normally perfused myocardium. First-pass perfusion imaging is generally performed at rest and pharmacologic stress (Al-Saadi et al., 2000), to assess the myocardial perfusion reserve (Wilke et al., 1999).

> **CMR Adenosine Stress Perfusion**

Adenosine is an endogenous nucleotide that promotes vasodilatation by activation of the α2 receptors in the vessels. In the field of CMR imaging, adenosine is most commonly used for stress perfusion imaging for the detection of CAD with an iv dosage of 140 μg/kg/min body weight per minute. The peak effect of adenosine occurs 2-3 min after start of the iv infusion, with an increase of the heart rate. After stopping the iv. infusion of adenosine, the heart rate returns to normal levels after 1-2 minutes (Pennell 2004). In CMR perfusion studies, adenosine stress testing is used to increase the differentiation in the first-pass delivery of the contrast agent between myocardial regions perfused by normal and abnormal coronary arteries. Under resting conditions differences in perfusion can only be seen for 90% or higher luminal narrowing of a coronary artery, and assuming there is no collateral supply. CMR adenosine stress perfusion is safe, and the occurrence of AV-block is very rare, occurring in < 1% of 9256 cases, and it has a very short half-life (< 10 seconds) (Al-Saadi and Bogaert J, 2004; Pennell 2004; Cerqueira et al., 1994).

> **Contrast Media**

Gadolinium chelates (Gd) are commonly used as paramagnetic contrast agents for myocardial perfusion and late gadolinium enhancement (LGE) CMR imaging. Gd is an extracellular paramagnetic contrast agent of low molecular weight (e.g. molecular weight of 938 for gadopentetate dimeglumine). After intravenous injection, it is carried to the right ventricular cavity, then to the left ventricular blood pool. Then it diffuses rapidly from the intravascular space into the myocardial extracellular space (Al-Saadi and Bogaert J, 2004). Gd cause shortening of the T1 relaxation times.

The Gd passage through the myocardium is usually monitored by T1-weighted imaging. Depending on the concentration and the time of wash-in and washout of the contrast agent in the extracellular space, the myocardial tissue appears bright with high Gd content and

dark with low Gd content. Therefore, myocardial perfusion imaging shows dark areas with low SI and bright areas with high SI by using contrast agents (Al-Saadi and Bogaert, 2004).

> **Late Gadolinium Enhancement**

LGE imaging was developed by Kim and Judd in 1996 (Kim & Judd, 1996) and is an excellent tool for assessment of tissue viability, e.g. in the diagnosis of CAD (Kim et al., 2000; Bruder et al., 2009; West et al., 2010; Grover et al., 2011). Today, LGE-CMR is an important imaging tool in both, congenital and acquired heart diseases, for detection of necrosis and scar tissue (Harris et al., 2007; Desai et al., 2004; Babu-Narayan et al., 2010). The basic principle of LGE rests on the differences in distribution volume between viable and non-viable myocardial tissue. After intravenous administration of Gd, its distribution in the myocardium is determined by cell-membrane integrity, and the loss of cell-membrane integrity is a key step in the loss of myocardial viability. The use of Gd in conjunction with T1 weighted inversion recovery imaging can be used to maximimize the contrast between normal and injured myocardium. Using this technique, normal myocardium is made to appear dark, and regions of myocardial infarction or scar appear bright (Kim et al., 2000).

> **CMR for Assessment of Myocardial Fibrosis**

Diffuse myocardial fibrosis (DMF) is an important marker in heart diseases. Increased DMF has been demonstrated to correlate with diastolic and systolic dysfunction, arrhythmia, and sudden cardiac death (Martin et al., 1980; Villari et al., 1993). Previous studies showed evidence for DMF in congenital and acquired heart disease (Broberg et al., 2010). The gold standard method in evaluations of DMF marker of heart diseases is endomyocardial biopsy, which is an invasive method and has several disadvantages, including risk of the hazard, sampling error, and high cost (Becker et al., 1991; Holzmann et al., 2008).

CMR T1 mapping is a non-invasive method that can differentiate between diffuse fibrosis and normal myocardium by using a Gd extracellular contrast agents. For cardiac applications, T1 mapping within a breathhold can be performed with an ECG-gated Look-Locker type of technique, where image data are read-out continuously after an initial inversion pulse, to reconstruct images for 10-20 times after inversion (TI's). More recently, an ECG-gated single-shot Modified Look and Locker Inversion-recovery (MOLLI) sequence, was described by Messroghli et al., which provides a high resolution T1 map of the myocardium (Messroghli et al., 2004). The MOLLI sequence acquires multiple single shot steady-state free precession images in the same slice and during the same cardiac

phase. The acquisition extends over ~10 heart beats, and the TI's are varied by shifting the time for application of the inversion pulse relative to the (diastolic) single-shot image acquisition. A disadvantage of MOLLI compared to the Look-Locker technique is that in general only a 5-9 images, corresponding to different TI's are acquired, compared to ~20 TI's that can be sampled with the Look-Locker technique. In addition, T1 mapping can be used to quantify the changes of concentration of Gd in myocardium and in the blood pool before and after Gd administration. This information can be used to differentiate between normal and abnormal myocardium, and further allows absolute quantification of the extracellular volume (ECV) (Sado et al., 2012; Messroghli et al., 2011). It has been shown for multiple pathologies (e.g. aortic stenosis, hypertrophic cardiomyopathy, dilated cardiomyopathy), that an expansion of the ECV is a marker of increased collagen and connective tissue accumulation in the interstitial space (Jerosch-Herold et al., 2008). Therefore, the T1 maping CMR technique is emerging as a method for quantitative assessment of myocardial fibrosis in ischemic heart disease.

1.3   Previous Studies

In 2004, Prakash et al. performed a study using CMR to examine the feasibility and potential clinical utility of CMR for the evaluation of ischemic heart disease in congenital and acquired heart disease. They applied first-pass perfusion and LGE in 30 patients (age: 0.3 to 40 years) and could show that CMR can evaluate myocardial perfusion and viability. However, absolute myocardial blood flow was not analyzed in this study (Prakash et al., 2004).

Mavrogeni et al. used CMR to visualize the coronary arteries, to evaluate cardiac function and to show scar tissue in 20 patients with KD, aged 7-12 years. They found aneurysms of the coronary arteries in 7 patients, scar tissue in 4 patients, and left ventricular dysfunction in 2 patients. First-pass perfusion imaging was not performed (Mavrogeni et al., 2006).

In 2009, Buechel et al. published a CMR perfusion study in pediatric patients. First-pass perfusion with adenosine was performed in 47 patients (age: 1 month - 18 years). Perfusion CMR showed a sensitivity of 87% and a specificity of 95% for the detection of myocardial ischemia. This study demonstrated the feasibility of perfusion CMR in children (Buechel et al., 2009).

A study using CMR during follow-up of 63 patients (median age: 14.6 years) with KD was published in 2011. The CMR protocol included rest and stress perfusion imaging with

adenosine, LGE imaging and magnetic resonance coronary angiography. CMR findings were compared with echocardiographic data. Aneurysms of the coronary arteries were identified in 15 patients. CMR imaging detected LGE in 5 patients, myocardial ischemia in 4 patients, and thrombus formation in 4 patients. In summary the authors concluded that CMR is a promising diagnostic tool during the long-term follow-up in KD (Tacke et al., 2011).

In another study rest and stress perfusion with adenosine, LGE and 3D whole-heart imaging were performed for assessment of myocardial ischemia in ALCPA patients (Secinaro et al., 2011). This study showed the role of CMR for the follow-up of ALCAPA patients after surgical repair.

Broberg et al. performed a study for detection and quantification of DMF in patients with TGA, repaired tetralogy of Fallot, or Eisenmenger syndrome. They found the evidence of increased diffuse fibrosis in this population, compared to normal controls, and a correlation of the fibrosis index with end-diastolic function, and also with LV-EF (Broberg et al., 2010).

There are only few CMR studies, which focus on ischemic heart disease in children. So far, the published studies have demonstrated the promising role of MRI for the detection of myocardial ischemia in children. But most CMR studies only used qualitative and/or semi-quantitative analysis of myocardial perfusion in children, and the data on T1 mapping in children with congenital heart disease is very sparse at the present time.

1.4 The Aim of This Study

Myocardial ischemia is a leading cause of myocardial infarction and sudden cardiac death. In children, it may occur after surgery for CHD involving the coronary arteries, in congenital coronary artery anomalies, and in patients with inflammatory disease of the coronary arteries such as KD. Therefore, assessment of myocardial ischemia is important in this population during the long-term follow up, but current diagnostic imaging methods, such as electrocardiography, stress echocardiography, SPECT and PET, are often limited in the pediatric population.

There are only few CMR studies which analyzed markers of myocardial ischemia in children. In order to avoid ionizing radiation, an inherent burden of nuclear imaging (PET and SPECT), this study used CMR imaging for the evaluation of ischemic heart disease in children. We utilized advanced CMR methods to assess myocardial blood flow, viability,

function and diffuse fibrosis, to guide further therapy, and in order to get a better understanding of the myocardial microcirculation in congenital and acquired heart disease. We further asked if CMR predicts the functional recovery after treatment therapy of these patients.

2. METHODS

2.1 Patients

Between 2005 and 2012, a total of 77 patients (50 male and 27 female; mean age 16 ± 11.7 years; range 1.15 – 64.3 years) with known or suspected myocardial ischemia underwent a CMR examination in the Department of Congenital Heart Disease and Pediatric Cardiology, University Hospital Schleswig-Holstein, Campus Kiel. Medical records were reviewed to collect the clinical characteristics of these patients.

The study population was further divided into 6 subgroups. The patient characteristics were summarized in **table 1**.

- **TGA – coronary problems**: 13 TGA patients (age**,** 12.3 ± 9.65 years; range, 1.15 to 30.7 years) after ASO who had known CAD such as occlusion, stenosis, hypoplasia of the coronary artery, and post myocardial infarction. One patient with diagnosis of LCA occlusion was treated by MIDCAB operation.

- **TGA – open coronaries**: 36 TGA patients (age, 14.9 ± 6.9 years; range, 1.3 to 25.6 years) after ASO without coronary problems.

- **Ross patients**: 12 patients (age, 24.4 ± 11.4 years; range, 7.5 to 53.8 years) after Ross procedure.

- **BWG patients**: 7 patients with ALCAPA (age, 11.9 ± 7.5 years; range, 1.7 to 20.9 years) after surgical treatment, such as re-implantation of LCA (n=6) and Tackeuchi procedure (n=1). Three of these patients had a CMR study before and after operation.

- **KD patients**: 4 patients with a previous history of KD (age, 10.5 ± 8.5 years; range, 1.9 to 19.2 years).

- **Other patients**: 5 patients (age, 20.5 ± 24.7 years; range, 4.5 to 64.3 years) with other diseases involving the coronary arteries such as coronary artery fistula (n=1), aberrant LCA (n=1), and post heart transplantation (n=3). The patient with the aberrant LCA had two MRI scans, before and after bypass surgery.

The control subjects included 68 heart-healthy volunteers and patients (age, 1 to 38 years). They were divided into 3 matched controls subgroups for perfusion study (n= 24), ECV study (n= 10), aortic function study in TGA patients after ASO (n= 34) (Table 1-3). They

were matched to the study subgroups for age and BSA. Control subjects were recruited among outpatients, medical students, healthy children of hospital staff, or from the department of pediatric neurology. In all controls, cardiac pathology had been excluded.

Table 1. Patient characteristics vs. matched normal controls for myocardial perfusion study

Subgroup	N	Sex (M/F)	BSA	Age at scan (years)	Matched normal controls					
					N	Sex (M/F)	BSA		Age at scan (years)	
TGA-coronary problems	13	8/5	1.2 ± 5.7	12.5 ± 9.0	17	11/6	1.2 ± 5.6	p = 0.8	11.5 ± 8.5	p = 0.96
TGA-open coronaries	36	22/14	1.4 ± 0.5	14.2 ± 7.4	17	11/6	1.2 ± 5.6	p = 0.3	11.5 ± 8.5	p = 0.35
Ross patients	12	11/1	1.8 ± 0.4	24.4 ± 11.7	15	15/3	1.8 ± 0.4	p = 0.9	24.0 ± 10.2	p = 0.93
BWG patients	7	4/3	1.4 ± 0.6	11.9 ± 7.5	17	11/6	1.2 ± 5.6	p = 0.5	11.5 ± 8.5	p = 0.52
KD patients	4	2/2	1.2 ± 0.6	9.8 ± 7.5	17	11/6	1.2 ± 5.6	p = 0.9	11.5 ± 8.5	p = 0.76
Other patients	5	3/2	1.3 ± 0.5	19.2 ± 22.3	17	11/6	1.2 ± 5.6	p = 0.9	11.5 ± 8.5	p = 0.24

Values are mean ± SD. M/F= male/female.

Table 2. Patient characteristics vs. matched normal controls for ECV study

Subgroup	N	Sex (M/F)	BSA	Age at scan (years)	Matched normal controls					
					N	Sex (M/F)	BSA		Age at scan (years)	
TGA-coronary problems	13	8/5	1.2 ± 5.7	12.5 ± 9.0	10	6/4	1.5 ± 0.3	p = 0.2	13.8 ± 3.7	p = 0.6
TGA-open coronaries	25	24/14	1.4 ± 0.5	14.2 ± 7.4	10	6/4	1.5 ± 0.3	p = 0.2	13.8 ± 3.7	p = 0.9
Ross patients	12	11/1	1.8 ± 0.4	24.4 ± 11.7	7	4/3	1.6 ± 1.2	p = 0.7	15.9 ± 1.1	p = 0.09

Values are mean ± SD. M/F= male/female.

Table 3. Clinical characteristics of TGA patients and control subjects in aortic function study

Variable	Patients (N=44)	Controls (N=34)	p-Value
Age (years)	11.8 ± 6.8	14.1 ± 8.0	0.30
Male/Female (n)	28/16	12/22	-
Weight (kg)	47.1 ± 31.0	43.4 ± 22.0	0.90
Height (cm)	140.5 ± 35.6	146.7 ± 26.9	0.60
BSA	1.3 ± 0.5	1.3 ± 0.5	0.98
SBP (mmHg)	102.2 ± 16.0	101.6 ± 10.5	0.80
DBP (mmHg)	54.5 ± 11.5	59.3 ± 12.5	0.08

Data are presented as mean ± SD. P-Values are from the Mann-Whitney-U test. SBP, systolic blood pressure; DBP, diastolic blood pressure; BSA, body surface area.

In this study, the coronary pattern in TGA patients is classified into 7 types depending on the Leiden classification (Gittenberger-de Groot et al., 1983) (Figure 6).

- The normal coronary pattern in TGA is: 1LCx-2R.
- The most frequent anomalies encountered are: 1L-2CxR, 2LCxR, 1R-2LCx, 1RL-2Cx, 1RLCx, 2LCx2R.
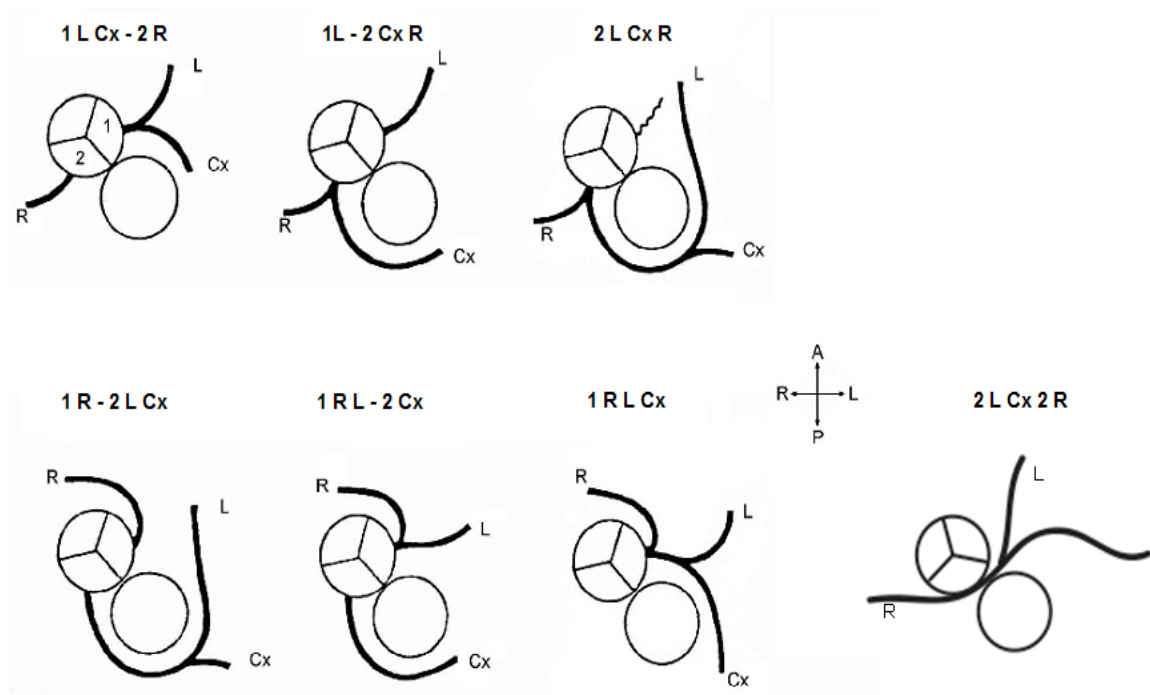
Figure 6. The Leiden classification for coronary pattern in TGA (Gittenberger-de Groot et al., 1983).

All patients underwent a CMR imaging protocol including first-pass perfusion and LGE imaging, T1-Mapping using the Look-Locker inversion recovery technique to evaluate myocardial perfusion, viability as well as LV fibrosis. Furthermore, CINE-MRI imaging was performed to assess ventricular function and coronary anatomy. The patient subgroups were compared to the healthy controls.

2.2 Image Acquisition

All studies were performed with a 3.0 Tesla Philips scanner (Achieva 3.0T, Philips Medical Systems, Best, Netherlands) using a phased-array coil for cardiac imaging (SENSE™ Cardiac coil, Philips Medical Systems, Netherlands). An intravenous line in an antecubital vein was inserted in all patients for the application of contrast media, adenosine, and sedation administration. Patients younger than 7 year olds were sedated with midazolam and propofol. Sedation was started with a bolus of midazolam (0.1mg/kg) and of propofol (1mg/kg). During the MR scan, propofol was infused with a dose of 3-5mg/kg/h. Adenosine and propofol were applied by using the MRI infusion system (MRidium™ 3850 Infusion pump, IRadimed, Florida, U.S.A). Electrocardiogram, blood pressure, oxygen saturation and breathing rate were monitored during the CMR scan by a MRI compatible monitor (In Vivo Precess™ 3160, Invivo, Orlando, FL). Systolic and diastolic blood pressures were

automatically measured every 10 minutes with an inflatable cuff placed over the left arm. A respiratory sensor was used for all patients during the CMR scan to monitor respiratory motion. Total scan time was approximately 60 to 90 minutes.

❖ **CINE CMR**

First, a series of scouts in axial, coronal, and sagittal orientation were performed. Then CINE-images were acquired using a gradient echo sequence to obtain axial, 2-chamber, 3-chamber, 4-chamber views, and a short axis stack. The sequence parameters were: field of view 280x224 mm, voxel size 1.88x1.94x6 mm, slice thickness 6-8 mm, TR/TE= 4.4/2.5ms, 25 cardiac phases. The short axis stack covered both ventricles from the base to the apex of the heart.

❖ **Perfusion Protocol**

For perfusion imaging, a T1-weighted, ECG-gated, single-shot, multi-slice gradient-echo sequence was used to visualize the first passage of Gd through the myocardium with the following parameters: repetition time 2.8 ms, echo time 1.4 ms, flip angle 20°, slice thickness 10 mm, gap 8 mm, field of view 300x200x28mm, voxel size 1.2x1.2x10 mm, 25 cardiac phases. For T1-weighting, a non-slice-selective saturation-recovery magnetization preparation was applied for each slice, to achieve identical T1-weighting of the signal in all slices, which was heart-rate independent. Perfusion imaging was planned from the 4 or 2-chamber views. Two (basal, mid-cavity) to three (basal, mid-cavity, and apical) short-axis slices were acquired during every heartbeat (Figure 7). First-pass perfusion imaging was performed for approximately 5-8 seconds before, and during the first pass of an injected Gd bolus (Magnevist, Bayer Schering Pharma AG, Germany) and recirculation of contrast (total acquisition time ~ 60 seconds). The contrast bolus corresponded to a dose of 0.03 mmol/kg and was followed by a normal saline flush of 20 ml. Blood pressure and heart rate were recorded before and after Gd injection. In our protocol, rest perfusion imaging was performed before the stress perfusion study.

The stress perfusion study followed approximately 15 minutes after rest perfusion imaging to allow for clearance of contrast from the blood before injecting the contrast bolus for stress perfusion imaging. CMR stress perfusion was started after 9 minutes of an infusion of adenosine (Adenoscan®, Sanofi-Synthelabo Ltd, Berlin, Germany) with adenosine doses increasing every 3 minutes (70µg/kg/min, 100µg/kg/min, 140µg/kg/min), or when the heart

rate had increased >10% at each infusion level. ECG, heart rate, blood pressure, pulse oximetry and breathing rate were monitored during and after performing stress adenosine.
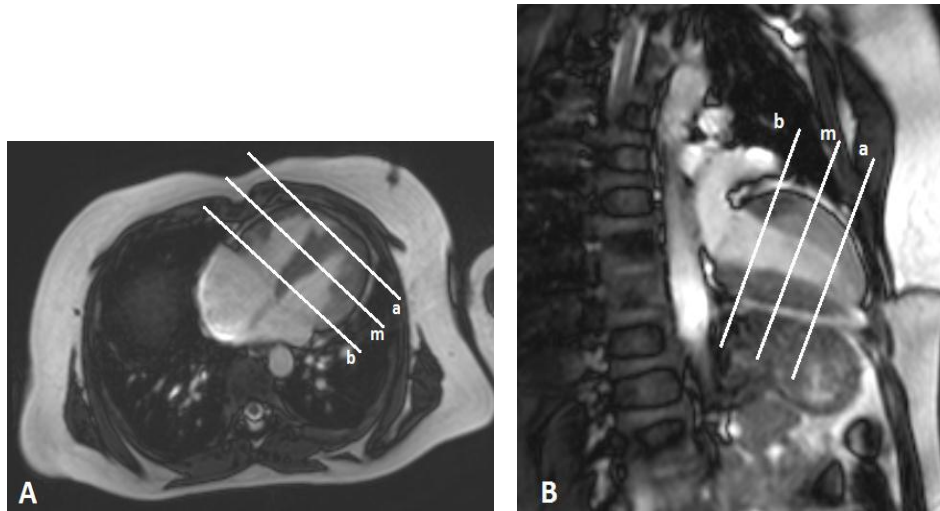
Figure 7. Perfusion imaging was planned from the 4 chamber views (A) and 4 chamber views in end-systolic. Three slices were acquired every beat heart in at basal (b), mid-cavity (m), and apical (a).

❖ **CMR Angiography**

Additionally, high resolution gadolinium-enhanced MR-angiography was performed in all patients for detailed 3D visualization of the aorta (Figure 29), using a keyhole technique, with the following imaging parameters: FOV 380x380 mm, 70 slices, keyhole percentage 20%, 20 dynamics, keyhole scan time 1.7 s, TR/TE=2.4/0.93 ms, scan duration 0:40 min. Gadolinium (Magnevist, Bayer Schering Pharma AG, Germany) was injected intravenously at a dose of 0.1 mmol/kg, with an injection rate of 2 ml/s, followed by a normal saline flush at the same rate. Healthy controls did not receive any contrast injections due to concerns by the ethics committee.

❖ **Late Gadolinium Enhanced CMR**

LGE studies using an ECG triggered 3D inversion recovery sequence were performed 10 – 15 minutes after stress perfusion study and contrast angiography (i.e. after a total of ~0.16 mmol/kg of contrast had been injected). The scan parameters were: repetition time 2.8 ms, echo time 1.4 ms, flip angle 15°, slice thickness 6-8 mm, field of view 300x178x80 mm, voxel size 1.17x1.27x10 mm, 25 cardiac phases, 20-24 slices, the trigger delay depended on the heart rate. The images were planed from short axis CINE images.

❖ **Look-Locker**

A Look-Locker sequence (temporal resolution, 40 ms; slice thickness, 8 mm; repetition time>3 R-R intervals) for the measurement of T1 was used for the detecting of myocardial fibrosis. The Look-Locker sequences were acquired before and after Gd infusion. All T1 measurements were performed in one and the same mid-ventricular plane.

❖ **Phase-Contrast CMR**

A phase-contrast cine pulse sequence, with through-plane velocity encoding, was applied for assessment of aortic pulse wave velocity (PWV) between the ascending aorta at the level of the sinotubular level, and the proximal descending aorta, with a slice plane intersecting the aorta at both locations at an approximately right angle. Phase-contrast flow velocity measurements in the proximal ascending aorta were also used for assessment of aortic valve competence. The phase-contrast sequence parameters were as follows: FOV 270x270 mm, voxel size 1.64x1.4x7 mm, TR/TE= 4.4/2.7 ms, max. velocity encoding: 200 cm/s.

2.3 Image Analysis

All CMR images were analyzed using a commercial software package (ViewForum 6.1, Philips Medical Systems, Best, Netherlands).

2.3.1 Segmentation of the Left Ventricle

Myocardial function and perfusion were analyzed according to the American Heart Association (AHA) 17-segment model (Cerqueira 2002). The LV was divided into three equal sections perpendicular to the long axis of the heart named basal, mid-cavity, and apical. The basal and mid cavity sections were further divided into 6 segments, and the apical section was divided into 4 segments. The first segment was defined in the anterior septal insertion of the right ventricle and started in a clockwise direction. Each segment corresponded to a coronary artery territory (Figure 8).

Left Ventricular Segmentation
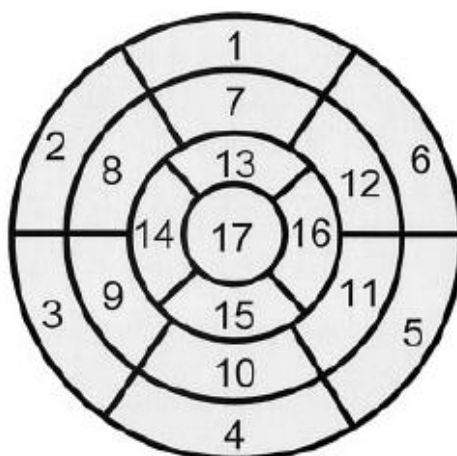
1. basal anterior	7. mid anterior	13. apical anterior
2. basal anteroseptal	8. mid anteroseptal	14. apical septal
3. basal inferoseptal	9. mid inferoseptal	15. apical inferior
4. basal inferior	10. mid inferior	16. apical lateral
5. basal inferolateral	11. mid inferolateral	17. apex
6. basal anterolateral	12. mid anterolateral	

Figure 8. The left ventricle was divided into 17 segments (Cerqueira 2002).

2.3.2 Quantitative Analysis of Global LV

The left ventricular volumes were measured by defining the endocardial and epicardial borders in the short axis stack of images at end-diastole and end-systole with a dedicated software program (ViewForum 6.1, Philips Medical Systems, Best, Netherlands). Papillary muscles were excluded for the quantification of ventricular volumes. When papillary muscles were well definable they were included for the calculation of left ventricular masses. Both left and right ventricular masses included the contribution from the cardiac septum. The volumes were calculated in each slice at end-diastole and end-systole images (Figure 9). Then the left ventricular volumes at end-diastole (EDV) and end-systole (ESV) were calculated with the Simpson's rule approach by summation of all the volumes in end-diastole and end-systole as described in previous studies (Sarwar et al., 2008; Graney et al., 1990).

Then ejection fraction (EF), stroke volume (SV), EDV index, ESV index, cardiac output (CO), and cardiac index (CI) were calculated from these values (Sarwar et al., 2008):

- SV (ml) = EDV–ESV

- EF (%) = (EDV – ESV)/EDV

- CO (ml/min) = SV x HR

- EDV index (ml/m^2)= EDV/BSA

- ESV index (ml/m^2)= ESV/BSA

- CI (l/min/m^2) = (SV x HR)/BSA

    (HR: heart rate; BSA: body surface area, according to the Mosteller formula: Height (cm) x Weight (kg)/3600).
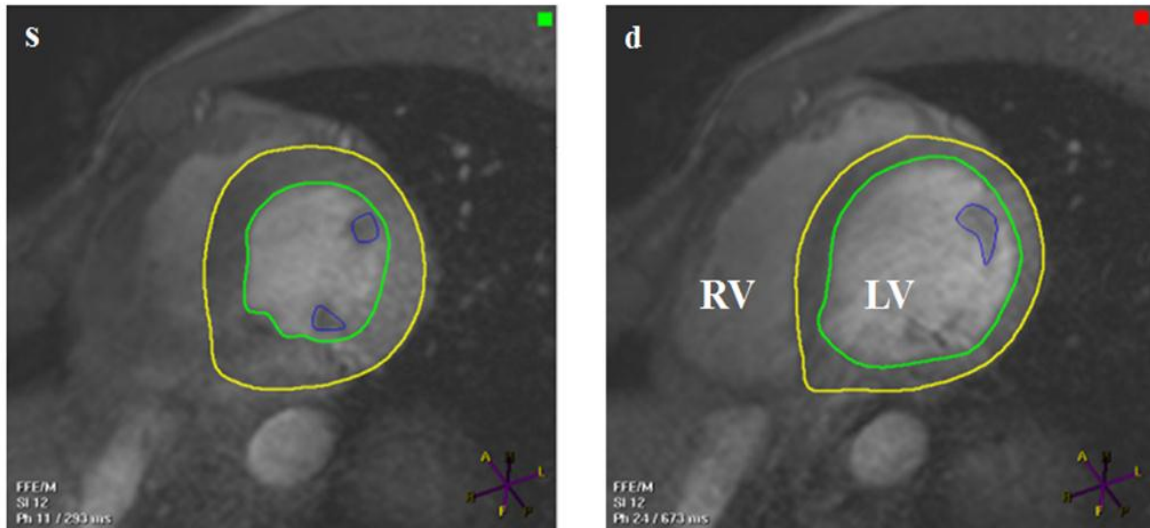
Figure 9. Endo and epicardial borders were defined from the short axis view at end-diastolic (d) and end-systolic (s) phases in the left ventricular.

2.3.3 Quantitative Analysis of LA Volume and Function

The left atrial (LA) volume was calculated on axial cine images at three phases during the cardiac cycle as previous description (Muellerleile et al., 2012): maximal LA volume just before mitral valve opening (LAV$_{max}$), minimal LA volume after mitral valve closure (LAV$_{min}$) and LA volume prior to atrial contraction (LAV$_{bac}$). LA endocardial contours were drawn manually slice by slice on axial cine CMR images in three phases of LAV$_{max}$, LAV$_{min}$, and LAV$_{bac}$ (Sarikouch et al., 2011); (Figure 10).
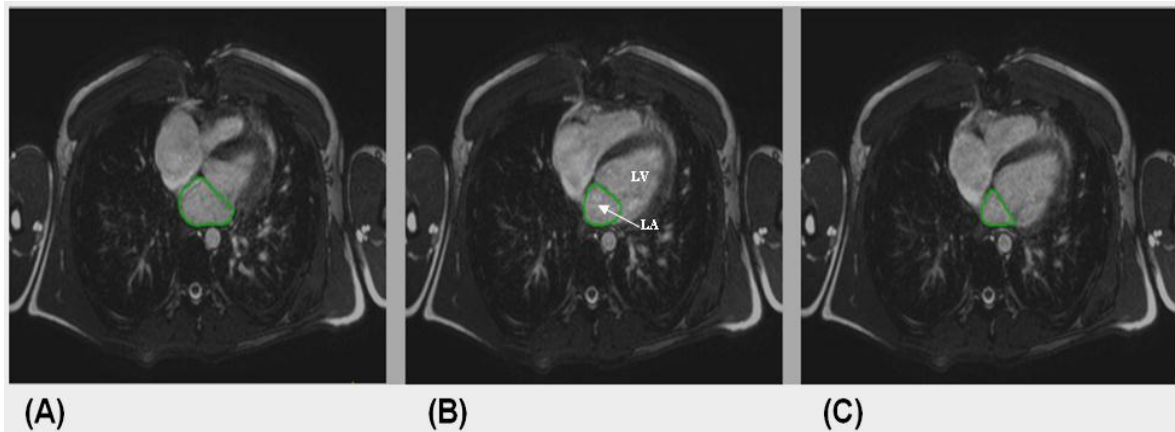
Figure 10. LA contours were defined from the axial images in a patient after Ross operation. A: LAV_{max}; B: LAV_{bac}; C: LAV_{min}

From the volumes we calculated other volumes and functional parameters:

- Total LA emptying volume is defined as the difference between LAV_{max} and LAV_{min}, and was calculated by the formula:

  Total LA emptying volume = LAV_{max}-LAV_{min}

- Total LA emptying volume was divided into LA passive emptying volume and LA contractile volume, and calculated by formulars:

  LA passive emptying volume = LAV_{max}–LAV_{bac}

  LA contractile volume = LAV_{bac}–LAV_{min}

- LAPEF = (LAV_{max}–LA passive emptying volume)*100/LAV_{max}

- LACEF = (LAV_{bac}–LA contractile volume)*100/LAV_{bac}

- LAREF = (LAV_{max}-V_{min})*100/LAV_{max}

2.3.4 First-Pass Perfusion Analysis

First-pass perfusion imaging was assessed qualitatively and semi-quantitatively. Furthermore, absolute quantification of myocardial perfusion was performed. Both, rest and stress perfusion studies were analyzed.

➤ **Qualitative Analysis**

First-pass perfusion imaging was assessed qualitatively by visual analysis of the contrast enhancement in different myocardial areas. For visual analysis the myocardial contrast

enhancement was viewed in cine mode for each slice, and by examining contrast enhancement in different myocardial segments in selected images during the wash-in phase of contrast. Perfusion defects were defined as relatively darker areas (i.e. with reduced signal intensity) in the LV wall after LV peak of contrast enhancement, and extending in time over at least several heart beats. The region of the perfusion defect at rest was compared with the same region at stress (Al-Saadi & Bogaert, 2004). The presence of a perfusion defect was assigned to the respective coronary artery based on the 17 segments AHA model (Cerqueira 2002), and coronary angiography data.
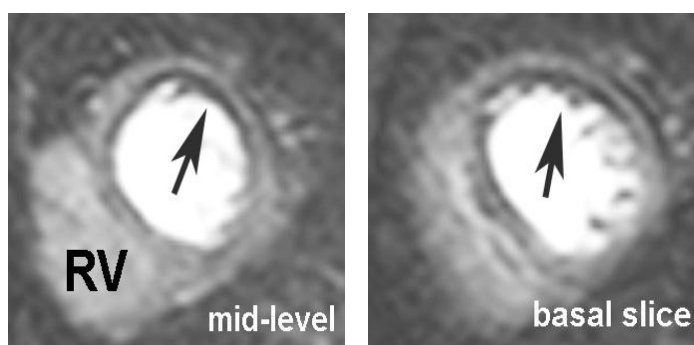
Figure 11. An example of mid and basal ventricular perfusion imaging with a perfusion defect in the anterior and anterolateral wall.

➢ **Semi-quantitative Analysis**

Semi-quantitative analysis allows measuring the changes in signal intensity during the transit of contrast agent through the heart. All endocardial and epicardial LV contours were drawn manually and the contours were first copied and then adjusted for images in a slice location. In addition the LV wall was divided into 16 segments according to the recommendation by the AHA for myocardial perfusion analysis (Cerqueira 2002) and the blood pool of the LV was defined (Figure 12).
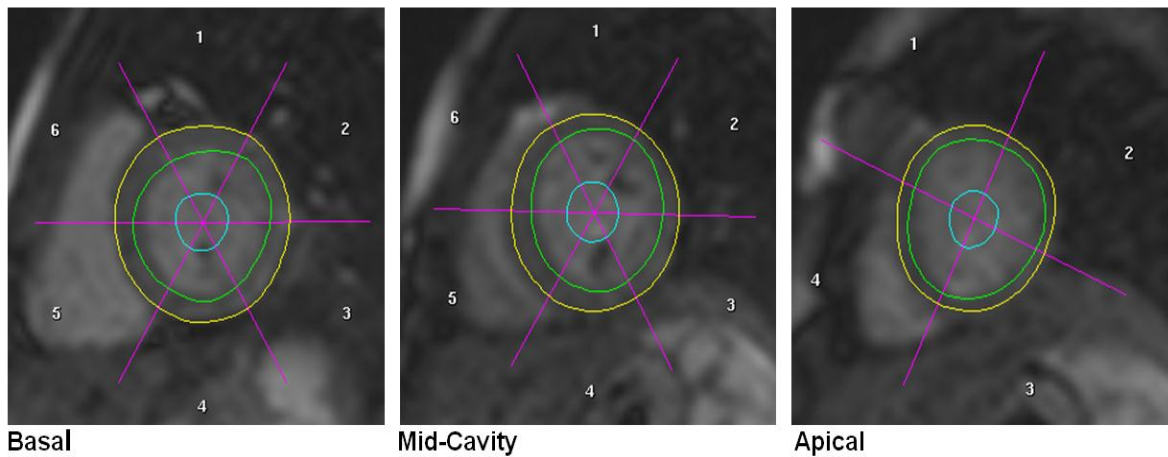
Figure 12. The LV was divided into 16 segments according to the AHA model for myocardial perfusion analysis (Cerqueira 2002). Six segments for the basal and mid-cavity portions, four segment for the apical portion.

Contour correction was necessary in most cases because of the movement of the heart during breathing. After contour correction, signal intensity curves for each myocardial segment were created by the software program. Parameters obtained by semi-quantitative analysis were the following (Keijer et al., 1995; Al-Saadi et al., 2000; Schwitter et al., 2001; Nagel et al., 2003; Jerosch-Herold et al., 2004):

a) **Up-slope parameter**: The race of change of the SI in LV cavity and myocardial tissue during the first pass of contrast agent.

b) **Time to peak**: The time from the onset of contrast enhancement (the foot of the SI curve) to the peak of the SI curve.

c) **Peak SI**: The peak value of SI time curve obtained from the myocardium during the first- pass of contract agent.

d) **Mean transit time**: The average time required for a contrast agent to pass through the ROI.

e) **Area under the SI curve**: The area under the SI curve from the foot of SI curve to a user-defined point.

Semi-quantitative and qualitative analyses were compared to improve diagnostic accuracy over visual analysis alone (Nagel E et al., 2003). The regions of perfusion defect were compared with the degree of signal intensity changes for each segment. These parameters were further used for absolute perfusion quantification.

➢ **Absolute Perfusion Quantification**

In contrast to qualitative and semi-quantitative myocardial perfusion analysis, the quantitative approach allows to calculate the absolute MBF in milliliters/minute/gram for each myocardial segment by a model-independent deconvolution (Jerosch-Herold et al., 2002). MBF was calculated for each segment of the LV at rest and stress by deconvolution of the myocardial signal intensity curves with an arterial input function measured in the left ventricular blood pool. This was performed with a Fermi function model of the myocardial impulse response. Then absolute MBF was estimated from the maximum amplitude of the Fermi impulse response, based on Zierler's central volume principle. Myocardial perfusion reserve index (MPRI) was calculated by dividing the absolute MBF at stress by the absolute MBF at rest.

2.3.5 LGE

LGE images were evaluated visually for areas of hyperenhancement indicating myocardial fibrosis. Myocardial fibrosis appears as bright signal in contrast to the dark appearance of the normal myocardium. We differentiated between subendocardial or transmural depending on the location and extent of the hyperenhancement.

Endocardial and epicardial contours of the LV were drawn in all short axis views that were divided into 6 segments based on the AHA model (Cerqueira 2002). The extent of hyperenhancement was quantified (percentage or volume) for each myocardial segment.

2.3.6 T1 Mapping Analysis

For each Look-Locker T1 mapping sequence, the endocardial and epicardial contours for the LV were drawn manually using QMass® MR software (Medis; Leiden, Netherlands). The LV wall was divided into six standard segments (Figure 13). The anterior junction between the LV and RV was used to define the first segment. The blood pool T1 was determined in the left ventricular cavity. The signal intensity during inversion recovery for each myocardial segment and the blood pool was calculated by the software. The resulting inversion-recovery curves were used to determine a segmental myocardial T1 value through exponential fitting. The reciprocal of T1, the relaxation rate constant R1, was then used for further analysis, as R1 is in principle linearly proportional to contrast agent concentration. The slope of the linear relationship between myocardial R1 and blood pool R1 before and after Gd administration defined the partition coefficient for Gd, λ_{Gd}. The myocardial volume

of Gd distribution, or myocardial extra-cellular volume fraction (MECVF) was obtained by multiplying each segmental partition coefficient for Gd by (1-hematocrit in percent/100) (Coelho-filho et al., 2013; Broberg et al., 2010). This correction accounts for the fact that the R1 in blood changes due to the addition of contrast in the partial volume which excludes red blood cells. The hematocrit values around 4 weeks before or after the time of the CMR were collected from the medical records. We used a hematocrit of 41% as a "default" value in patients without hematocrit data at the time of the CMR exam. Then global MECVF was calculated by averaging the values in 6 myocardial segments.
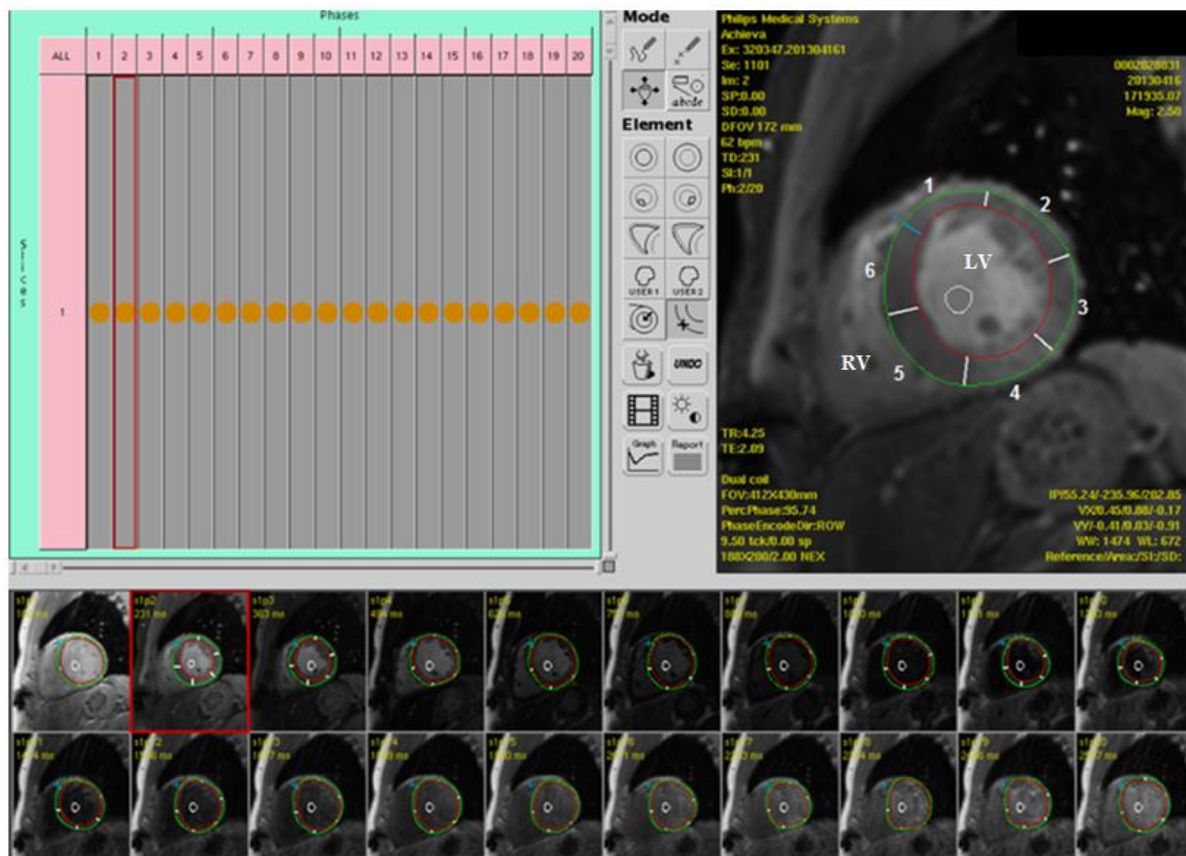
Figure 13. Look-Locker imaging was analyzed by using QMass® MR software. Endocardial and epicardial contours were defined in the LV. The LV wall was divided into 6 standard segments.

2.3.7 Functional Analysis of the Aorta

All CMR images for functional analysis of the aorta were analyzed using a commercial software package (ViewForum 6.1, Philips Medical Systems, Best, Netherlands).

❖ **Aortic Area**

The maximal and minimal areas of the aorta (A_{max} and A_{min}) were determined at four locations (Figure 14):

1) Aortic root at the level of the sinus of valsalva,

2) Ascending aorta,

3) Descending aorta at the level of the isthmus,

4) Descending aorta above the diaphragm.

Area measurements were also used for further calculations, specifically the aortic distensibility calculation. The measurements were made at the time of the maximal distension of the aorta.

❖ **Aortic Distensibility**

Aortic distensibility was assessed from two-dimensional axial cine images at the aortic root, and the ascending aorta as well as in the descending aorta at the level of the aortic isthmus and above the diaphragm in patients and controls. The systolic and diastolic blood pressures (P_{max} and P_{min}) were obtained non-invasively using a CMR-compatible monitor with sphygmomanometer (Invivo Precess^{TM} 3160, Invivo, Orlando, USA), with the cuff placed around the right arm.

Distensibility was calculated according to the following formula (Nollen et al., 2004):

$$\text{Distensibility} = (A_{max} - A_{min})/[A_{min} \times (P_{max} - P_{min})]$$
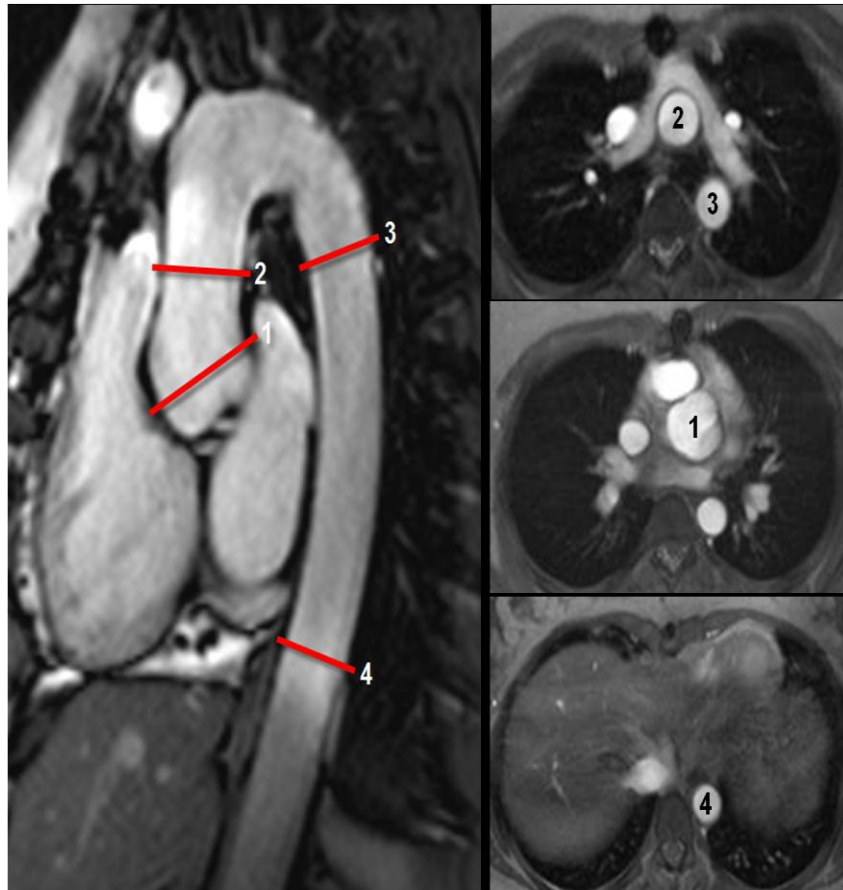
Figure 14. Aortic area measurements. Aortic area was assessed from axial MR images acquired with a gradient echo cine sequence at three different locations of the thoracic aorta: aortic root (1), ascending aorta (2), descending aorta at the aortic isthmus (3), descending aorta above the diaphragm (4). Aortic area measurements were used for distensibility estimation.

❖ **Aortic Flow**

Aortic flow measurements were analyzed from phase-contrast cine sequences by using a commercial software package (ViewForum 6.1, Philips Medical Systems, Best, Netherlands) to obtain aortic regurgitation (AR) parameter. Endovascular contours were drawn for the aorta to obtain AR parameters and flow curves data. AR was defined as the following levels (Globits et al., 1992):

1) Mild: the regurgitant fraction was 5%-15%.
2) Moderate: the regurgitant fraction was 16%-30%.
3) Moderate to severe: the regurgitant fraction was 31-50%.
4) Severe: the regurgitant fraction was >50%.

❖ **Aortic Pulse Wave Velocity**

Aortic pulse wave velocity (PWV) was determined from aortic flow versus time curves, as the ratio of the aortic segment length, (Δx, meters; Figure 15.A) divided by the time delay of the distal flow curve, relative to the proximal flow curve (Δt, seconds; Figure 15.B):

PWV= Δx/Δt.
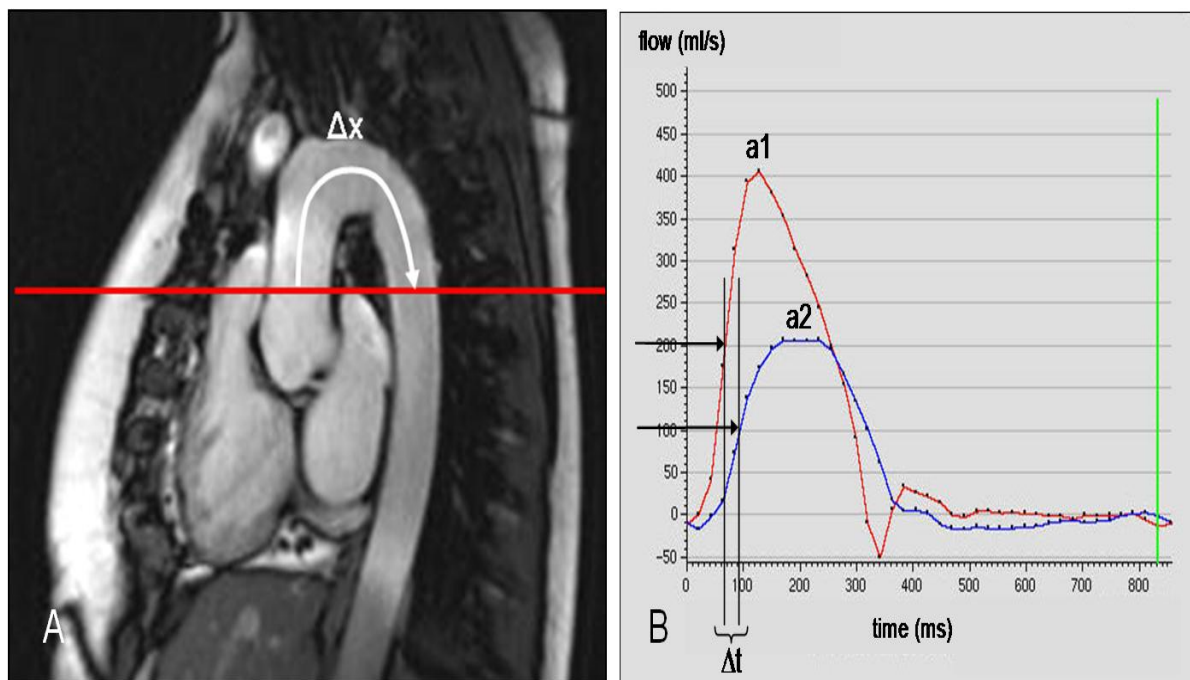
Figure 15. Pulse wave velocity. A) This sagittal image of the aorta was generated with a gradient echo cine sequence and shows the sites where phase contrast cine images were acquired. First, the distance along a midline through the aortic arch (Δx) between the measurement locations in the ascending and descending aorta was measured. B) Next, the transit delays (Δt) of the systolic flow curves in the descending (a1) relative to the ascending (a2) aorta were determined.

2.4 Statistical Analysis

Statistical testing and data analysis were performed using Microsoft Excel and IBM SPSS Statistics for Windows version 21. The data were expressed as mean values and standard deviations or median values and range. Two-tailed Mann-Whitney-U test for non-parametric samples was used to compare data between subgroups and healthy controls. Correlation was tested with Spearman's rank correlation coefficients. Chi-square tests were used to compare

the frequency of presented perfusion defect cross the subgroups. A p-value <0.05 was considered as statistically significant.

3. RESULTS

3.5 Patient Findings

Seventy-seven patients and 68 healthy subjects participated in this study from 2005 to 2013. There were no differences in age, height, weight, and body surface area between each subgroup and age matched healthy controls, and between the two subgroups of TGA patients. Forty-nine patients (89%) had an operation before the CMR examination. Most surgical procedures were performed at the Universitätsklinikum Schleswig-Holstein, Campus Kiel (85%). Medication was used during the follow up in each subgroup are summarized in table 4. Medication in TGA patients was significantly different between TGA-coronary problems and TGA-open coronaries (Table 4).

Table 4. Cardiac medications during the follow-up in each subgroup

Subgroups	Aspirin	Warfarin	Diuretics	ACE	B-blocker	CA
TGA-coronary problems	6/13	0	0	2/13	3/13	1/13
TGA-open coronaries	0	0	0	1/36	0	1/36
Ross patients	0	0	0	2/12	1/12	0
BWG patients	3/7	1/7	1/7	3/7	1/7	0
KD patients	3/4	1/4	1/4	1/4	0	0
Other patients	2/5	0	1/5	1/5	3/5	0

ACE: Angiotensin-converting enzyme inhibitors; **CA**: Calcium channel blockers. The frequencies for each medication across subgroups are significantly different ($p<0.05$, Chi-square test).

TGA patients. Eleven patients (85%) in TGA-coronary problems, and 33 patients (91.7%) in TGA-open coronaries underwent one-stage ASO. The mean age at ASO was 7.6 ± 3.3 days in TGA-coronary problems, and 8.5 ± 5.7 days in TGA-open coronaries. Two patients in TGA-coronary problems, and three patients in TGA-open coronaries underwent two-stage ASO. The age at operation in the latter patients ranged from 11.6 to 24.4 months. One patient with LCA occlusion in TGA-coronary problems was treated by MIDCAB operation. The coronary

artery patterns in TGA patients are described in figure 15. Table 5 describes in detail the coronary status of patients in TGA-coronary problems.
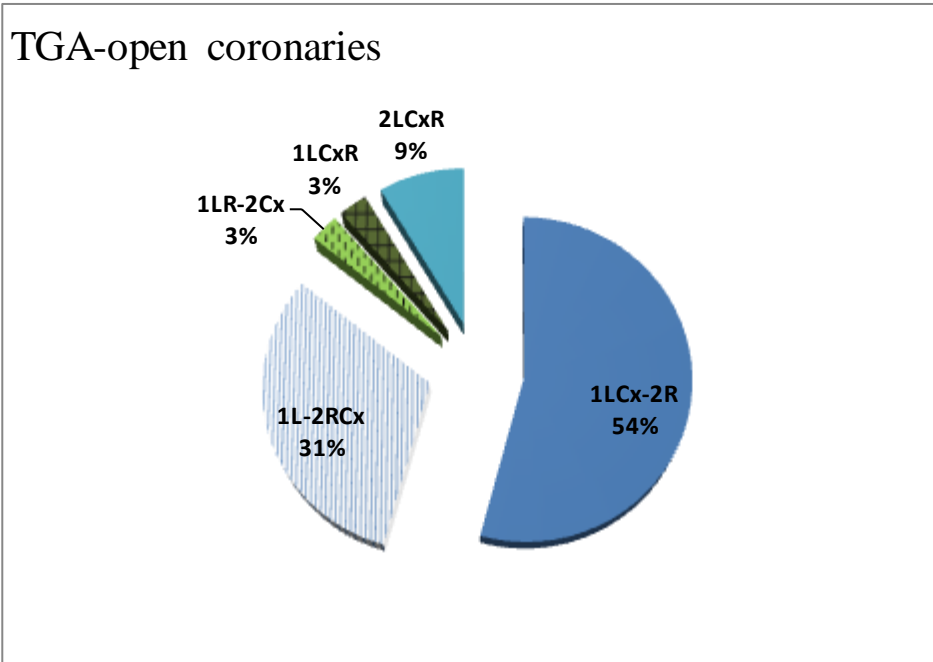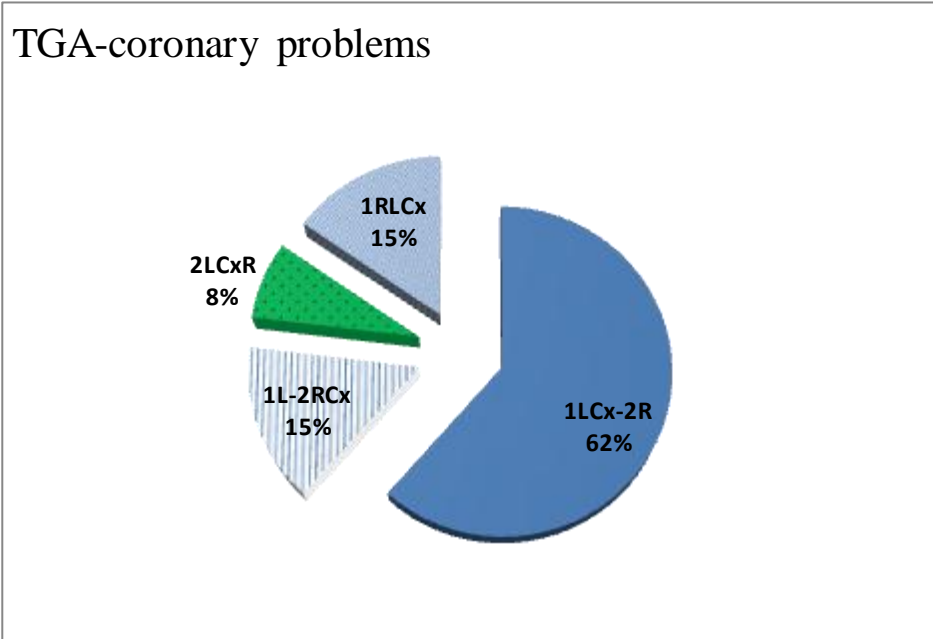
Figure 15. Coronary pattern in 2 subgroups of TGA patients.

Table 5. Coronary artery problems in 13 TGA patients in TGA-coronary problems

Patients	Coronary artery problems	Course of the coronary arteries
1	CFX closure	1LCx-2R
2	Hypoplastic LCA	1LCx-2R
3	Anomalous LCA	1LCx-2R
4	Hypoplastic LCA	1LCx-2R
5	LCA closure	1L-2RCx
6	LCA closure	1LCx-2R
7	Ramus circumflex closure	1LCx-2R
8	LCA occlusion	2LCxR
9	LCA closure	1L-2RCx
10	RCA closure	1RLCx
11	LCA occlusion	1LCx-2R
12	LCA occlusion	1RLCx
13	Post myocardial infarction	1LCx-2R

CFX**:** circumflex artery, LCA: left coronary artery, RCA: right coronary artery

Ross patients. The patient characteristics in this subgroup are summarized in Table 1. Most patients were asymptomatic post operation. Only one patient had an episode of syncope and was treated by Beta-blocker and ACE.

BWG. All BWG patients (n=7) were treated by surgery for anatomical correction of the coronary artery. Patient characteristics were described in table 1 and in the chapter above. Two patients had symptoms of chest pain and syncope before surgery. LCA was showed slightly stenosis post-operation in a patient. All patients were asymptomatic post-surgery.

Kawasaki Syndrome. Patient characteristics were described in Table 1. None of those patients had symptoms of myocardial ischemia before the CMR exam. Cardiac operations were not performed in Kawasaki Syndrome.

Other patients. In this subgroup, 1 patient with aberrant of LCA was treated by MIDCAP operation. CMR before surgery showed an anomalous origin of the LCA from the right sinus

of Valsalva. After surgery CMR was repeated and showed that both RCA and LCA originated from the aortic root, and MBF at stress and MPR were increased and the patient was asymptomatic post-operation. The characteristics in the group of the other patients are described in table 1.

3.2 Cardiac MRI

Sixteen children (25.61%) were sedated with midazolam and propofol during CMR scan. Sedation-related complications did not occur.

3.2.1 Left Ventricular Volumes and Function

Volumetric and functional parameters of the LV for each subgroup are summarized in (Table 6 to 11). In 15 patients we found a reduced LVEF (<40%) including 4 patients in TGA-coronary problems, one patient in TGA-open coronaries, 4 patient in subgroup of Ross patients, 4 BWG patients, and 1 patient after heart transplantation and 1 patient with aberrant LCA. Ross patients and BWG patients had a significantly reduced LVEF compared to the control group (Ross patients: 54.84 ± 8.73 vs. controls 65.03 ± 3.06, p=0.03; BWG patients: 50.7 ± 9.8 vs. controls 64.6 ± 3.9, p=0.05). LV EDV index in the 2 subgroups of TGA patients was significant higher than in the controls (p<0.05).

Table 6. Left ventricular volumes and function in TGA-coronary problems.

Parameters	TGA-coronary problems (N = 13)	Controls (N = 13)	p-Value
LV – EDV (ml)	103.0 ± 67.5	78.8 ± 45.0	0.45
LV – EDV index (ml/m^2)	80.0 ± 25.5	60.0 ± 16.6	0.04
LV – ESV (ml)	49.0 ± 44.0	29.3 ± 18.2	0.44
LV – ESV index (ml/m^2)	36.0 ± 21.0	21.9 ± 8.2	0.06
LV – EF (%)	57.0 ± 13.4	64.7 ± 4.0	0.26
LV – SV (ml)	54.0 ± 30.2	61.0 ± 33.3	0.61
LV – SV index (ml/m^2)	44.0 ± 11.5	40.6 ± 9.7	0.36
LV – CO	4.4 ± 2.2	4.8 ± 2.2	0.68
LV – CO index	3.8 ± 1.4	3.3 ± 0.6	0.51
LV – mass (g)	69.0 ± 45.9	81.7 ± 52.2	0.51
LV – mass index (g/m^2)	56.0 ± 20.8	53.0 ± 19.0	0.54

Values are mean ± SD. P-values are from the Mann-Whitney-U test.

Table 7. Left ventricular volumes and function in TGA-open coronaries.

Parameters	TGA-open coronaries (N = 36)	Controls (N = 13)	p-Value
LV – EDV (ml)	116.0 ± 59.4	78.8 ± 45.0	0.07
LV – EDV index (ml/m^2)	80.6 ± 22.0	60.0 ± 16.6	0.01
LV – ESV (ml)	46.5 ± 29.0	29.3 ± 18.2	0.08
LV – ESV index (ml/m^2)	32.0 ± 12.6	21.9 ± 8.2	0.02
LV – EF (%)	61.6 ± 7.0	64.7 ± 4.0	0.13
LV – SV (ml)	69.6 ± 33.0	61.0 ± 33.3	0.46
LV – SV index (ml/m^2)	49.0 ± 11.0	40.6 ± 9.7	0.02
LV – CO	5.0 ± 2.0	4.8 ± 2.2	0.74
LV – CO index	3.7 ± 1.1	3.3 ± 0.6	0.36
LV – mass (g)	84.0 ± 38.3	81.7 ± 52.2	0.82
LV – mass index (g/m^2)	59.8 ± 18.0	53.0 ± 19.0	0.30

Values are mean ± SD. P-values are from the Mann-Whitney-U test.

Table 8. Left ventricular volumes and function in patients after Ross procedure.

Parameters	Ross patients (N = 12)	Controls N = 15	p-Value
LV – EDV (ml)	229.0 ± 83.0	-	-
LV – EDV index (ml/m^2)	123.3 ± 42.1	-	-
LV – ESV (ml)	112.0 ± 55.0	-	-
LV – ESV index (ml/m^2)	59.4 ± 30.5	-	-
LV – EF (%)	55.0 ± 8.7	65.0 ± 3.1	0.03
LV – SV (ml)	121.0 ± 37.0	83.0 ± 25.0	0.04
LV – SV index (ml/m^2)	65.6 ± 15.7	44.8 ± 6.7	<0.001
LV – CO	8.0 ± 2.3	5.1 ± 1.7	0.025
LV – CO index	4.4 ± 1.2	3.4 ± 0.7	0.012
LV – mass (g)	143.0 ± 57.0	125 ± 49.3	0.516
LV – mass index (g/m^2)	75.0 ± 24.0	66.3 ± 15	0.277

Values are mean ± SD. P-values are from the Mann-Whitney-U test.

Table 9. Left ventricular volumes and function in patients with BWG.

Parameters	BWG patients (N = 7)	Controls (N = 13)	p-Value
LV – EDV (ml)	116.0 ± 63.0	78.8 ± 45.0	0.27
LV – EDV index (ml/m^2)	84.0 ± 30.3	60.0 ± 16.6	0.16
LV – ESV (ml)	61.5 ± 37.5	29.3 ± 18.2	0.07
LV – ESV index (ml/m^2)	41.9 ± 18.3	21.9 ± 8.2	0.02
LV – EF (%)	50.7 ± 10.0	64.7 ± 4.0	0.005
LV – SV (ml)	55.4 ± 26.0	61.0 ± 33.3	0.57
LV – SV index (ml/m^2)	42.0 ± 15.0	40.6 ± 9.7	0.81
LV – CO	4.4 ± 1.5	4.8 ± 2.2	0.95
LV – CO index	3.5 ± 1.5	3.3 ± 0.6	0.13
LV – mass (g)	87.0 ± 53.0	81.7 ± 52.2	0.81
LV – mass index (g/m^2)	61.4 ± 22.0	53.0 ± 19.0	0.48

Values are mean ± SD. P-values are from the Mann-Whitney-U test.

Table 10. Left ventricular volumes and function in with a history of KD.

Parameters	KD patients (N = 4)	Controls (N = 13)	p-Value
LV – EDV (ml)	106.4 ± 62.0	78.8 ± 45.0	0.45
LV – EDV index (ml/m^2)	88.5 ± 25.0	60.0 ± 16.6	0.03
LV – ESV (ml)	42.0 ± 25.4	29.3 ± 18.2	0.63
LV – ESV index (ml/m^2)	35.0 ± 14.4	21.9 ± 8.2	0.10
LV – EF (%)	61.4 ± 5.5	64.7 ± 4.0	0.24
LV – SV (ml)	66.7 ± 42.0	61.0 ± 33.3	0.87
LV – SV index (ml/m^2)	55.0 ± 12.0	40.6 ± 9.7	0.10
LV – CO	4.9 ± 2.6	4.8 ± 2.2	0.95
LV – CO index	4.4 ± 1.3	3.3 ± 0.6	0.13
LV – mass (g)	69.5 ± 43.0	81.7 ± 52.2	0.87
LV – mass index (g/m^2)	56.0 ± 13.0	53.0 ± 19.0	0.87

Values are mean ± SD. P-values are from the Mann-Whitney-U test.

Table 11. Left ventricular volumes and function in other patients.

Parameters	Other patients (N = 5)	Controls (N = 13)	p-Value
LV – EDV (ml)	79.0 ± 32.0	78.8 ± 45.0	1.00
LV – EDV index (ml/m^2)	62.5 ± 22.0	60.0 ± 16.6	0.85
LV – ESV (ml)	38.3 ± 25.0	29.3 ± 18.2	0.31
LV – ESV index (ml/m^2)	28.5 ± 15.0	21.9 ± 8.2	0.51
LV – EF (%)	55.2 14.5	64.7 ± 4.0	0.24
LV – SV (ml)	40.7 ± 11.0	61.0 ± 33.3	0.24
LV – SV index (ml/m^2)	34.0 ± 12.2	40.6 ± 9.7	0.38
LV – CO	3.6 ± 0.9	4.8 ± 2.2	0.33
LV – CO index	3.0 ± 0.9	3.3 ± 0.6	0.84
LV – mass (g)	70.0 ± 26.3	81.7 ± 52.2	1.00
LV – mass index (g/m^2)	54.0 ± 19.2	53.0 ± 19.0	0.92

Values are mean ± SD. P-values are from the Mann-Whitney-U test. Heart transplantation (n=3), aberrant LCA (n=1), coronary fistula (n=1).

3.2.2 Myocardial Perfusion

Rest perfusion was performed in 48 patients (87.3%) and stress perfusion with adenosine was performed in 47 patients (85.5%). All of the 46 patients (83.6%) successfully completed both rest and adenosine stress perfusion. They did not complain of chest pain, and AV block did not occur during stress testing.

Hemodynamic data during perfusion CMR imaging are shown in table 12. During stress perfusion, heart rate increased from 79.8 ± 18.7 to 104.8 ± 19.9 ($p < 0.001$).

Table 12. Hemodynamic parameters perfusion imaging

Parameters	Rest	Stress	p-Value
Heart rate, per min	79.8 ± 18.7	104.8 ± 19.9	<0.001
Systolic BP, mmHg	99.2 ± 15.2	98.2 ± 20.3	0.97
Diastolic BP, mmHg	49.7 ± 13.8	49.7 ± 19.2	0.99
Mean BP, mmHg	68.9 ± 14.4	69.0 ± 19.9	0.98

Values are presented as mean $\pm$ SD. BP= blood pressure.

P-values are from the Mann-Whitney-U test.

Visual analysis of myocardial perfusion imaging showed regions of perfusion defects at rest and stress perfusion in subgroups (table 13). No region of perfusion defects were found in TGA-open coronaries, Ross patients, and the healthy controls.

Table 13. Presence of visual perfusion defect assessed by qualitative myocardial perfusion analysis.

Group	Rest perfusion	Stress perfusion
TGA-coronary problems	5/13 (38.5%)	8/13 (61.5%)
TGA-open coronaries	0/36	0/36
Ross patients	0/12	0/12
BWG patients	1/7 (14.3%)	4/7 (57.1%)
KD patients	0/4	1/4 (25%)
Other patients	1/5 (10%)	2/5 (40%)

The presence of perfusion defects was not significantly higher during stress compared to rest ($p > 0.05$). However, the frequency of perfusion defects is significantly different between subgroups at rest and stress (rest, $p < 0.001$; stress, $p = 0.003$; Chi-square tests).

The results of absolute quantification of myocardial perfusion are presented in Table 14. At rest, MBF was not different between each subgroup and healthy controls (Figure 18). However, MBF at stress was significantly reduced in the 2 subgroups of TGA patients compared with the controls (TGA-coronary problems: 1.94 ± 0.58 vs. 3.71 ± 1.25, $p < 0.001$; TGA-open coronaries: 2.57 ± 0.71 vs. 3.71 ± 1.25, $p < 0.001$), (Figure 19-20). MPR was significantly reduced in both subgroups of TGA patients in comparison to the healthy controls (TGA-coronary problems: 2.2 ± 0.8 vs. 4.1 ± 1.3; $p < 0.001$; TGA-open coronaries: 3.22 ± 1.06 vs. 4.13 ± 1.27; $p = 0.02$), (Figure 21-22). MBF at stress (1.94 ± 0.58 vs. 2.57 ± 0.71, $p = 0.014$) and MPR (2.2 ± 0.8 vs. 3.2 ± 1.1; $p = 0.023$) were significantly reduced in TGA-coronary problems compared to TGA-open coronaries.

In a TGA patient with coronary problem, we found an aberrant LCA in this patient by using CMR. Myocardial perfusion CMR showed a region of perfusion defect in anteroseptal. The patient was treated by MIDCAP operation. Post-operation, the patient was repeated CMR exam and we did not found any region of perfusion defect in LV myocardial wall. In addition, semiquantitative analysis showed that SI in antero-septal segment increased post-operation as compared to previous exam (Figure 16).
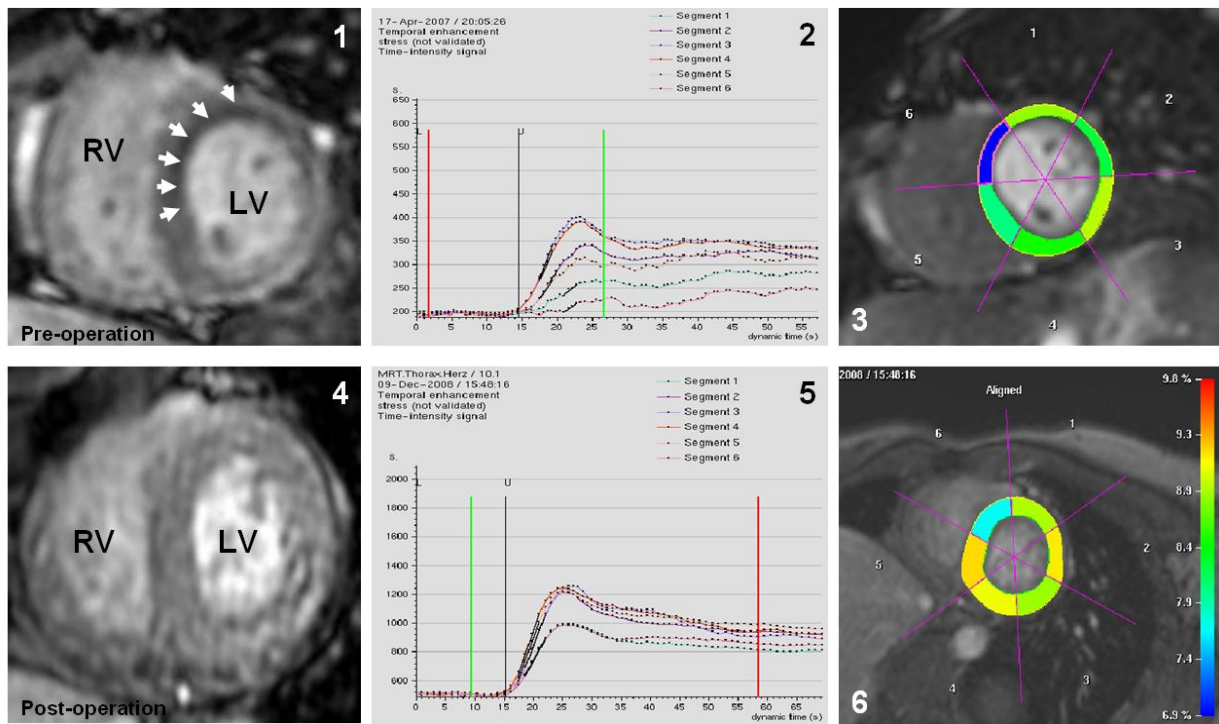
Figure 16. Visual analysis and semiquantitative analysis of myocardial perfusion CMR in a TGA patient with an aberrant of LCA. Pre-operation, visual analysis first-pass perfusion CMR showed a region of myocardial perfusion defect in anteroseptal (1), semiquantitative showed that SI was slightly increased after at peak of contrast agent in anteroseptal (2-3). Post-MIDCAP operation, qualitative analysis showed no regional myocardial ischemia in this area (4), and SI was significantly increased in this area (5-6).

We found that in Kawasaki patients, MBF at stress was impaired (2.49 ± 0.58 vs. controls 3.71 ± 1.25, p=0.013), but MPR was not significantly reduced (2.85 ± 1.27 vs. controls 4.1 ± 1.3, p=0.05). MBF at stress and MPR in subgroup 6 were not significantly reduced as compared to age matched controls (table 14).

In a patient with coronary fistula, CMR exams were performed pre-operation and 1.5 years after the operation. Pre-operation, MBF at stress (3.05 ml/g/min) and MPR (3.08 ml/g/min) reduced as compared to normal controls. Post-operation, quantitative analysis showed that MBF (3.50 ml/g/min) at stress and MPR (4.86 ml/g/min) increased.

In a patient with aberrant LCA, quantitative MBF analysis showed that MBF at stress (2.71 ml/g/min) and MPR (2.56 ml/g/min) impaired. Post-operation, quantitative analysis had demonstrated that MBF at stress and MPR increased post-operation (MBF: 3.11 ml/g/min, MPR: 4.00 ml/g/min) (Figure 17).
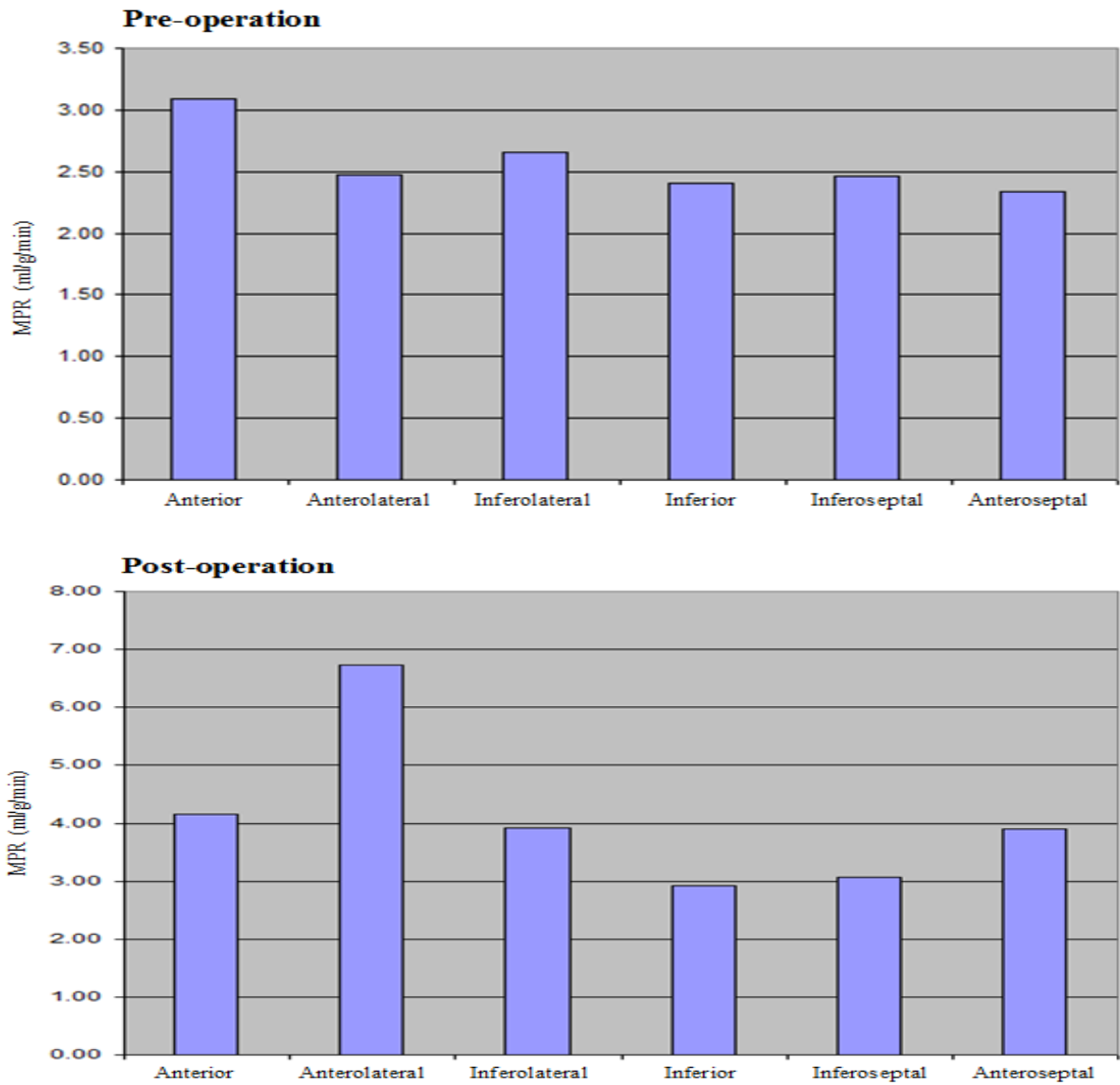
Figure 17. MPR values in each myocardial segment in a patient with aberrant LCA pre- and post - MIDCAP operation. MPR values increased post-operation in all myocardial segments.
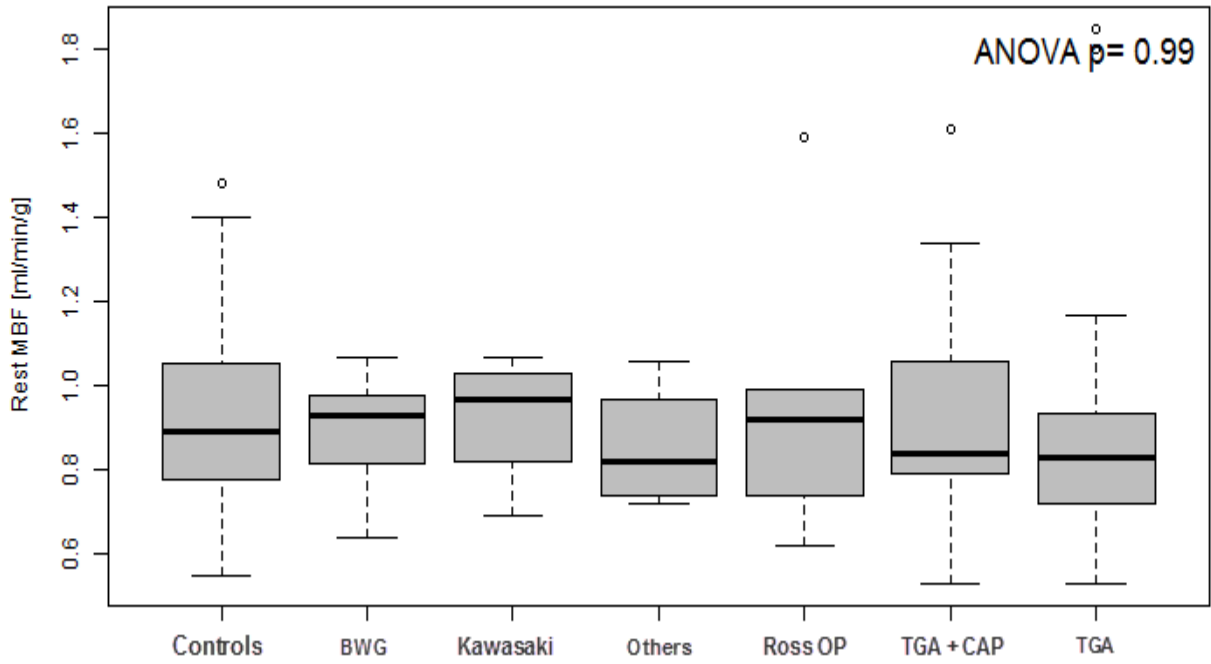
Figure 18. Comparison of mean MBF at rest between patients and controls.
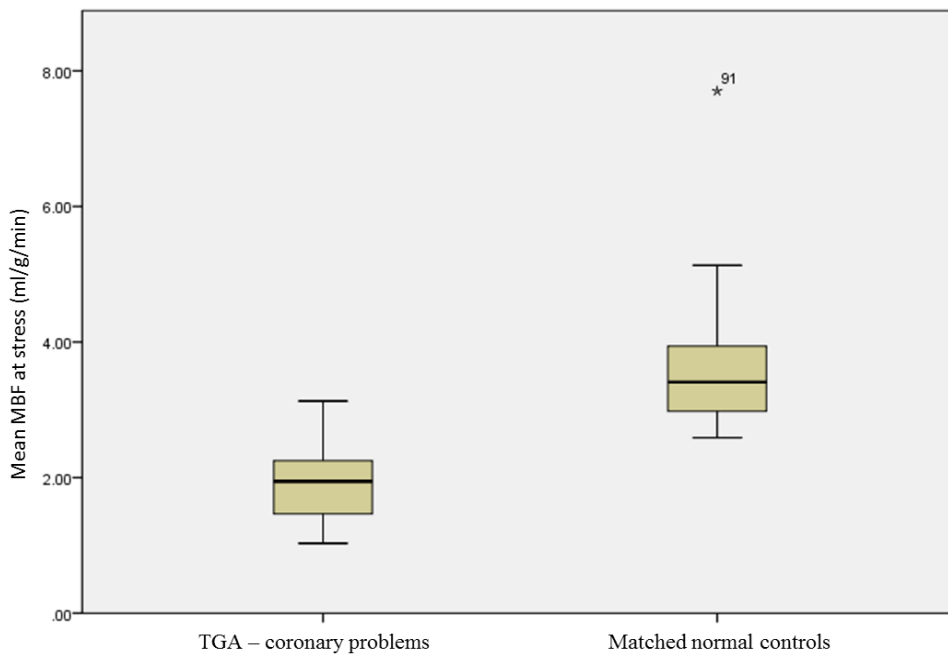
Figure 19. Comparison of mean MBF at stress between TGA – coronary problems and matched normal controls (p-value < 0.01; Mann-Whitney-U test).
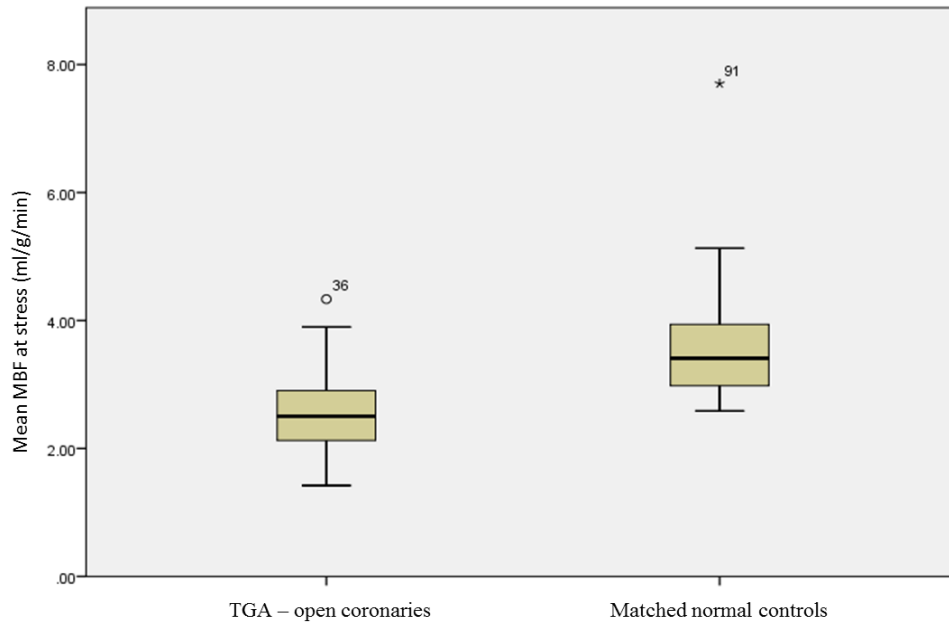
Figure 20. Comparison of mean MBF at stress between TGA – open coronaries and matched normal controls (p-value < 0.01; Mann-Whitney-U test).
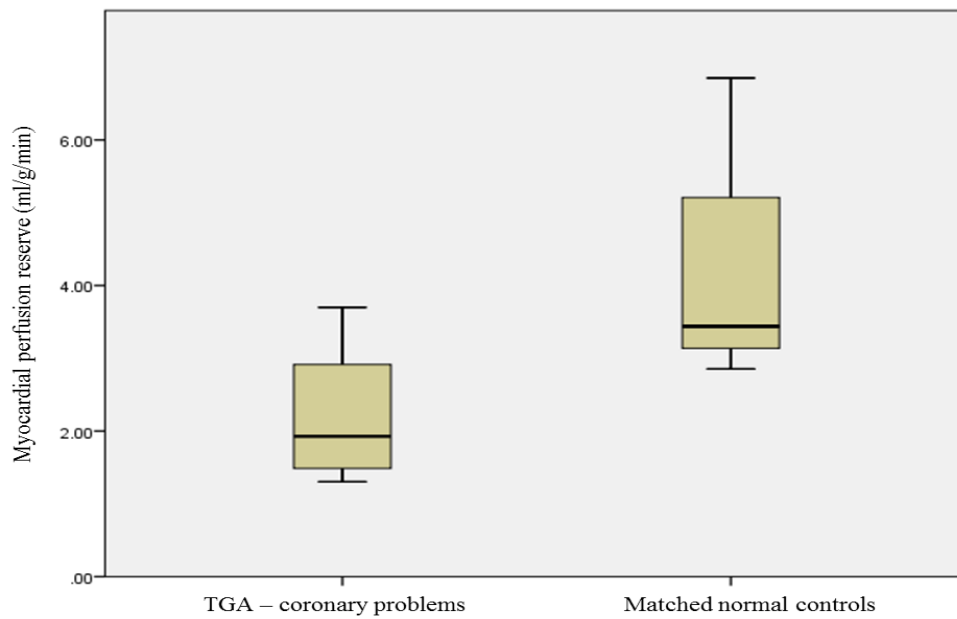
Figure 21. Mean MPR in TGA patients after ASO with coronary problems versus mean MPR in normal subjects (p-value = 0.0001; Mann-Whitney-U test).
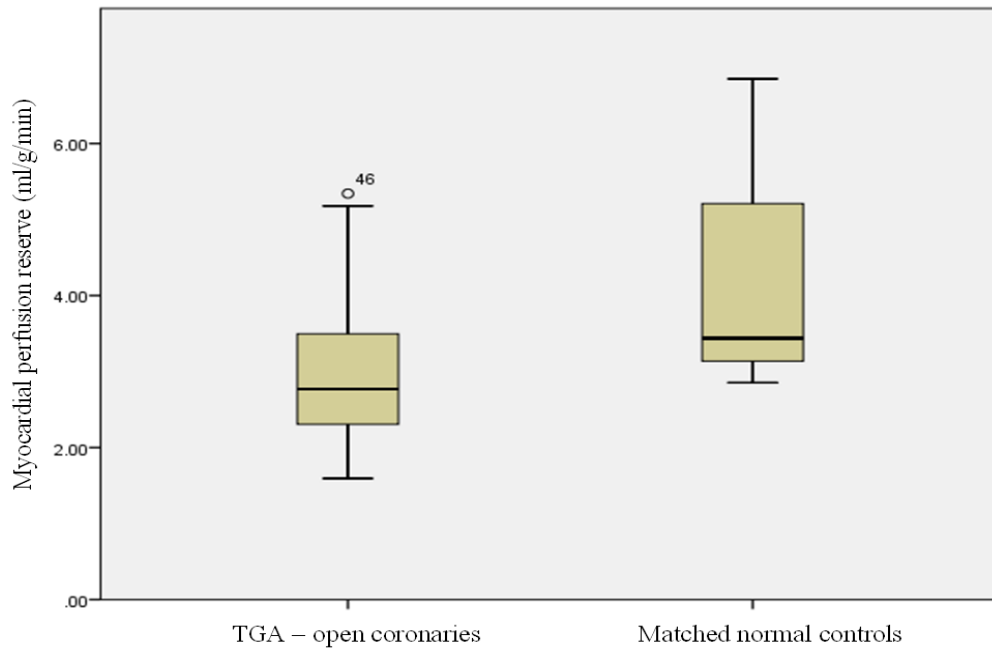
Figure 22. Mean MPR in TGA – open coronaries versus mean MPR in normal controls (p-value = 0.02; Mann-Whitney-U test).
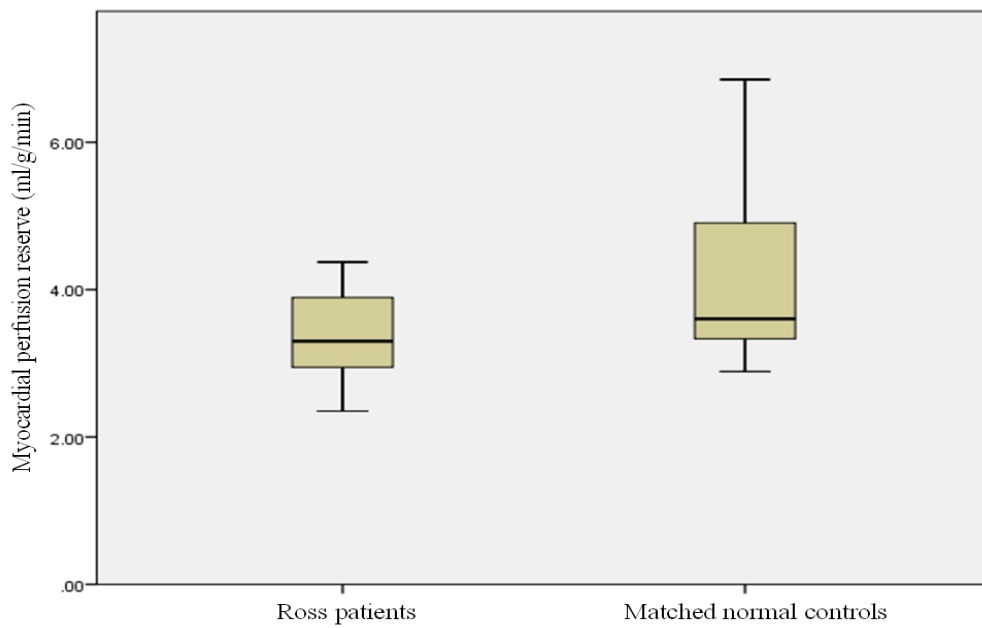
Figure 23. Mean MPR in Ross patients versus mean MPR in matched normal controls (p-value = 0.6; Mann-Whitney-U test).

Table 14. Absolute quantification of myocardial perfusion.

Patients		Controls	Mean MBF at rest			Mean MBF at stress			Mean MPR		
Subgroups	N	N	Patients	Controls	p	Patients	Controls	p	Patients	Controls	p
TGA-coronary problems	13	17	0.93 ± 0.29	0.93 ± 0.22	0.61	2.02 ± 0.53	3.70 ± 1.25	<0.01	2.28 ± 0.83	4.07 ± 1.23	<0.01
TGA-open coronaries	36	17	0.88 ± 0.28	0.93 ± 0.22	0.54	2.57 ± 0.71	3.70 ± 1.25	<0.01	3.04 ± 1.06	4.07 ± 1.23	0.02
Ross patients	5	15	0.97 ± 0.37	0.93 ± 0.28	0.88	3.41 ± 0.76	3.79 ± 1.48	0.86	3.39 ± 0.91	4.15 ± 1.16	0.60
BWG patients	7	17	0.89 ± 0.15	0.93 ± 0.22	0.82	2.75 ± 0.86	3.70 ± 1.25	0.08	3.20 ± 1.17	4.07 ± 1.23	0.22
KD patients	4	17	0.93 ± 0.16	0.93 ± 0.22	0.96	2.49 ± 0.58	3.70 ± 1.25	0.01	2.85 ± 1.27	4.07 ± 1.23	<0.05
Other patients	4	17	0.86 ± 0.15	0.93 ± 0.22	0.47	2.46 ± 0.83	3.70 ± 1.25	0.18	2.96 ± 1.28	4.07 ± 1.23	0.08

Values are mean ± SD; p-values are from the Mann-Whitney-U test for patient group against controls. MPR: myocardial perfusion reserve. Data were compared to matched normal control groups.

3.2.3 Late Gadolinium Enhancement

LGE was performed in 24 cases (43.6% of all patients). LV scar was observed in 11 of 55 patients (20%) with a mean volume 5.1 ± 4.7 cm^3. We found LGE in 4 cases (30.8%) in TGA-coronary problems; 1 case (9.1%) in Ross patients; 5 cases (71.4%) with BWG (Figure 24); 1 case (20%) in subgroup of other patients. There was no scar in TGA-open coronaries, KD patients, and normal subjects. RV scar was not found in all patients.
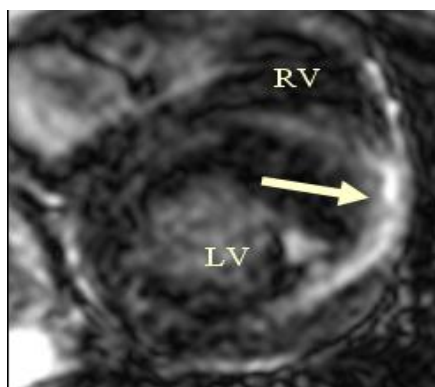
Figure 24. LGE was identified anterior, anterolateral, and anteroseptal in the LV in a BWG patient. LV: left ventricle; RV: Right ventricle.

3.2.4 T1 Mapping

Look-Locker T1 imaging was performed in 37 of 77 patients (TGA – coronary problems, n=4; TGA – open coronaries, n=29; Ross patients, n=4). The results were compared to matched normal controls (n=10). T1 mapping showed increased extracellular matrix expansion suggestive of diffuse fibrosis in TGA – coronary problems (0.3 ± 0.03 vs. 0.26 ± 0.02, p=0.014), TGA – open coronaries (0.31 ± 0.07 vs. 0.26 ± 0.02, p=0.028), and Ross patients (0.3 ± 0.002 vs. 0.26 ± 0.02, p=0.017) as compared to matched normal subjects. We did not find any correlation between mean ECV in each subgroups and LVEF, ESV index and EDV index, respectively (Spearman's rho).
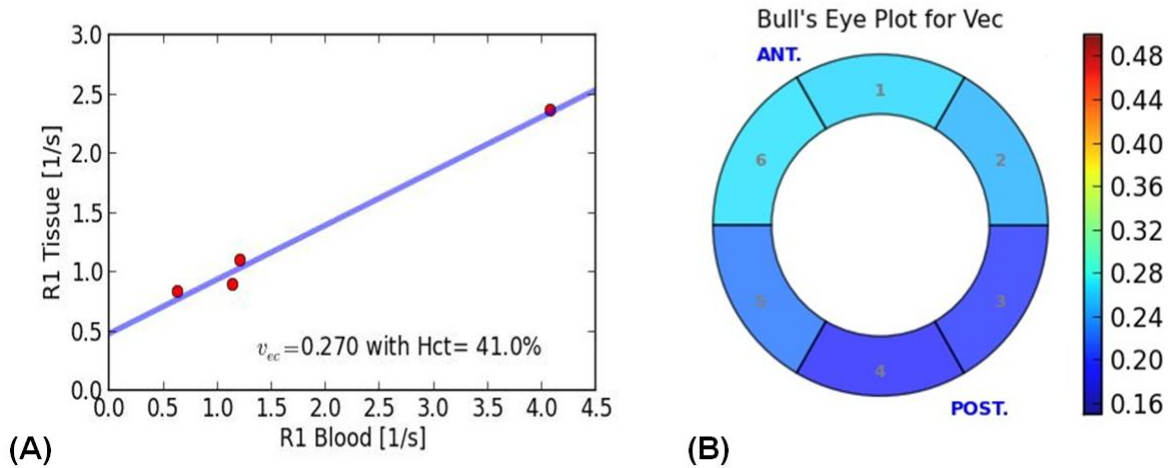
Figure 25. An example of T1 measurement in a patient after Ross operation. (A) Derivation of the partition coefficient by calculating the slope of the linear relationship between R1 for myocardium versus R1 for the blood pool from all R1 measurements. (B) Bull's eye maps for the ECV results in each myocardial wall segment.
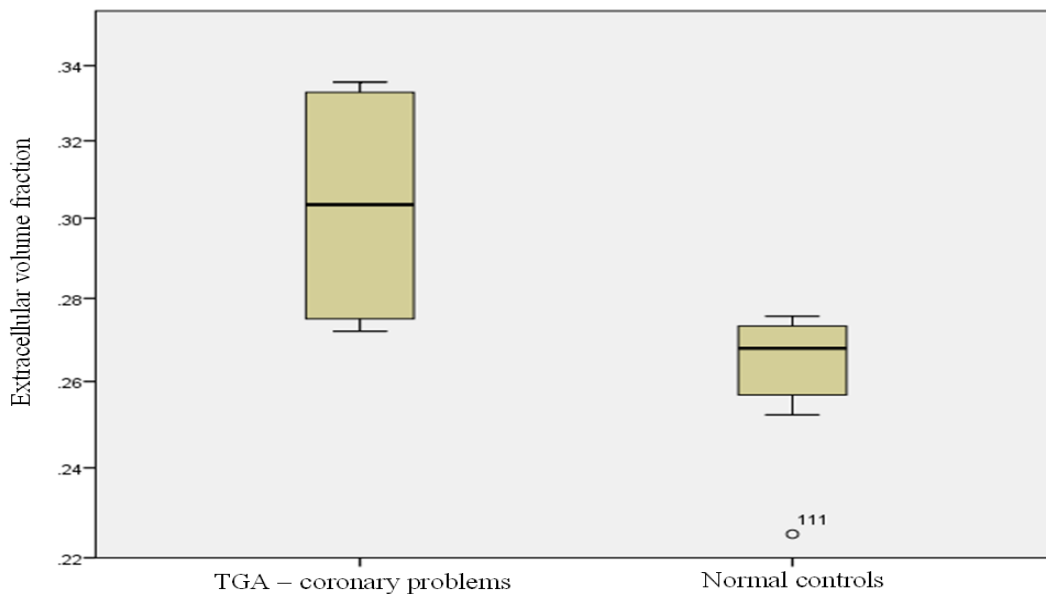
Figure 26. Comparison of mean extracellular volume fraction (ECV) between TGA-coronary problems and matched normal controls. Mean ECV increased in patients as compared to controls ($p=0.014$); (Mann-Whitney-U test).
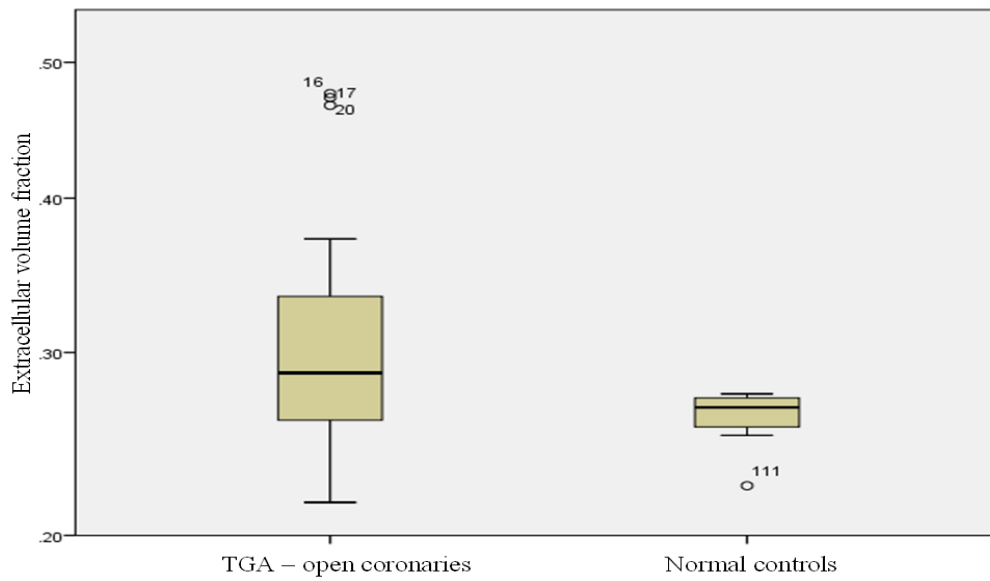
Figure 27. Comparison of mean extracellular volume fraction (ECV) between TGA-open coronaries and matched normal controls. Mean ECV increased in patients as compared to controls (p=0.028); (Mann-Whitney-U test).
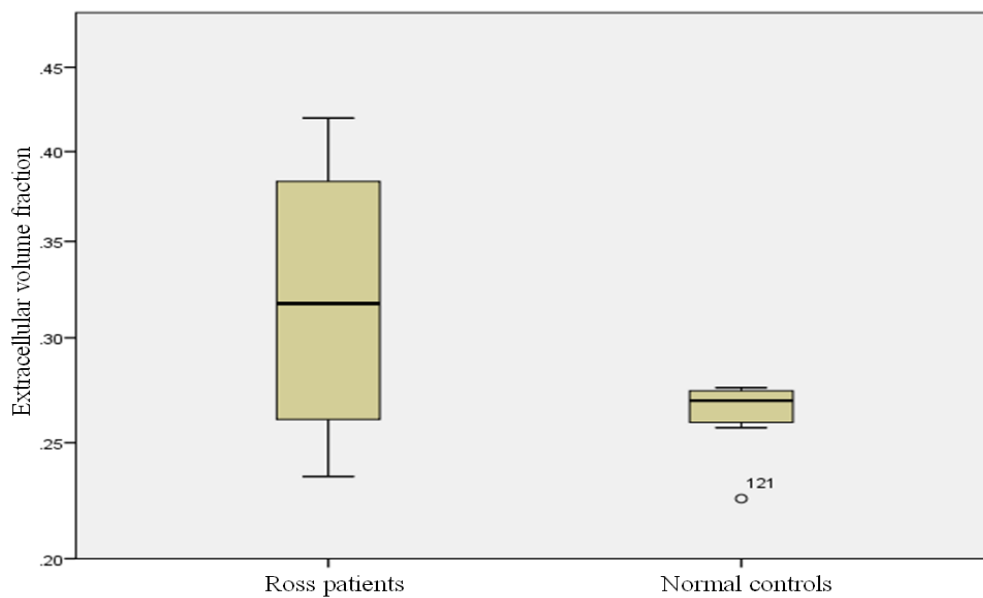
Figure 28. Comparison of mean extracellular volume fraction (ECV) between Ross patients and matched normal controls. Mean ECV increased in patients as compared to controls (p=0.017); (Mann-Whitney-U test).

3.2.5 Aortic Function in TGA Patients after One-Stage ASO

44 TGA patients with one-stage ASO and 34 healthy controls participated in this study to evaluate aortic function. The patient characteristics were summarized in table 3. There were not different in age, weight, height, BSA and blood pressure between patients and normal controls. Phase-contrast cine imaging for assessment of PWV and aortic regurgitation (AR) was applied in 44 patients and 30 controls. PWV assessment was not possible in 11 patients, and AR could not be measured in 7 patients because of susceptibility artefacts from surgical implants or sedation problems. In all other patients image quality was considered good or excellent.

❖ **Aortic Distensibility**

Distensibility of the aortic root, ascending aorta, and descending aorta at the isthmus were significantly lower in TGA patients as compared to normal subjects (Table 16). However, wall distensibility of the descending aorta at the level of the diaphragm was not significantly different from the normal controls. We did not find a significant association of aortic stiffness and myocardial perfusion reserve (Spearman's rho test).

❖ **Aortic Pulse Wave Velocity**

Aortic pulse wave velocity data of patients and normal subjects was summarized in table 16. PWV in all TGA patients was not significant different from the normal controls (patients, 4.2 ± 1.9 vs. controls, 3.3 ± 0.5; $p = 0.08$). In addition, PWV was not increased in children after one-stage ASO (patients, 4.18 ± 2.13; controls, 3.21 ± 0.48; $p = 0.43$), but adult patients who underwent one-stage ASO had a significantly higher PWV than controls (patients, 4.51 ± 1.10; controls, 3.39 ± 0.64; $p = 0.03$).

❖ **LA Volume and LV Function**

LA volume and LVEF, LVESD, LVEDV in TGA patients were not significantly different from the normal controls. However, LV-mass was significantly increased in TGA patients as compared to healthy subjects ($p = 0.02$) (table 15).

❖ **Aortic Regurgitation** (AR) values in patients and normal subjects were presented in Table 15. Mean AR value in patients was significantly higher than normal controls ($p<0.01$).
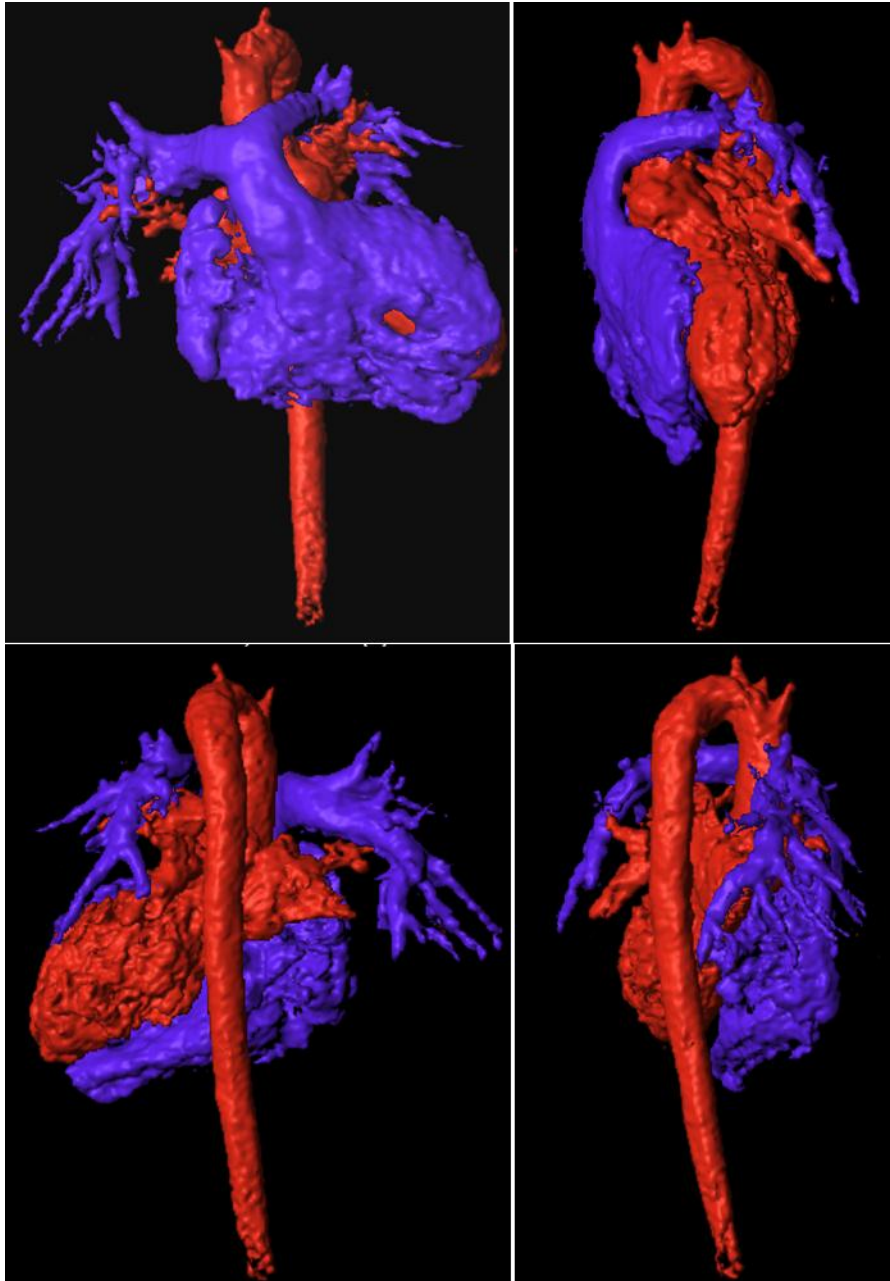
Figure 29. Three-dimensional volume rendered gadolinium-enhanced MR-angiography in a patient with TGA showing the bifurcation of the pulmonary arteries in front of the aorta after ASO with Lecompte procedure. Note the steep course of the aortic arch.

Table 15. Comparison of CMR measurements in TGA patients and controls

Variable	Patients (N=44)	Controls (N=34)	p Value
Maximal aortic area (mm²/m)			
Aortic root	648.7 ± 261.5	356.8 ± 113.4	<0.01
Ascending aorta	331.0 ± 140.0	315.4 ± 89.3	0.99
Descending aorta at the isthmus	179.1 ± 92.1	153.9 ± 36.7	0.35
Descending aorta at the level of the diaphragm	142.1 ± 59.9	129.0 ± 32.1	0.42
AR percentage (%, range)	6.0 (0.3-44.5)	0.6 (0 - 3.8)	<0.01
LVEF (%)	61.5 ± 8.7	60.1 ± 5.6	0.21
LVSV (ml/m)	44.6 ± 19.1	40.6 ± 11.2	0.47
LVEDV (ml/m)	75.2 ± 38.5	68.4 ± 20.8	0.95
LVESV (ml/m)	30.6 ± 21.5	29.5 ± 11.6	0.41
LV mass (g/m)	53.9 ± 22.2	42.7 ± 14.4	<0.05
LA Vol$_{max}$ (g/m)	39.1 ± 22.4	39.4 ± 13.8	0.38
LA Vol$_{min}$ (g/m)	20.1 ± 12.3	17.8 ± 6.7	0.71
LA Vol$_{ac}$ (g/m)	27.5± 16.7	23.4 ± 9.0	0.76
Distensibility (10^{-3} mmHg^{-1})			
Aortic root	4.1 ± 2.3	9.1 ± 4.7	<0.01
Ascending aorta	5.1 ± 2.9	10.8 ± 5.5	<0.01
Descending aorta at the isthmus	7.1 ± 3.3	9.1 ± 5.1	<0.02
Descending aorta at the level of the diaphragm	9.1 ± 4.5	9.9 ± 4.9	0.28
PWV (m/s)	4.2 ± 1.9	3.3 ± 0.5	0.08

Data are presented as mean ± SD or median and range. P-Values are from the Mann-Whitney-U test. AR, aortic regurgitation; LVEF, left ventricular ejection fraction; LVSV, left ventricular stroke volume; LVEDV, left ventricular end-diastolic volume; LVESV, left ventricular end-systolic volume; LA Vol$_{max}$, maximal left atrial volume; LA Vol$_{min}$, minimal left atrial volume; LA Vol$_{ac}$, left atrial volume just before atrial contraction; PWV, pulse wave velocity.

4. DISCUSSION

In children, myocardial ischemia may occur during childhood in several conditions, such as after surgery for CHD involving the coronary artery, in congenital coronary abnormalities and after surgery for treatment, and in patients with inflammatory disease of the coronary arteries such as Kawasaki disease (Angelini 2007; Hauser et al., 2001; Maiers & Hurwitz, 2008; Vogel et al., 1991; Daniels et al., 2012). Assessment of myocardial ischemia in these populations is important because adverse cardiac events may occur (Pasquali et al., 2002; Legendre et al., 2003; Raja et al., 2005; Hauser et al., 2001; Kazmierczak et al., 2013; Ramírez et al., 2011). We used CMR imaging as a non-invasive and radiation-free method for assessment of myocardial blood flow, viability, heart function, and diffuse myocardial fibrosis in such patients to evaluate ischemic heart disease.

4.1 Myocardial Perfusion

4.1.1 Myocardial Perfusion after Coronary Reimplantation in Patient after ASO and Ross Operation

Reimplantation of the coronary arteries is one of the most difficult procedures during ASO and Ross operation (Jatene 1976; Ross 1967). The ASO is a common surgical procedure for the anatomic repair of TGA, while the Ross procedure is a surgical method for replacement of aortic valve disease to avoid the use of long-term anticoagulation and to achieve the potential for autograft growth in children (Losay et al., 2001; Pasquali et al., 2002; Svensson et al., 2003). However, reimplantation of the coronary arteries into the aortic root is used for those operations. The major concern about mortality and long-term outcome after these operations mainly depend on the myocardial perfusion provided by the transferred coronary arteries. Reimplantation of the coronary arteries in ASO and Ross operation may have some effects on coronary blood flow (Bengel et al., 1998; Hutter et al., 2000; Hauser et al., 2001). We applied advanced CMR methods to assess myocardial perfusion in those patients. To our knowledge, this is the first study reports the use of CMR imaging approach to quantify of absolute myocardial perfusion in patients after ASO and Ross operation.

a) Myocardial Perfusion in TGA Patients after ASO

The successful of the ASO mainly depends on the coronary blood flow supplied by the transferred coronary arteries may result myocardial ischemia and infarction (Jatene et al., 1976). After the ASO, coronary artery obstruction in TGA patients was documented in the

literatures (Bonhoeffer et al., 1997). In our study subgroup, in TGA patients (n=13) after ASO had known or suspected coronary problems as occlusion, stenosis or hypoplasia (table 5), we found that regional ischemia presented in 8 patients (61.3%) by visual analysis. In addition, using quantification of absolute myocardial perfusion, MBF at stress and MPR were significantly impaired in TGA-coronary problems when compared to normal subjects. However, mean MBF value at rest was normal and it is remain unclear in the present study. Nevertheless, visual analysis and quantitative myocardial blood flow method by CMR demonstrated that regional ischemia was detected and coronary blood flow was significantly reduced in this group. The reasons of the reduction of coronary blood flow in TGA patients with coronary problems are clear in the study because coronary artery problems (Table 5) were presented in all patients. In addition, LGE was found in 30.1 % patients and coronary angiography data showed that coronary stenosis in 23.1% and occlusion in 76.9% in TGA-coronary problems. These findings may cause an impairment of coronary blood flow of TGA patients after the ASO in this group.

In TGA patients (n=36) after ASO with patent epicardial coronaries (TGA – open coronaries) were asymptomatic of myocardial ischemia. Visual analysis of myocardial perfusion CMR showed no region of perfusion defect and LGE in all patients. In addition, mean MBF value at rest is normal. However, mean MBF at stress and MPR values were significantly reduced as compared to healthy controls. Although coronary problems were not presented in this group, our data suggests that MBF is effected in these patients after ASO, possibly due to endothelial or smooth muscle dysfunction, both of which can impair vasodilation (Bartoloni et al., 2006). The face of the transferred coronary arteries after the ASO is at risk of dysfunction and it has been assessed in previous studies (Vogel et al., 1991; Tane et al., 1995; Manso et al., 2010). Our findings are similar to two previous studies in TGA patients after ASO by PET (Bengel et al., 1998; Hauser et al., 2001). By quantitative PET analysis, those studies showed that MBF was significantly reduced in TGA patients after ASO with asymptomatic with myocardial ischemia. Therefore, by quantification of MBF by CMR, our data proved that coronary blood flow was affected after reimplantation of the coronary artery in TGA patients after ASO. In addition, the results of the present study suggest that quantification of myocardial perfusion by CMR is important for early diagnosis of impairment of coronary blood flow in the follow-up of TGA patients after ASO, because all TGA patients in this subgroup showed no symptoms of myocardial ischemia, and visual analysis showed no evidence of myocardial ischemia, independent of whether the TGA patients had coronary problems or not.

Although all patients in TGA-coronary problems had known coronary artery problems, mean MBF at rest was not different from the normal controls. The reason of normal mean MBF values at rest in TGA-coronary problems remains unclear in this study because in this group coronary problems were found in all patients, and 30.7 % patients were detected LGE.

In TGA-open coronaries, our results show that mean MBF at rest was not significantly lower normal subjects. That may be because myocardial ischemia was not severe in this group. In addition, we found that these patients were asymptomatic with myocardial ischemia. Furthermore, LGE was negative in all patients in TGA-open coronaries. However, mean MBF at stress and MPR are reduced in both TGA groups. These results demonstrate the important role of adenosine stress test, and the combination of both rest and stress techniques is important for the detection of myocardial ischemia in TGA patients after ASO. In addition, our finding shows that coronary blood flow is reduced not only in TGA patients that have known or suspected coronary problems but also in patients after ASO with patent epicardial coronaries. This study suggests that it is important to evaluate myocardial ischemia in patients after the ASO.

b) Myocardial Pefusion in Patients after Ross Procedure

In patients after Ross operation, visual analysis myocardial perfusion CMR showed region of perfusion defect in only 1 patient (8.3%). MBF at rest and stress, and MRP were not reduced as compared to normal controls. These results show that MBF is not impaired in patients after Ross operation. This finding is in accordance with quantitative myocardial perfusion by PET in patients (n=9) after Ross operation (Hauser et al., 2001). The Ross procedure is accepted as a surgical method for replacement of aortic valve disease to avoid the use of long-term anticoagulation and to achieve the potential for autograft growth in children and adult (Ross 1967). Reimplantation of the coronary arteries is used in this procedure and the adequacy of coronary artery perfusion is one of the major concerns post-operation (Ross 1967; Somerville et al., 1979). However, our findings show that coronary blood flow may not be affected after the Ross procedure in this study. The small number of patients (n=6) after Ross operation is the main limitation in the study. However, assessment of coronary blood flow is important in patients after reimplantation of the coronary arteries and this study represents the first application of this new approach of quantification of absolute myocardial perfusion by CMR as a non-invasive method in the follow-up in this population.

c) The Difference in Myocardial Blood Flow after Coronary Reimplantation in Patients after ASO and Ross Procedure.

Reimplantation of the coronary arteries was performed in both ASO and Ross operation in our study. However, our results show that stress MBF was reduced in TGA patients (TGA-open coronaries) after ASO but normal in the Ross subgroup. This finding is consistent with a previous study using quantification of MBF by PET in patients after ASO and Ross operation (Hauser et al., 2001). With quantitative MBF by PET, Hauser and colleagues measured absolute myocardial blood flow in patients after reimpalntation after ASO and Ross procedure. That study also found that MBF was impaired in TGA patients after ASO but not in patients after Ross operation. However, there are some factors that may effect to coronary blood flow in TGA patients after ASO. Because TGA is commonly associated with unusual coronary artery origins and courses (Martins & Castela, 2008; Sim et al., 1994). The ASO is the treatment of choice in neonates for anatomical correction in TGA (Jatene 1976). After coronary reimplantation in ASO, the growth of coronary artery anastomoses and their patency are the major concerns in this population. In our study, TGA patients were performed one stage ASO: 8.5 ± 5.7 days, two stages ASO: 1.3 ± 0.1 years. In addition, some authors showed that coronary artery obstructions were observed in TGA patients after ASO by using selective coronary angiography. Otherwise, the Ross operation was performed later (12.7 ± 5.5 years).

4.1.2 BWG

ALCAPA is a rare congenital coronary artery abnormality and is associated with early infant mortality and adult sudden death (Wesselhoeft et al., 1968). After surgical correction, BWG patients may at high risk of myocardial ischemia (Davis et al., 2001; Dodge-Khatami et al., 2002; Wesselhoeft et al., 1968). In this study, we describe the use of CMR for evaluation of myocardial perfusion in ALCAPA patients after anatomical surgery correction with suspected myocardial ischemia.

This is also the first study that describes the method of quantification of absolute myocardial perfusion in BWG patients using CMR imaging. Two previous studies reported the use of myocardial perfusion CMR at rest and stress with adenosine for detection of myocardial ischemia in ALCAPA patients (Secinaro et al., 2011; Buechel et al., 2009), and found the areas of perfusion defects in BWG patients by qualitative analysis. However, these studies did not carry out semi-quantitative and quantitative myocardial perfusion analysis, and did

not study controls, and they were the main limitations in the studies. In the present study, we further applied qualitative, semi-quantitative, and quantitative analysis of myocardial perfusion for evaluation of myocardial ischemia in BWG patients.
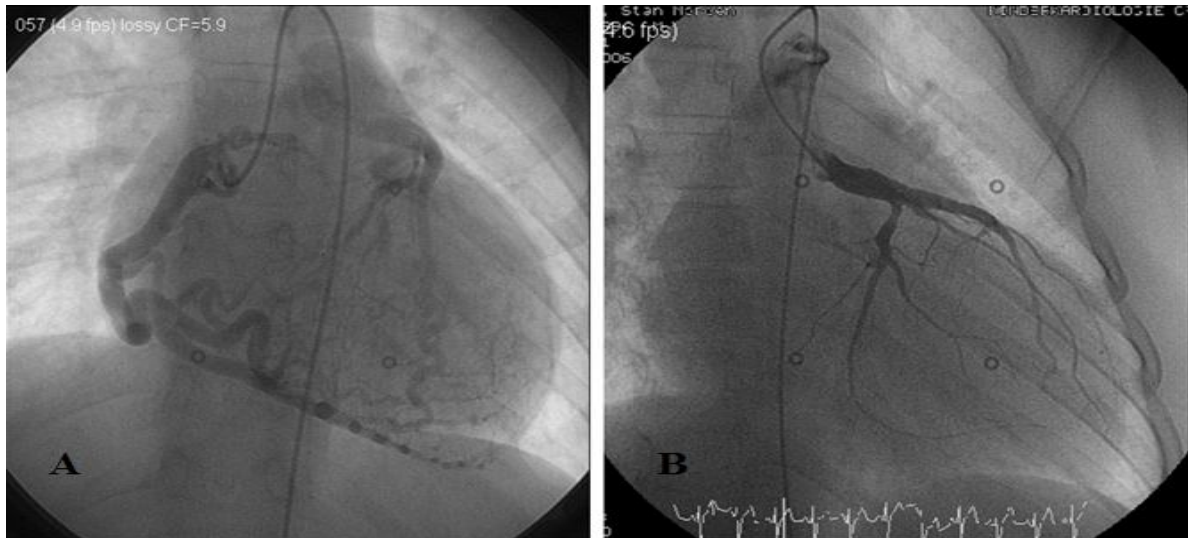
Figure 30. Pre- and post-operative coronary angiography, patient with ALCAPA. A: Pre-op injection into the dilated RCA and retrograde staining of the LCA and MPA. B: Post-Op injection into the LCA from the left coronary sinus.

In BWG patients (n=7), our results showed that areas with perfusion defect were present in 4 patients (57.1%). LGE presented in 5 of 7 patients (71.4) and in a patient LCA was noted slightly stenosis by coronary angiography. These finding may suggest a severe myocardial ischemia in this group. However, our data showed that mean MBF at rest and stress, and mean MPR were not significantly lower normal controls. This remains unclear in the study. However, the number of BWG patients in this study was small, because it is rare congenital coronary abnormally (Bland et al., 1933). Coronary blood flow was not significantly reduced in this group as compared to normal controls may be due to the development of coronary collateral circulation (Figure 30) before operation and therefore in some BWG patients who were diagnosed in adulthood without any myocardial ischemia symptoms as previous descriptions (Dodge-Khatami et al., 2002; Wesselhoeft et al., 1968). This may also explain that some patients are asymptomatic. In short, we described the application of CMR in evaluation of myocardial perfusion in BWG patients. Importantly, we first applied the method of quantification of myocardial blood flow by CMR imaging and found that it is a useful method to detect myocardial ischemia in this population.

4.1.3 Kawasaki Disease

KD is one of the most common acquired heart diseases in children in the developed countries. Coronary artery aneurysms and stenosis may develop long-term during childhood in KD (Tanaka et al., 1986). They are major complications that may lead to myocardial ischemia and adverse cardiac events in KD (Dajani et al., 1993). Myocardial perfusion CMR has demonstrated to be a useful method for detection of myocardial ischemia in KD (Tacke et al., 2011). However, previous studies showed regions of myocardial perfusion defects by visual analysis, and have limitation in quantification of absolute myocardial perfusion by CMR (Prakash et al., 2004; Mavrogeni et al., 2006; Tacke et al., 2011). In the present study, we first applied the method to assess absolute myocardial perfusion by CMR and detect myocardial ischemia during follow-up in children with a history of KD.

A previous study of patients with KD (n=10) showed that mean MBF at rest was normal and however, mean MBF at stress and flow reserve were significantly lower than normal controls by using PET (Muzik et al., 1996). Because patients who have KD during childhood may develop long-term coronary aneurysm and subsequent coronary artery stenosis, and may lead to chronic myocardial ischemia or infarction (Neuburger et al., 2005; Tanaka., 1986). In the present study, similar to the findings by Muzik and colleagues (Muzik et al., 1996), we also found a normal mean MBF value at rest, and reduced mean MBF at stress and MPR by using CMR technique. Our data show that only 1 patient presented region of perfusion defect in antero- and inferoseptal at rest by visual analysis, while visual analysis at rest was normal in all patients. In addition, X-ray coronary angiography data reported that coronary artery stenosis was not present in all KD patients, and a small area of coronary aneurysm was shown in a patient.

These findings suggest that CMR can be used to detected myocardial ischemia in the follow-up KD patients. However, the limitation of our study is a small sample size (n=4) of patients with Kawasaki disease. Nevertheless, we could show that CMR is a useful method to quantify absolute myocardial perfusion in patients with a history of KD.

4.1.4 Other Patients

First-pass perfusion CMR was also used to detect myocardial perfusion in patients with suspected myocardial ischemia, such as patients after heart transplantation, one patient with a coronary artery fistula, and one patient with an aberrant LCA.

Coronary fistula is rare congenital coronary abnormalities (Krause 1865). Assessment of myocardial ischemia is important in this population because adverse cardiac events can occur before and after surgical treatment (Valente et al., 2010; Canga et al., 2012). In this study, we first described an application of CMR to quantify myocardial blood flow in a patient with coronary fistula pre- and post-operation. This patient was asymptomatic with myocardial ischemia. CMR exam pre-operation, visual analysis showed region of myocardial perfusion defect in lateral wall of the LV. CMR exam was repeated after 1.5 years post-operation and showed no regional ischemia by visual analysis. In addition, quantitative analysis showed that MBF at stress and MPR increased post operation. We found that CMR can be used as a good method to evaluate the result of the surgical treatment in patient with coronary fistula. Although the small sample size of coronary fistula patient is the limitation in this study. However, our data shows the advantage of CMR for evaluation of myocardial ischemia in patients with coronary fistula.

Cardiac allograft vasculopathy is the major cause of death in patients after heart transplantation and remains to limit the long-term success of this operation (Kaye et al., 1993). A previous study used CMR for quantitative myocardial perfusion in patients after heart transplantation and showed that MPR reduced in patients after heart transplantation (Muehling et al., 2003). In our study, two other patients in this subgroup after heart transplantation had no clinical symptoms of myocardial ischemia. Visual analysis showed no regional myocardial ischemia. However, MBF at stress and MPR were reduced in these patients as compared to normal controls. These results are conformity with previous findings by Muehling and colleagues (Muehling et al., 2003). This is the second study that described quantification method of myocardial perfusion by using CMR. The number of patients after heart transplantation is small in this study as compared to the previous study. However, our findings provide data about using CMR to quantify myocardial perfusion in combination with evaluation of LV function, and LGE in patients after heart transplantation.

An aberrant LCA is a rare congenital coronary artery anomaly that may lead to myocardial ischemia (Tuo et al., 2012; Yamanaka & Hobbs, 1990). After surgical treatment myocardial ischemia and sudden death can occur due to development of stenosis or closure of LCA (Krasuski et al., 2011). In this study, we first describe the use of CMR for detection of myocardial ischemia in a patient with diagnosis of aberrant LCA. This patient had symptom of chest pain with suspected myocardial ischemia. We found an abnormal coronary artery anatomy in this patient (aberrant LCA) and the patient was indicated to use beta-blocker and

ASS. CMR exam showed that region of perfusion defect presented in antero-septal. Quantitative MBF analysis showed that MBF at stress (2.71 ml/g/min) and MPR (2.56 ml/g/min) impaired. The patient was performed MIDCAP operation for anatomical correction of the coronary artery. Post-operation, visual analysis showed no region of perfusion defect. Quantitative analysis had demonstrated that MBF at stress and MPR increased post-operation (Figure 17). In addition, this result corresponds with clinical status after the surgery, the patient was asymptomatic with myocardial ischemia and therefore, Beta-blocker was excluded from the medication. In short, our study shows the advantage of using CMR for detection of myocardial ischemia in patients with aberrant LCA and in the long-term follow-up these patients after surgical treatment. We report the first experience of quantitative myocardial perfusion analysis in a patient with aberrant LCA.

The small sample size of patients in this group is a limitation of our study. However, most of them are rare congenital coronary abnormalities. Nevertheless, we could show that CMR is a useful method to quantify absolute myocardial perfusion in patients with abnormal coronary artery and in patients after heart transplantation.

4.1.5 The Importance of Absolute Quantification of Myocardial Perfusion by CMR

The assessment of myocardial perfusion by CMR is widely applied for the evaluation of myocardial ischemia in clinical practice as a non-invasive method (Coelho-Filho et al., 2013). Visual analysis of myocardial perfusion can show perfusion defects in patients with myocardial ischemia. This method is routinely used in clinical practice for detection of myocardial ischemia (Schwitter et al., 2011; Ntsinjana et al., 2011). But, visual analysis can not exclude myocardial ischemia (Nandalur et al., 2007). Therefore, a method to quantify absolute myocardial perfusion is important for a more precise diagnosis of myocardial ischemia. Previous studies showed the role of absolute quantification of MBF by CMR, SPECT, and PET in cardiac disease (Morton et al., 2012; Hauser et al., 2001; Muzik et al., 1996). However, PET and SPECT are limited in pediatric patients due to the use of ionizing radiation. Therefore, quantification of MBF by CMR is a promising approach for the evaluation of ischemic heart disease in children (Morton et al., 2012; Gupta et al., 2011; Jerosch-Herold 2010), but is not applied as a routine method in clinical practice so far. To our knowledge, this is the first study which used quantification of absolute myocardial perfusion in congenital and acquired heart disease in pediatric patients by CMR. Our data

shows that quantification of myocardial perfusion can detect reduced myocardial perfusion in patients with no visual perfusion defects and can improve diagnostic accuracy in patients with presented perfusion defects.

4.2 Late Gadolinium Enhancement

LGE imaging by CMR was developed by Kim and Judd in 1996 (Kim & Judd., 1996). Since then LGE has been applied for detection of myocardial fibrosis or scar tissue in heart diseases. However, LGE technique has been widely applied in adult cardiology (Beek et al., 2003; Bruder et al., 2009) and there were not many studies in children (Babu-Narayan 2010). Previous studies demonstrated the feasibility of the combination of CMR perfusion imaging and LGE for detection MF with the role of Gd in congenital and acquired heart disease (Prakash et al., 2004; Valsangiacomo Buechel et al., 2009; Tacke et al., 2011; Secinaro et al., 2011). In the present study, we applied LGE technique to detect MF in patients with congenital and acquired heart disease.

In patients after ASO with coronary problems, LV scar was detected in 30.8 % patients. Therefore, we also found that MBF at stress and MPR were impaired in this group. Coronary problems may be the reason of presented LGE after ASO. However, in TGA-open coronaries LGE was not presented in all patients. A previous study has described the use of LGE CMR to detect MF in patients after ASO (Buechel et al., 2009). However, there was no area of MF that was detected in that study.

Previous study showed that LGE CMR can be used to observe myocardial fibrosis in BWG patients (Buechel et al., 2009). In the present study, we found that LV scar presented in 5 BWG patients (71.4%). This result is similar to a previous finding by Secinaro and colleagues (Secinaro et al., 2011). However, in our study, we further quantified the extent of hyperenhancement in percentage or volume for each myocardial segment.

4.3 CMR for Assessment Myocardial Fibrosis

Myocardial fibrosis (MF) is characterized by an increase of collagen composition and is one of the most common histological features of cardiac failure (Schaper et al., 1992). It leads to impaired diastolic and systolic functions and is related to major adverse cardiac events (Bello et al., 2003; Kwong et al., 2008). Endomyocardial biopsy is the gold standard to evaluate MF in different cardiac diseases. However, it is an invasive procedure with higher and prone to sampling error (Holzmann et al., 2008; Becker et al., 1991). A non-invasive

approach, such as LGE imaging with CMR has become the method of choice to detect MF in children (Mavrogeni et al., 2006; Prakash et al., 2004; Buechel et al., 2009). The visualization of focal MF, due to myocardial infarction, can be accurately identified in clinical practice by LGE CMR imaging (Kim et al., 1999; Wagner et al., 2003). However, LGE imaging has limitations to detect diffuse and generalized MF (Mewton et al., 2011). Therefore, Messroghli and colleagues firstly described Modified Look and Locker Inversion-recovery (MOLLI) sequence in 2004 (Messroghli et al., 2004). Since then, studies demonstrated that T1 mapping CMR can be used to assess DMF by quantification of myocardial ECV as a non-invasive and radiation-free method in animal and human (Broberg et al., 2010; Messroghli et al., 2011; Sado et al., 2012). However, this method has been not widely applied in clinical practice. In this study we used a Look-Locker sequence for T1 mapping, in addition to LGE imaging, to measure also DMF in patients after ASO and Ross operations, and in normal subjects.

In TGA patients after ASO, our results showed that mean myocardial ECV values are increased in TGA patients with coronary problems (table 5) and in patients after ASO with patent epicardial coronaries, compared to normal controls. Only one previous CMR study had described DMF in TGA patients and found that an abnormal fibrosis index was present in 10 of 11 TGA patients (Broberg et al., 2010). However, all TGA patients in this study were patients with a systemic RV. In addition, there was a correlation between EDV index and fibrosis index. This study demonstrates that CMR imaging method can be used to quantify DMF in different forms of CHD. Our data indicate that DMF increases in patients after ASO in TGA-coronary problems and TGA-open coronaries. However, there was no relationship between DMF, and LVEF, EDV index, and ESV index, respectively.

In patients after Ross operation, mean myocardial ECV increased compared to normal subjects. To the best of our knowledge, this is the first study that used CMR technique to detect myocardial diffuse fibrosis in this population. A previous study demonstrated that DMF is related to LV function and commonly related to diastolic and systolic function (Conrad et al., 1995). However, our data can not demonstrate correlations between myocardial fibrosis index and LV function in patients after Ross operation. The main limitation of our study was a small number of Ross patients (4 of 12 patients) and it is difficult to detect correlations. However, our study shows that CMR imaging can be used to detect DMF in patients after Ross procedure as a non-invasive diagnostic imaging tool.

4.4 Left Ventricular Function

CMR imaging is considered as the most accurate diagnostic imaging approach for the assessment of ventricular volumes and function in heart diseases (Lorenz et al., 1999; Sechtem et al., 1987). In the present study, using CMR imaging method we found that mean LV-EF values were normal in TGA-coronary problems, TGA-open coronaries, in KD patients, and were significantly reduced in patients after Ross procedure and BWG patients.

Pulmonary autograft replacement of the aortic valve is used in the Ross operation with potential for annulus growth, and it is therefore the technique of choice to treat aortic valve disease for children and young adults (Turrentine et al., 2001; Ross 1967). The function of the aortic root replacement is a major concern after the operation and it has been assessed in previous studies (Grotenhuis et al., 2006; Puranik et al., 2009; Goda et al., 2012). Dilatation of the pulmonary autograft and aortic valve insufficiency are main complications after the Ross procedure and they have been demonstrated their effect on the LV function (Grotenhuis et al. 2006). By using CMR, Grotenhuis and colleagues showed that dilation and decreased distensibility of the aortic root, and aortic insufficiency lead to impair systolic function. Decreased LV-EF was correlated with dilation and impaired distensibility of the aortic root, and aortic regurgitation (AR) fraction, and the AR fraction was significantly correlated with increased LV-EDV index (Grotenhuis et al., 2006). In our patients after Ross operation, mean LV-EF is significantly reduced compared to healthy controls. LV-EF values are lower 50% in 4 patients. In addition, aortic insufficiency presents in 7 of 12 patients (AR fraction, 20.4 ±11.7 %). Our findings are in accordance with the previous study by Grotenhuis et al. (Grotenhuis et al., 2006). The impairment of LV-EF may be caused by dilation and decreased distensibility of the aortic root, and AR. However, lack of the data to evaluate the function of the aortic root and LV- EDV volume in this group is the main limitation in this study.

In BWG patients, mean LV-EF was significantly impaired compared to normal controls, and LV-EF values were lower than 50% in 5 patients (71.4%). Our results are different from a previous study by Secinaro et al. They also used CMR, and showed that the mean LV function was normal in six ALCAPA patients (Secinaro et al., 2011). Our results might be explained by the presence of LGE in 5 patients (71.4 %). An increase in MF has been demonstrated that may lead to LV systolic and diastolic dysfunction (Villari et al., 1993; St John Sutton et al., 1980).

In TGA patients after ASO, our findings show that mean EV-EF is normal in both subgroups of TGA after ASO. However, in TGA-coronary problems we found that LV-EF was reduced below 50% in 4/13 (30.8 %) patients in this group. In addition, our data showed that 3/4 of these patients presented with LGE in the LV and this may be a cause of impaired LV-EF in these patients (Villari et al., 1993; St John Sutton et al., 1980).

4.5 Comparison of CMR with Other Diagnostic Imaging Techniques

CMR imaging has emerged as a non-invasive and radiation-free diagnostic imaging modality for evaluation of ischemic heart disease in children (Buechel et al., 2009). Although ECG can be used for diagnose of myocardial ischemia, but a normal ECG result does not exclude ischemic heart disease. In addition, exercise ECG has some limitations for the evaluation myocardial ischemia in pediatric patients (Rhodes et al., 2000). X-ray coronary angiography is known as a gold standard for detection of ischemic heart disease (Scanlon et al., 1999). However, it is an invasive method and imposes a radiation burden.

Most of the noninvasive imaging methods can be used to evaluate myocardial ischemia, such as SPECT, PET, and CMR. Previous studies demonstrated the abilities of SPECT, PET, and CMR in the detection of ischemic heart disease (Rickers et al., 2000; Hernandez-Pampaloni et al., 2003; Puranik et al., 2010; Jaarsma et al., 2012). However, compared to SPECT and PET, the main advantages of CMR are the use of non-ionizing radiation and high spatial resolution (Jaarsma et al., 2012). In addition, the present study shows that CMR is feasible for the evaluation of myocardial ischemia in children with congenital and acquired heart diseases, and provides the ability to quantify absolute myocardial perfusion, scar tissue, extracellular matrix expansion suggestive of diffuse myocardial fibrosis, and LV function. To the best of our knowledge, CMR T1 mapping was the first non-invasive diagnostic imaging tool that has ability to quantify DMF. More recently, a similar method has been proposed, using CT, but the accuracy of ECV evaluation may be lower.

4.6 Aortic Function in TGA Patients after the ASO

❖ **Aortic Dimensions and Aortic Insufficiency**

Significant enlargement of the aortic root was found in our TGA patients, whereas cross-sectional areas of the ascending and descending aorta were not significantly different from the control group. Aortic root enlargement after ASO has previously been reported from our group (Kramer et al., 2003) and by other echocardiographic studies (McMahon et al., 2004;

Hourihan et al., 1993). A CMR study by Grotenhuis et al. in 15 TGA patients also revealed significantly increased aortic root diameters (Grotenhuis et al., 2008). Furthermore, they showed that patients with AR had even larger aortic root diameters. This is in agreement with our findings in that TGA patients with a higher degree of AR had a larger cross-sectional area of the aortic root. However, only a small number of patients (n= 4) had more than mild AR and higher degree AR was infrequent (n= 1).

❖ **Aortic Distensibility**

In agreement with data from echocardiographic and CMR studies, we found reduced distensibility of the aortic root in TGA patients after ASO (Grotenhuis et al., 2008; Murakami et al., 2000). This finding was explained among other factors by the increased aortic wall stress of the dilated aortic root (Grotenhuis et al., 2008; Murakami et al., 2000). However, our results did not show any significant relation between the normalized aortic cross-sectional area and its distensibility. Probably, other factors contribute to reduced distensibility. Niwa et al. observed abnormalities of elastic fibres, smooth muscle, collagen, and ground substance of the medial layer already in the native aortic wall of neonates with TGA, which may affect distensibility (Niwa et al., 2001). Alternatively in surgical patients, fibrous tissue around the transposed arteries after ASO or the pulmonary artery branches embracing the aorta after Lecompte maneuver may impede aortic root distensibility. Stefanadis et al. detected in animals after experimental aortic dissection severe structural changes of the aortic wall and a decrease of distensibility and argued that this may be caused by damaging of the vasa vasorum (Stefanadis et al., 1995; Stefanadis et al., 1993).

The impairment of arterial distensibility is a known risk factor for cardiovascular morbidity and mortality (Laurent et al., 2006; Eren et al., 2004) because of the development of systolic arterial hypertension (Stefanadis et al., 1993), premature atherosclerosis (Farrar et al., 1991) and aneurysm formation (Wilson et al., 2003). It may also adversely affect ventriculo-arterial coupling due to the increased ventricular afterload, with the consequence of LV hypertrophy and dysfunction in the long-term (Eren 2004; Mottram et al., 2005; Lartaud-Idjouadiene et al., 1999). In addition, we found that the decreased aortic distensibility is accompanied by increased LA volumes. LA size has been reported to be a marker of LV diastolic dysfunction (Pritchett et al., 2005; Kaminski et al., 2011). Therefore, our data suggest that impaired aortic distensibility is likely to contribute to LV diastolic dysfunction in TGA patients.

❖ **Aortic Pulse Wave Velocity**

Another surrogate marker for an impaired aortic elasticity is the increase of PWV. PWV was not increased in children after one-stage ASO, but adult patients who underwent one-stage ASO had a significantly higher PWV than controls. Previous studies which analyzed aortic PWV after ASO revealed conflicting results. While Grotenhuis et al. observed an increased aortic PWV investigating a small cohort of 15 patients by CMR with an age range from 12-21 years (Grotenhuis et al., 2008), Agnoletti et al. found normal data by using applanation tonometry in children aged 5-7 years (Agnoletti et al., 2008). Considering that we evaluated both, children and adults, we are in agreement with these studies, as we found a normal PWV in small children and increased values in adolescents and young adults. However, an increased PWV can be expected within an aortic root with reduced distensibility, which was demonstrated in this and previous studies (Grotenhuis et al., 2007).

4.7 Study Limitations

There are some limitations to the present study. Because some congenital heart diseases are relatively rare, the sample size of patients in each subgroup is relatively small, and that made it difficult to detect correlations within subgroups. The range of age in our patients was high (between 1 and 64 years). However, the mean of age, height, weight, and BSA were not significantly different as compared to matched normal controls. In addition, patients younger than 7 years old (25.61%) had to be sedated with midazolam and propofol, which had a slight influence on blood pressure. The change of blood pressure may have an effect on myocardial perfusion. However, there were no patients or normal controls with severely reduced blood pressure in this study. Moreover, the ECV and LGE are not affected by reduced blood pressure.

In addition, the heart rate in children is usually higher than in adults and this may affect the quality of the images. All CMR exams were performed in all patients due to clinical indication. However, a comparison CMR with conventional coronary angiography is limited because they were not indicated in all patients. In some TGA patients, PWV and AR assessment were not possible because of metal artefacts from surgical implants. Nevertheless, we have reported the application of CMR in the assessment of myocardial blood flow, viability, and diffuse fibrosis in congenital and acquired heart disease and aortic function in TGA patients after ASO. The CMR protocol was not completed in some patients, because they woke up early from sedation.

5. SUMMARY

Myocardial ischemia may occur after surgical correction of congenital heart defects involving the coronary arteries, in patients with congenital coronary artery anomalies, or in acquired heart disease. To assess myocardial ischemia disease in children, we used cardiac MRI as a non-invasive and radiation-free method to evaluate myocardial perfusion, viability, diffuse myocardial fibrosis, and heart function, to guide further therapy and for a better understanding of the pathophysiology of the microcirculation.

In this study, a total of 77 patients and 68 healthy controls were enrolled. In 13 TGA patients (26.5%) with known or suspected coronary problems, such as occlusion, stenosis or hypoplasia. We found that 7/13 (53.8%) had regional ischemia, scar tissue in 4/13 (30.8%) and regional or global impairment of LV function in 4/13 (30.8%). In addition, absolute quantification of myocardial perfusion showed that coronary blood flow was impaired, and T1 mapping showed extracellular matrix expansion suggestive of diffuse myocardial fibrosis. As a consequence of our findings, one patient received MIDCAB surgery, and 4 patients (30.8%) were treated medically.

In another TGA group (n=36) with patent epicardial coronaries, we also found that global coronary blood flow is impaired after the ASO. In addition, T1 mapping showed an increase of ECV. However, no focal regions of hypoperfusion or LGE were found in this group.

In addition, in TGA patients with single-stage ASO, aortic root dilatation and impaired bioelastic properties of the thoracic aorta were present and were related to LV diastolic dysfunction but we did not find a significant association of aortic stiffness and myocardial perfusion reserve.

In patients after Ross operation (n=12), coronary blood flow was not significantly reduced as compared to matched normal controls, and only 1 patient showed a perfusion defect. However, we found that mean ECV was increased, and mean LVEF was significantly reduced in this group.

In BWG patients (n=7), we found regions of perfusion defects in 4/7 (57.1%) of patients. Scar tissue was detected in 5 cases (71.4%), and LVEF was significantly impaired in BWG patients.

In patients with a history of Kawasaki Syndrome (n=4), a region of impaired myocardial perfusion was present in one patient. Global MBF at stress, and MPR were impaired in this

group. LGE was not present. Additionally, in other patients with coronary problems, including an aberrant LCA (n=1), coronary fistula (n=1) and status post heart transplantation (n=2) our study showed that CMR imaging can be used to detect regional myocardial ischemia by visual qualitative, semi-quantitative, and quantitative myocardial perfusion analysis. In addition, LGE CMR also was used to uncover regions of focal myocardial fibrosis in this population.

The present study shows that CMR imaging can provide a comprehensive assessment of myocardial perfusion, viability and function, and myocardial tissue characteristic in children with congenital and acquired heart disease. We used CMR as a non-invasive method for evaluation myocardial perfusion in children with a spectrum of cardiac diseases. Importantly, this is the first study that used quantification of myocardial perfusion to measure absolute MBF in such diseases. We found that it is a useful method for the early diagnosis of myocardial ischemia in children, even in the absence of ischemic symptoms. The combination of first-pass perfusion imaging and LGE can increase the diagnostic accuracy for the detection of ischemic heart diseases. Contrast enhanced CMR provides an accurate quantification of areas of scar and viable tissue in children. T1 mapping as used in our study can additionally detect diffuse myocardial fibrosis. It provides information about myocardial tissue pathology and seems to be a useful method for assessment of interstitial fibrosis in children with congenital and acquired heart disease.

In conclusion, the present study provides new evidence with CMR techniques of increased diffuse myocardial fibrosis in TGA patients after ASO, and in patients after Ross. In addition, assessment of aortic function in TGA patients after ASO showed that the aortic wall is stiffer than in controls, which may be an important cardiovascular risk factor. Therefore, we suggest that these patients have regular follow-ups after ASO even in adulthood to detect early onset of degenerative cardiovascular disease.

6. LIST OF REFERENCES

Alexander RW, Griffith GC. Anomalies of the coronary arteries and their clinical significance. Circulation 1956; 14(5):800–805.

Al-Saadi N, Nagel E, Gross M, et al. Noninvasive detection of myocardial ischemia from perfusion reserve based on cardiovascular magnetic resonance. Circulation 2000; 101(12): 1379–1383.

Al-Saadi N and Bogaert J. Myocardial perfusion. In: Bogaert J, Dymarkowski S, Taylor AM, editors. Clinical cardiac MRI. 1st ed. Germany: Springer. 2004; 7:143-167.

Agnoletti G, Ou P, Celermajer DS, et al. Acute angulation of the aortic arch predisposes a patient to ascending aortic dilatation and aortic regurgitation late after the arterial switch operation for transposition of the great arteries. J Thorac Cardiovasc Surg 2008; 135:568-572.

Angelini P, Velasco JA, Flamm S. Coronary anomalies: incidence, pathophysiology, and clinical relevance. Circulation 2002; 105(20):2449–2454.

Angelini P. Coronary artery anomalies: an entity in search of an identity. Circulation 2007; 115(10):1296–305.

Askenazi J, Nadas AS. Anomalous left coronary artery originating from the pulmonary artery. Report on 15 cases. Circulation 1975; 51(6):976–987.

Atkinson DJ, Burstein D, Edelman RR. First-pass cardiac perfusion: evaluation with ultrafast MR imaging. Radiology 1990; 174:757–62.

Auerbach MA, Schoder H, Hoh C, et al. Prevalence of myocardial viability as detected by positron emission tomography in patients with ischemic cardiomyopathy. Circulation 1999; 99(22):2921–2926.

Babu-Narayan SV. The role of late gadolinium enhancement cardiovascular magnetic resonance in the assessment of congenital and acquired heart disease. Prog Pediatr Cardiol 2010; 28(1-2):11–19.

Barnard CN. A human cardiac transplant: an interim report of a human successful operation performed at Groote Schuur Hospital, Cape Town. S Afr Med J 1967; 41(48):1271-4.

Bartolani G, Bianca S, Patane L, Mignosa C. Pathology of coronary narrowing after arterial switch operation: autopsy findings in 2 patients who died within 3 months of surgical treatment and review of the literature. Cardiovasc Pathol 2006; 15(1):49-54.

Bateman TM, Heller GV, McGhie AI, et al. Diagnostic accuracy of rest/stress ECG-gated Rb-82 myocardial perfusion PET: comparison with ECG-gated Tc-99m sestamibi SPECT. J Nucl Cardiol 2006; 13:24–33.

Bateman TM. Advantages and disadvantages of PET and SPECT in a busy clinical practice. J Nucl Cardiol 2012; 19(1):S3–11.

Becker AE, Heijmans CD, Essed CE. Chronic non-ischemic congestive heart disease and endomyocardial biopsies. Worth the extra? Eur Heart J 1991; 12:218-23.

Beek AM, Kühl HP, Bondarenko O, et al. Delayed contrast-enhanced magnetic resonance imaging for the prediction of regional functional improvement after acute myocardial infarction. J Am Coll Cardiol 2003; 42(5):895-901.

Bello D, Shah DJ, Farah GM, et al. Gadolinium cardiovascular magnetic resonance predicts reversible myocardial dysfunction and remodeling in patients with heart failure undergoing beta-blocker therapy. Circulation 2003; 108:1945–53.

Bengel FM, Hauser M, Duvernoy CS, et al. Myocardial blood flow and coronary flow reserve late after anatomical correction of transposition of the great arteries. J Am Coll Cardiol 1998; 32:1955–1961.

Berman DL, Hachamovitch R, Shaw LJ, et al. Roles of nuclear cardiology, cardiac computed tomography and cardiac magnetic resonance: assessment of patients with suspected coronary artery disease. J Nucl Med 2006; 47:74–82.

Bianca S, Ettore G. Sex ratio imbalance in transposition of the great arteries and possible agricultural environmental risk factors. Images Paediatr Cardiol 2001; 8:10-14.

Bland EF, White PD, Garland J. Congenital anomalies of the coronary arteries: report of an unusual case associated with cardiac hypertrophy. Am Heart J 1933; 8:787–801.

Bonhoeffer P, Bonnet D, Piéchaud JF, et al. Coronary artery obstruction after the arterial switch operation for transposition of the great arteries in newborns. J Am Coll Cardiol 1997; 29(1):202–6.

Broberg CS, Chugh SS, Conklin C, Sahn DJ, Jerosch-Herold M. Quantification of diffuse myocardial fibrosis and its association with myocardial dysfunction in congenital. Circ Cardiovasc Imaging 2010; 3(6):727–734.

Bruder O, Schneider S, Nothnagel D, et al. EuroCMR (European Cardiovascular Magnetic Resonance) Registry results of the German Pilot phase. JACC 2009; 54(15):1457–1466. doi: 10.1016/j.jacc.2009.07.003. Epub 2009 Aug 13.

Buechel ERV, Balmer C, Bauersfeld U, Kellenberger CJ, Schwitter J. Feasibility of perfusion cardiovascular magnetic resonance in paediatric patients. J Cardiovasc Magn Reson 2009; 11:51. doi: 10.1186/1532-429X-11-51.

Canga Y, Ozcan KS, Emre A, et al. Coronary artery fistula: review of 54 cases from single center experience. Cardiol J 2012; 19(3):278-86.

Cerqueira MD, Verani MS, Schwaiger M, Heo J, Iskandrian AS. Safety profile of adenosine stress perfusion imaging: results from the Adenoscan Multicenter Trial Registry. J Am Coll Cardiol 1994; 23(2):384–89.

Cerqueira MD. Standardized myocardial segmentation and nomenclature for tomographic imaging of the heart: A statement for healthcare professionals from the Cardiac Imaging Committee of the Council on Clinical Cardiology of the American Heart Association. Circulation 2002; 105(4):539–542.

Charitos EI, Stierle U, Hanke T, Schmidtke C, Sievers H-H, Richardt D. Long-term results of 203 young and middle-aged patients with more than 10 years of follow-up after the original subcoronary Ross operation. Ann Thorac Surg 2012; 93(2):495-502.

Cheitlin MD, De Castro CM, Mcallister HA. Sudden death as a complication of anomalous left coronary origin from the anterior sinus of valsalva: A not-so-minor congenital anomaly. Circulation 1974; 50(4):780–787.

Cheitlin MD, MacGregor J. Congenital anomalies of coronary arteries: role in the pathogenesis of sudden cardiac death. Herz 2009; 34(4):268–79.

Chung KJ, Simpson IA, Glass RF, Sahn DJ, Hesselink JR. Cine magnetic resonance imaging after surgical repair in patients with transposition of the great arteries. Circulation 1988; 77:104–9.

Coelho-Filho OR, Mongeon FP, Mitchell R, et al. The role of transcytolemmal water exchange in magnetic resonance measurements of diffuse myocardial fibrosis in hypertensive heart disease. Circ Cardiovasc Imaging 2013; 6:134–141.

Conrad CH, Brooks WW, Hayes JA, Sen S, Robinson KG, Bing OH. Myocardial fibrosis and stiffness with hypertrophy and heart failure in the spontaneously hypertensive rat. Circulation 1995; 9(1):161-70.

Dajani AS, Taubert KA, Gerber MA, et al. Diagnosis and therapy of Kawasaki disease in children. Circulation 1993; 87(5):1776–1780.

Daniels LB, Tjajadi MS, Walford HH, et al. Prevalence of Kawasaki disease in young adults with suspected myocardial ischemia. Circulation 2012; 125(20):2447–53.

Davis JA, Cecchin F, Jones TK, Portman MA. Major coronary artery anomalies in a pediatric population: incidence and clinical importance. J Am Coll Cardiol 2001; 37(2):593–7.

Desai MY, Lima JA, Bluemke DA. Cardiovascular magnetic resonance imaging: current applications and future directions. Methods Enzymol 2004; 386:122-48.

Dodge-Khatami A, Mavroudis C, Backer CL. Anomalous origin of the left coronary artery from the pulmonary artery, collective review of surgical therapy. Ann Thorac Surg 2002; 946 – 955.

Driscoll DJ. Coronary artery anomalies. In: Driscoll DJ, editor. Fundamentals of pediatric cardiology. 1st ed. Minnesota: Lippincott Williams & Wilkins. 2006;14:162–166.

Earls JP, Ho VB, Foo TK, Castillo E, Flamm SD. Cardiac MRI: recent progress and continued challenges. J Magn Reson Imaging 2002; 16(2):111–27.

Eren M. Relation between aortic stiffness and left ventricular diastolic function in patients with hypertension, diabetes, or both. Heart 2004; 90(1):37–43.

Farrar DJ, Bond MG, Riley W a., Sawyer JK. Anatomic correlates of aortic pulse wave velocity and carotid artery elasticity during atherosclerosis progression and regression in monkeys. Circulation 1991; 83(5):1754–1763.

Fratz S, Hauser M, Bengel FM, et al. Myocardial scars determined by delayed-enhancement magnetic resonance imaging and positron emission tomography are not common in right ventricles with systemic function in long-term follow up. Heart 2006; 92(11):1673–1677.

Gaibazzi N, Reverberi C, Lorenzoni V, Molinaro S, Porter TR. Prognostic value of high-dose dipyridamole stress myocardial contrast perfusion echocardiography. Circulation 2012; 126(10):1217–24.

Geva T. Magnetic resonance imaging: historical perspective. J Cardiovasc Magn Reson 2006; 8(4):573-80.

Ghosh N, Rimoldi OE, Beanlands RSB, Camici PG. Assessment of myocardial ischaemia and viability: role of positron emission tomography. Eur Heart J 2010; 31(24):2984-95.

Gittenberger-de Groot AC, Sauer U, Oppenheimer-Dekker A, Quagebeur JM. Coronary arterial anatomy in transposition of the great arteries: a morphologic study. Pediatr Cardiol 1983; 4(1):15–24.

Globits S, Frank F, Mayr H, Neuhold A, Glogar D. Quantitative assessment of aortic regurgitation by magnetic resonance imaging. Eur Heart J 1992; 13(1):78-83.

Goda M, Gewillig M, Eyskens B, Heying R, Cools B, Rega F, Meyns B. Mechanism of autograft insufficiency after the Ross operation in children. Cardiol Young 2013; 23(4):523-9.

Görler H, Ono M, Thies A, et al. Long-term morbidity and quality of life after surgical repair of transposition of the great arteries: atrial versus arterial switch operation. Interactive cardiovascular and thoracic surgery 2011; 12(4):569–74.

Cranney GB, Lotan CS, Dean L, Baxley W, Bouchard A, Pohost GM. Left ventricular volume measurement using cardiac axis nuclear magnetic resonance imaging. Validation by calibrated ventricular angiography. Circulation 1990; 82:154-163.

Greenwood JP, Maredia N, Younger JF, et al. Cardiovascular magnetic resonance and single-photon emission computed tomography for diagnosis of coronary heart disease (CE-MARC): a prospective trial. Lancet 2012; 379(9814):453–60.

Grotenhuis HB, Ottenkamp J, Fontein D, et al. Aortic elasticity and left ventricular function after arterial switch operation: MR imaging – initial experience. Radiology 2008; 249:801-809.

Grotenhuis HB, Ottenkamp J, Westenberg JJ, et al. Reduced aortic elasticity and dilatation are associated with aortic regurgitation and left ventricular hypertrophy in nonstenotic bicuspid aortic valve patients. J Am Coll Cardiol 2007; 49:1660-1665.

Grotenhuis HB, Westenberg JJ, Doornbos J, et al. Aortic root dysfunctioning and its effect on left ventricular function in Ross procedure patients assessed with magnetic resonance imaging. Am Heart J 2006; 152:e1-8.

Grover-McKay M, Ratib O, Schwaiger M, et al. Detection of coronary artery disease with positron emission tomography and rubidium 82. Am Heart J 1992; 123:646–652.

Grover S, Srinivasan G, Selvanayagam JB. Evaluation of myocardial viability with cardiac magnetic resonance imaging. Prog Cardiovasc Dis 2011 ;54(3):204-14.

Hauser M, Bengel FM, Kühn A, et al. Myocardial blood flow and flow reserve after coronary reimplantation in patients after arterial switch and ross operation. Circulation 2001; 103(14):1875–80.

Harris MA, Johnson TR, Weinberg PM, Fogel MA. Delayed-enhancement cardiovascular magnetic resonance identifies fibrous tissue in children after surgery for congenital heart disease. J Thorac Cardiovasc Surg 2007; 133(3):676-81.

Heneghan MA, Biancaniello TM, Heidelberger E, Peterson SB, Marsh MJ, Lauterbur PC. Nuclear magnetic resonance zeugmatographic imaging of the heart: application to the study of ventricular septal defect. Radiology 1982; 143:183–6.

Hernandez-Pampaloni M, Allada V, Fishbein MC, Schelbert HR. Myocardial perfusion and viability by positron emission tomography in infants and children with coronary abnormalities: Correlation with echocardiography, coronary angiography, and histopathology. J Am Coll Cardiol 2003; 41(4):618-626.

Herrington CS, Tsirka AE. Pediatric cardiac transplantation. Semin Thorac Cardiovasc Surg 2004; 16(4):404-9.

Higgins CB, Sechtem UP, Pflugfelder P. Cine MR: evaluation of cardiac ventricular function and valvular function. Int J Card Imaging 1988; 3:21–8.

Hoffman JIE, Kaplan S. The incidence of congenital heart disease. J Am Coll Cardiol 2002; 39(12):1890–900.

Holzmann M, Nicko A, Kühl U, et al. Complication rate of right ventricular endomyocardial biopsy via the femoral approach: a retrospective and prospective study analyzing 3048 diagnostic procedures over an 11-year period. Circulation 2008; 118(17):1722-8.

Hourihan M, Colan SD, Wernovsky G, Maheswari U, Mayer JE, Sanders SP. Growth of the aortic anastomosis, annulus, and root after the arterial switch procedure performed in infancy. Circulation 1993; 88:615-620

Hourihan M, Colan SD, Wernovsky G, et al. Growth of the aortic anastomosis, annulus, and root after the arterial switch procedure performed in infancy. Circulation 1993; 88(2):615–620.

Hutter PA, Bennink GB, Ay L, Raes IB, Hitchcock JF, Meijboom EJ. Influence of coronary anatomy and reimplantation on the long-term outcome of the arterial switch. Eur J Cardiothorac Surg 2000; 18:207–213.

Jaarsma C, Leiner T, Bekkers SC, et al. Diagnostic performance of noninvasive myocardial perfusion imaging using single-photon emission computed tomography, cardiac magnetic resonance, and positron emission tomography imaging for the detection of obstructive coronary artery disease: a meta-anal. J Am Coll Cardiol 2012; 59(19):1719–28.

Jacobs ML, Mavroudis C. Anomalies of the coronary arteries: nomenclature and classification. Cardiol young 2010; 20(3):15-9.

Jadvar H, Strauss HW, Segall GM. SPECT and PET in the evaluation of coronary artery disease. Radiographics 1999; 19(4):915-2.

Jatene AD, Fontes VF, Paulista PP, Souza LC, Neger F, Galantier M, Sousa JE. Anatomic correction of transposition of the great vessels. J Thorac Cardiovasc Surg 1976; 72(3):364-70.

Jerosch-Herold M, Swingen C, Seethamraju RT. Myocardial blood flow quantification with MRI by model-independent deconvolution. Medical physics 2002; 15:886–897.

Jerosch-Herold, M, Seethamraju, R, Swingen, C, Wilke, N, Stillman, A. Analysis of myocardial perfusion MRI. J Magn Reson Imaging 2004; 19(6):758–770.

Jerosch-Herold M, Sheridan DC, Kushner JD, et al. Cardiac magnetic resonance imaging of myocardial contrast uptake and blood flow in patients affected with idiopathic or familial dilated cardiomyopathy. Am J Physiol Heart Circ Physiol 2008; 295(3):H1234-H1242.

Jerosch-Herold M. Quantification of myocardial perfusion by cardiovascular magnetic resonance. J Cardio Magn Reson 2010; 12:57.

Kaye MP. The Registry of the International Society for Heart and Lung Transplantation: Tenth Official Report—1993. J Heart Lung Transplant 1993; 12:541-548.

Kaminski M, Steel K, Jerosch-Herold M, et al. Strong cardiovascular prognostic implication of quantitative left atrial contractile function assessed by cardiac magnetic resonance imaging in patients with chronic hypertension. J Cardiovasc Magn Reson 2011; 13:42. doi:10.1186/1532-429X-13-42.

Kashyap R, Mittal BR, Bhattacharya A, Manojkumar R, Singh S. Exercise myocardial perfusion imaging to evaluate inducible ischaemia in children with Kawasaki disease. Nucl Med Commun 2011; 32(2):137–41.

Kato H, Sugimura T, Akagi T, et al. Long-term consequences of Kawasaki disease. A 10- to 21-year follow-up study of 594 patients. Circulation 1996; 94:1379–1385.

Kato H. Kawasaki disease. In: Cardiology 3rd ed, Crawford MH, DiMarco JP, Paulus WJ, et al, editors. Philadelphia. Elsevier. 2010; 7:1613-1626.

Kaufmann BA, Wei K, Lindner JR. Contrast echocardiography. Curr Probl Cardiol 2007; 32(2):51–96.

Kawasaki T. Acute febrile mucocutaneous syndrome with lymphoid involvement with specific desquamation of the fingers and toes in children. Arerugi 1967; 16:178–222.

Kazmierczak PA, Ostrowska K, Dryzek P, Moll JA, Moll JJ. Repair of anomalous origin of the left coronary artery from the pulmonary artery in infants. Interact Cardiovasc Thorac Surg 2013; 0:1–5.

Keijer JT, Van Rossum AC, Van Eenige MJ, Karreman AJ, Hofman MBM and Visser CA. Semiquantitation of regional myocardial blood flow in normal human subjects using first pass magnetic resonance imaging. Am Heart J 1995; 1301893-901.

Kim RJ, Chen EL, Lima JA, Judd RM. Myocardial Gd-DTPA kinetics determine MRI contrast enhancement and reflect the extent and severity of myocardial injury after acute reperfused infarction. Circulation 1996; 94(12):3318–3326.

Kim RJ, Fieno DS, Parrish TB, et al. Relationship of MRI delayed contrast enhancement to irreversible injury, infarct age, and contractilefunction. Circulation 1999; 100:1992–2002.

Kim RJ, Wu E, Rafael A, et al. The use of contrast-enhanced magnetic resonance imaging to identify reversible myocardial dysfunction. N Engl J Med 2000; 343:1445–1453.

Kimball RT. Transposition of the Great Arteries. In: Grawford H.M, DiMarco J.P, Paulus W.J, editors. Cardiology. 3^rd^ed . Mosby Elsevier 2010; P.1485-1488.

Kimball RT. Transposition of the Great Arteries. In: Grawford H.M, DiMarco J.P, Paulus W.J, editors. Cardiology. 3^rd^ed . Mosby Elsevier 2010; P.1487.

Kirklin JW, Blackstone EH, Tchervenkov CI, Castaneda AR. Clinical outcomes after the arterial switch operation for transposition. Patient, support, procedural, and institutional risk factors. Congenital Heart Surgeons Society. Circulation 1992; 86(5):1501-15.

Klein C, Nekolla SG, Bengel FM, et al. Assessment of myocardial viability with contrast-enhanced magnetic resonance imaging: comparison with positron emission tomography. Circulation 2002; 105(2):162–167.

Krahwinkel W, Ketteler T, Wolfertz J, et al. Detection of myocardial viability using stress echocardiography. Eur Heart J 1997; 18 Suppl D:D111–6.

Kramer HH, Scheewe J, Fischer G, et al. Long term follow-up of left ventricular performance and size of the great arteries before and after one- and two-stage arterial switch operation of simple transposition. Eur J Cardiothorac Surg 2003; 24:898-905.

Krasuski RA, Magyar D, Hart S, et al. Long-term outcome and impact of surgery on adults with coronary arteries originating from the opposite coronary cusp. Circulation 2011; 123(2):154–62.

Krause W. Uber den Ursprung einer Akzessorischen A. coronaria aus der A. pulmonalis. Z Ratl Med 24. 1865;225-227.

Kutty S, Olson J, Danford CJ, et al. Ultrasound contrast and real-time perfusion in conjunction with supine bicycle stress echocardiography for comprehensive evaluation of surgically corrected congenital heart disease. Eur Heart J Cardiovasc Imaging 2012; 13(6):500-9.

Kwong RY, Sattar H, Wu H, et al. Incidence and prognostic implication of unrecognized myocardial scar characterized by cardiac magnetic resonance in diabetic patients without clinical evidence of myocardial infarction. Circulation 2008; 118:1011–20.

Lalezari S, Bruggemans EF, Blom NA, Hazekamp MG. Thirty-year experience with the arterial switch operation. Ann Thorac Surg 2011; 92(3):973–9.

Lange R, Cleuziou J, Hörer J, et al. Risk factors for aortic insufficiency and aortic valve replacement after the arterial switch operation. Eur J Cardiothorac Surg 2008; 34:711-717.

Lartaud-Idjouadiene I, Lompre AM, Kieffer P, et al. Cardiac consequences of prolonged exposure to an isolated Increase in aortic stiffness. Hypertension 1999; 34(1):63–69.

Laurent S, Cockcroft J, Van Bortel L, et al. Expert consensus document on arterial stiffness: methodological issues and clinical applications. Eur Heart J 2006; 27(21):2588–605.

Legendre a, Losay J, Touchot-Koné a, et al. Coronary events after arterial switch operation for transposition of the great arteries. Circulation 2003; 108(1):II186–90.

Lorenz CH, Walker ES, Morgan VL, Klein SS, Graham TP Jr. Normal human right and left ventricular mass, systolic function, and gender differences by cine magnetic resonance imaging. J Cardiovasc Magn Reson 1999; 1(1):7-21.

Losay J, Touchot A, Capderou A, et al. Aortic valve regurgitation after arterial switch operation for transposition of the great arteries: incidence, risk factors, and outcome. J Am Coll Cardiol 2006; 47(10):2057–62.

Losay J, Touchot A, Serraf A, et al. Late outcome after arterial switch operation for transposition of the great arteries. Circulation 2001; 104(12 Suppl 1):I121-6.

Manso B, Castellote A, Dos L, Casaldaˊliga J. Myocardial perfusion magnetic resonance imaging for detecting coronary function anomalies in asymptomatic paediatric patients with a previous arterial switch operation for the transposition of great arteries. Cardiology in the Young 2010; 20, 410–417.

Maiers J, Hurwitz R. Identification of coronary artery disease in the pediatric cardiac transplant patient. Pediatr cardiol 2008; 29(1):19–23.

Martins P, Castela E. Transposition of the great arteries. Orphanet J Rare Dis. 2008; 3:27. doi: 10.1186/1750-1172-3-27.

Mavrogeni S, Papadopoulos G, Douskou M, et al. Magnetic resonance angiography, function and viability evaluation in patients with Kawasaki disease. J Cardiovasc Magn Reson 2006; 8(3):493–498.

McMahon CJ, Ravekes WJ, Smith EO, et al. Risk factors for neo-aortic root enlargement and aortic regurgitation following arterial switch operation. Pediatric cardiology 2004; 25(4):329–35.

Mersich B, Studinger P, Lenard Z, Kadar K, Kollai M. Transposition of great arteries is associated with increased carotid artery stiffness. Hypertension 2006; 47(6):1197–202.

Messroghli DR, Nordmeyer S, Dietrich T, et al. Assessment of diffuse myocardial fibrosis in rats using small-animal Look-Locker inversion recovery T1 mapping. Circ Cardiovasc Imaging 2011; 4:636–640.

Messroghli DR, Radjenovic A, Kozerke S, Higgins DM, Sivananthan MU, Ridgway JP. Modified look-locker inversion recovery (MOLLI) for high-resolution T1 mapping of the heart. Magn Reson Med 2004; 146:141–146.

Mewton N, Liu CY, Croisille P, et al. Assessment of myocardial fibrosis with cardiovascular magnetic resonance. J Am Coll Cardiol 2011; 57:891–903.

Morrison ML, Sands AJ, McCusker CG, et al. Exercise training improves activity in adolescents with congenital heart disease. Heart 2013; 99(15):1122-8.

Morton G, Ishida M, Schuster A, et al. Perfusion cardiovascular magnetic resonance: Comparison of an advanced, high-resolution and a standard sequence. J Cardio Magn Reson 2012; 14(1):34.

Morton G, Chiribiri A, Ishida M, et al. Quantification of absolute myocardial perfusion in patients with coronary artery disease: comparison between cardiovascular magnetic resonance and positron emission tomography. J Am Coll Cardiol 2012; 60(16):1546-55.

Mottram PM, Haluska BA, Leano R, Carlier S, Case C, Marwick TH. Relation of arterial stiffness to diastolic dysfunction in hypertensive heart disease. Heart 2005; 91:1551-1556

Muellerleile K, Groth M, Saring D, et al. Evaluation of different magnetic resonance imagingtechniques for the assessment of active left atrial emptying. Eur Radiol 2012; 22(9):1904-11

Mühling O, Jerosch-Herold M, Nabauer M, Wilke N. Assessment of ischemic heart disease using magnetic resonance fi rst-pass perfusion imaging. Herz 2003; 28(2):82-89.

Mulvagh SL. Advances in myocardial contrast echocardiography and the role of adenosine stress. Am J Cardio 2004; 94(2A):12D–18D.

Murakami T, Nakazawa M, Momma K, Imai Y. Impaired distensibility of neo-aorta after arterial switch procedure. Ann Thorac Surg 2000; 70:1907-1910.

Muzik O, Paridon SM, Singh TP, Morrow WR, Dayanikli F, Di Carli MF. Quantification of myocardial blood flow and flow reserve in children with a history of Kawasaki disease and normal coronary arteries using positron emission tomography. J Am Coll Cardiol 1996; 28:757–62.

Nagel E, Klein C, Paetsch I, Hettwer S, Schnackenburg B, Wegscheider K, Fleck E. Magnetic resonance perfusion measurements for the noninvasive detection of coronary artery disease. Circulation 2003; 108(4):432-7.

Nandalur KR, Dwamena BA, Choudhri AF, Nandalur MR, Carlos RC. Diagnostic performance of stress cardiac magnetic resonance imaging in the detection of coronary artery disease: a meta-analysis. J Am Coll Cardiol 2007; 50(14):1343–53.

Newburger JW, Takahashi M, Gerber MA, et al. Diagnosis, treatment, and long-term management of Kawasaki disease: a statement for health professionals from the Committee on Rheumatic Fever, Endocarditis, and Kawasaki Disease, Council on Cardiovascular Disease in the Young, American Heart Association. Pediatrics 2004; 114(6):1708-33.

Nickel T, Bigdeli A, von Ziegler F, et al. Coronary dilatation after heart transplantation. Transplantation 2011; 92(6):697–702.

Niwa K, Perloff JK, Bhuta SM, et al. Structural abnormalities of great arterial walls in congenital heart disease: light and electron microscopic analyses. Circulation 2001; 103:393-400.

Nollen GJ, Groenink M, Tijssen JG, Van Der Wall EE, Mulder BJ. Aortic stiffness and diameter predict progressive aortic dilatation in patients with Marfan syndrome. Euro Heart J 2004; 25(13):1146–52.

Ntsinjana HN, Hughes ML, Taylor, AM. The role of cardiovascular magnetic resonance in pediatric congenital heart disease. J Cardio Magn Reson 2011; 13(1),51.

Ogden JA. Congenital anomalies of the coronary arteries. Am J Cardiol 1970; 25(4):474–9.

Pasquali SK. Coronary artery pattern and outcome of arterial switch operation for transposition of the great arteries: A meta-analysis. Circulation 2002; 106(20):2575–2580.

Pennell DJ. Cardiovascular magnetic resonance and the role of adenosine pharmacologic stress. Am J Cardiol 2004; 94(2A):26D–32D.

Perloff JK. Congenital coronary arterial fistula. In: Clinical Recognition of Congenital Heart Disease. Perloff JK, editor. Elsevier Science 2003; 22:443-456.

Perloff JK. Anomalous Origin of the Left Coronary Artery from the Pulmonary Trunk. In: Perloff JK, ed. The Clinical Recognition of Congenital Heart Disease. Elsevier Science 2003; 21:430-442.

Porter TR, Xie F, Silver M, Kricsfeld D, Oleary E. Real-time perfusion imaging with low mechanical index pulse inversion Doppler imaging. J Am Coll Cardiol 2001; 37(3):748-53.

Prakash A, Powell AJ, Krishnamurthy R, Geva T. Magnetic resonance imaging evaluation of myocardial perfusion and viability in congenital and acquired pediatric heart disease. Am J Cardiol 2004; 93(5):657–61.

Pritchett AM, Mahoney DW, Jacobsen SJ, Rodeheffer RJ, Karon BL, Redfield MM. Diastolic dysfunction and left atrial volume: a population-based study. J Am Coll Cardiol 2005; 45(1):87–92.

Puranik R, Tsang VT, Broadley A, et al. Functional outcomes after the Ross (pulmonary autograft) procedure assessed with magnetic resonance imaging and cardiopulmonary exercise testing. Heart 2010; 96:304-308.

Puranik R, Muthurangu V, Celermajer DS, Taylor AM. Congenital heart disease and multi-modality imaging. Heart Lung Circ 2010; 19(3):133-44.

Raja SG, Shauq A, Kaarne M. Outcomes after arterial switch operation for simple transposition. Asian Cardiovasc Thorac Ann 2005; 13(2):190-8.

Ramírez S, Curi-Curi PJ, Calderón-Colmenero J, et al. Outcomes of coronary reimplantation for correction of anomalous origin of left coronary artery from pulmonary artery. Rev Esp Cardiol 201; 64(8):681-7.

Rhodes J, Ubeda Tikkanen A, Jenkins KJ. Exercise testing and training in children with congenital heart disease. Circulation 2010; 122(19):1957-67.

Rickers C, Sasse K, Buchert R, et al. Myocardial viability assessed by positron emission tomography in infants and children after the arterial switch operation and suspected infarction. J Am Coll Cardiol 2000; 36(5):1676–83.

Roberts WC, Shirani J. The four subtypes of anomalous origin of the left main coronary artery from the right aortic sinus (or from the right coronary artery). Am J Cardiol 1992; 70(1):119-21.

Ross D. Replacement of aortic and mitral valves with a pulmonary autograft. Lancet 1967; 290(7523):956–958

Roussel JC, Baron O, Périgaud C, et al. Outcome of heart transplants 15 to 20 years ago: graft survival, post-transplant morbidity, and risk factors for mortality. J Heart Lung Transplant 2008; 27(5):486–93.

Sado DM, Flett AS, Banypersad SM, et al. Cardiovascular magnetic resonance measurement of myocardial extracellular volume in health and disease. Heart 2012; 98(19):1436-41.

Salerno M, Beller GA. Noninvasive assessment of myocardial perfusion. Circ Cardiovasc Imaging 2009; 2(5):412–24.

Samánek M. Boy girl ratio in children born with different forms of cardiac malformation. Pediatr Cardiol 1994; 15:53-7.

Samánek M, Slavík Z, Zbořilová B, Hroboňová V, Voříšková M, Škovránek J. Prevalence, treatment, and outcome of heart disease in live-born children: A prospective analysis of 91,823 live-born children. Pediatric Cardiology 1989; 10(4):205–211.

Sampson UK, Limaye A, Dorbala S, et al. Diagnostic accuracy of rubidium-82 myocardial perfusion imaging with hybrid positron emission tomography/ computed tomography (PET-CT) in the detection of coronary artery disease. J Am Coll Cardiol 2007; 49:1052–1058.

Sarwar A, Shapiro MD, Abbara S, Cury RC. Cardiac magnetic resonance imaging for the evaluation of ventricular function. Semin Roentgenol 2008; 43(3):183-92.

Scanlon PJ, Faxon DP, Audet AM, et al. ACC/AHA guidelines for coronary angiography: executive summary and recommendations. A report of the American College of Cardiology/American Heart Association Task Force on Practice Guidelines (Committee on Coronary Angiography) developed in collaboration with the Society for Cardiac Angiography and Interventions. Circulation 1999; 99(17):2345-57.

Schaefer S, Malloy CR, Katz J, Parkey RW, Buja LM, Willerson JT, Peshock RM. Gadolinium-DTPA-enhanced nuclear magnetic resonance imaging of reperfused

myocardium: identification of the myocardial bed at risk. J Am Coll Cardiol 1988; 12:1064–72.

Schaper J, Speiser B. The extracellular matrix in the failing humanheart. Basic Res Cardiol 1992; 87(1):303–9.

Schwitter J, Nanz D, Kneifel S, et al. Assessment of myocardial perfusion in coronary artery disease by magnetic resonance: a comparison with positron emission tomography and coronary angiography. Circulation 2001; 103:2230–2235.

Schwitter J and Arai AE. Assessment of cardiac ischaemia and viability: role of cardiovascular magnetic resonance. Euro Heart J 2011; 32,799–809.

Secinaro A, Ntsinjana H, Tann O, et al. Cardiovascular magnetic resonance findings in repaired anomalous left coronary artery to pulmonary artery connection (ALCAPA). J Cardiovasc Magn Reson 2011; 13**:27**

Sechtem U, Pflugfelder PW, Gould RG, Cassidy MM, Higgins CB. Measurement of right and left ventricular volumes in healthy individuals with cine MR imaging. Radiology 1987; 163(3):697-702.

Sim EK, van Son JA, Edwards WD, Julsrud PR, Puga FJ. Coronary artery anatomy in complete transposition of the great arteries. Ann Thorac Surg 1994; 57(4):890-4.

Singh TP, Muzik O, Forbes TF, Di Carli MF. Positron emission tomography myocardial perfusion imaging in children. Pediatr Cardiol 2003; 24:138–144.

Somerville J, Saravalli O, Ross D, Stone S. Long-term results of pulmonary autograft for aortic valve replacement. Br Heart J 1979; 42(5):533-40.

Sridharan S, Price G, Tann O, et al. Kawasaki disease. In: Sridharan S, Price G, Tann O, Hughes M, Muthurangu V, Taylor AM, editors. Cardiovascular MRI in congenital heart disease. 1st ed. Berlin: Springer; 2010. P.140.

St John Sutton MG, Lie JT, Anderson KR, O'Brien PC, Frye RL. Histopathological specificity of hypertrophic obstructive cardiomyopathy. Myocardial fibre disarray and myocardial fibrosis. Br Heart J 1980; 44(4):433-43.

Stefanadis CI, Vlachopoulos C, Karayannacos P, et al. Effect of vasa vasorum flow on structure and function of the aorta in experimental animals. Circulation 1995; 91:2669-2678.

Stefanadis CI, Karayannacos PE, Boudoulas HK, et al. Medial necrosis and acute alterations in aortic distensibility following removal of the vasa vasorum of canine ascending aorta. Cardiovasc Res 1993; 27:951-956

Stehlik J, Edwards LB, Kucheryavaya AY, et al. The registry of the International Society for Heart and Lung Transplantation: Twenty-eighth adult heart transplant report--2011. J Heart Lung Transplant 2011; 30(10),1078-94.

Sundaram PS, Padma S. Role of myocardial perfusion single photon emission computed tomography in pediatric cardiology practice. Ann Pediatr Cardiol 2009; 2(2):127-39.

Svensson LG, Blackstone EH, Cosgrove DM. Surgical options in young adults with aortic valve disease. Curr Probl Cardiol 2003; 28(7):417-80.

Tacke CE, Kuipers IM, Groenink M. Cardiac magnetic resonance imaging for noninvasive assessment of cardiovascular disease during the follow-up of patients with Kawasaki disease.. Circ Cardiovasc Imaging 2011; 4(6):712-20.

Tanaka N, Naoe S, Masuda H, Ueno T. Pathological study of sequelae of Kawasaki disease (MCLS). With special reference to the heart and coronary arterial lesions. Acta Pathologica Japonica 1986; 36(10):1513–1527.

Tanel RE, Wernovsky G, Landzberg MJ, Perry SB, Burke RP. Coronary artery abnormalities detected at cardiac catheterization following the arterial switch operation for transposition of the great arteries. Am J Cardiol 1995; 76(3):153-7.

Tuo G, Marasini M, Brunelli C, Zannini L, Balbi M. Incidence and clinical relevance of primary congenital anomalies of the coronary arteries in children and adults. Cardiol young 2013; 23(3):381-6.

Turrentine MW, Ruzmetov M, Vijay P, Bills RG, Brown JW. Biological versus mechanical aortic valve replacement in children. Ann Thorac Surg 2001; 71:S356–60.

Urrutia-S CO, Falaschi G, Ott DA, Cooley DA. Surgical management of 56 patients with congenital coronary artery fistulas. Ann Thorac Surg 1983; 35(3):300–307.

Valente AM, Lock JE, Gauvreau K, et al. Predictors of long-term adverse outcomes in patients with congenital coronary artery fistulae. Circ Cardiovasc Interv 2010; 3(2):134–9.

Villari B, Campbell SE, Hess OM, et al. Influence of collagen network on left ventricular systolic and diastolic function in aortic valve disease. J Am Coll Cardiol 1993; 22(5):1477-84.

Vogel M, Smallhorn JF, Gilday D, et al. Assessment of myocardial perfusion in patients after the arterial switch operation. J Nucl Med 1991; 32(2):237–41.

Wagner A, Mahrholdt H, Holly TA, et al. Contrast-enhanced MRI and routine single photon emission computed tomography (SPECT) perfusion imaging for detection of subendocardial myocardial infarcts: an imaging study. Lancet 2003; 361:374 –379.

Wei K, Jayaweera AR, Firoozan S, et al. Quantification of myocardial blood flow with ultrasound-induced destruction of microbubbles administered as a constant venous infusion. Circulation 1998; 97:473–83.

Weindling SN, Wernovsky G, Colan SD, et al. Myocardial perfusion, function and exercise tolerance after the arterial switch operation. J Am Coll Cardiol 1994; 23(2):424–33.

Wesselhoeft H, Fawcett JS, Johnson AL. Anomalous origin of the left coronary artery from the pulmonary trunk: its clinical spectrum, pathology, and pathophysiology, based on a review of 140 cases with seven further cases. Circulation 1968; 38(2):403–425.

West AM, Kramer CM. Cardiovascular magnetic resonance imaging of myocardial infarction, viability, and cardiomyopathies. Curr Probl Cardiol 2010; 35(4):176-220.

White CW, Wright CB, Doty DB, et al. Does visual interpretation of the coronary arteriogram predict the physiologic importance of a coronary stenosis? N Engl J Med 1984; 310: 819–24.

Wilke NM, Jerosch-Herold M, Zenovich A, Stillman AE. Magnetic resonance first-pass myocardial perfusion imaging: clinical validation and future applications. J Magn Reson Imaging 1999; 10(5):676–85.

Wilson KA, Lee AJ, Lee AJ, et al. The relationship between aortic wall distensibility and rupture of infrarenal abdominal aortic aneurysm. J Vasc Surg 2003; 37(1):112–7.

Yacoub MH, Radley-Smith R. Anatomy of the coronary arteries in transposition of the great arteries and methods for their transfer in anatomical correction. Thorax 1978; 33(4):418–24.

Yamanaka O, Hobbs RE. Coronary artery anomalies in 126,595 patients undergoing coronary arteriography. Cathet Cardiovasc Diagn 1990; 21(1):28–40.

7. ACKNOWLEDGEMENTS

8. CURRICULUM VITAE

Name: Hoang Minh

Family Name: Pham

Sex: Male

Date of Birth: 15.07.1979

Place of Birth: Hau Giang Province,Viet Nam

Nationality: Vietnamese

Marital status: Married

Address: Can Tho City General Hospital

Intensive Care Unit

206, Cach Mang Thang 8 street, Ninh Kieu district, Can Tho City, Vietnam.

Email: Phamhoangminhvn@gmail.com

❖ **Education:**

2011 – 2013: Doctoral student in UKSH - Kiel - Germany.

Training in CMR imaging in pediatric and adult congenital heart disease.

2005 – 2007: Training in adult cardiology in Choray Hospital – Ho Chi Minh City – Vietnam.

Training in Echocardiography – Heart Institute – Ho Chi Minh City – Vietnam.

1999 – 2005: Medical student in Can Tho University of Medicine and Pharmacy – Can Tho City – Vietnam.

❖ **Working experience:**

2009 – 2011: Intensive Care Unit – Can Tho City General Hospital – Can Tho City – Vietnam.

2009 – 2010: General Internal Medicine Department - Can Tho City General Hospital – Can Tho City – Vietnam.

2007 – 2008: Emergency Department. Can Tho City General Hospital – Can Tho City – Vietnam.

❖ **Scholarship:** ,,Kinderherzen-wollen-leben e.V.'', Beethovenstraße 15-19, 24534 Neumünster (Feb.2013 – Dec. 2013).

❖ **Publications in recent 3 years:**

1. Implications of early aortic stiffening in patients with transposition of the great arteries after arterial switch operation. Voges I, Jerosch-Herold M, Hedderich J, Hart C, Petko C, Scheewe J, Andrade AC, **Pham M**, Gabbert D, Kramer HH, Rickers C. Circ Cardiovasc Imaging. 2013 Mar 1; 6(2):245-53. doi: 10.1161/CIRCIMAGING. 112.000131. Epub 2013 Jan 30.

2. Response to letter regarding article, "implications of early aortic stiffening in patients with transposition of the great arteries ffter arterial switch operation". Voges I, Jerosch-Herold M, Hedderich J, Hart C, Petko C, Scheewe J, Andrade AC, **Pham M**, Gabbert D, Kramer HH, Rickers C. Circ Cardiovasc Imaging. 2013 Jul, *6(4): e24.* doi: 10.1161/CIRCIMAGING.113.000557.

3. Adverse results of a decellularized tissue-engineered pulmonary valve in humans assessed with magnetic resonance imaging. Voges I, Bräsen JH, Entenmann A, Scheid M, Scheewe J, Fischer G, Hart C, Andrade A, **Pham HM**, Kramer HH, Rickers C. Eur J Cardiothorac Surg. 2013 Jun 30.

4. Determination of volume-time curves for the right ventricle and its outflow tract for functional analyses. Gabbert DD, Entenmann A, Jerosch-Herold M, Frettlöh F, Hart C, Voges I, **Pham M**, Andrade A, Pardun E, Wegner P, Hansen T, Kramer HH, Rickers C. Magn Reson Med. 2013 Feb 4. doi: 10.1002/mrm.24609.

❖ **Conferences:**

1. XLI Congresso Nazionale Società Italiana di Cardiologia Pediatrica with la Sezione di Cardiochirurgia Pediatrica e delle Cardiopatie Congenite della SICCH in BARI, Itália, 2011. It was choosen one of the best abstracts in 43. Jahrestagung der Deutschen Gesellschaft für Pädiatrische Kardiologie, in Weimar, october 2011.

Myokardiale Perfusions- und Vitalitäts-Untersuchungen bei Patienten mit Hypoplastischem Linksherzsyndrom im Stadium der Fontan-Zirkulation. C. Rickers, P. Wegner, M. Jerosch-Herold, E. Pardun, C. Hart, I. Voges, **M. Pham**, A. Andrade, H.-H. Kramer (Kiel, Germany - Boston, USA).

2. ESC Congress 2012, Munich, agost 2012. Poster - Myocardial blood flow and viability in children with congenital or aquired coronary disease. **Pham M**, Jerosch-Herold M, Andrade AC, Voges I, Hart C, Hansen T, Kramer H-H, Rickers C.

3. ESC Congress 2012, Munich, agost 2012. Oral presentation - Maladaptive aortic bioelastic properties and diastolic dysfunction in patients with Tetralogy of Fallot (ToF) post surgical repair during long-term follow-up. Andrade AC, Voges I, Jerosch-Herold M, **Pham M**, Hart C, Hansen T, Kramer H-H, Rickers C.

4. Jahrestagung der Norddeutschen Gesellschaft für Kinder- und Jugendmedizin (NDGKJ), Kiel, 2012. MRT-Normalwerte für Dehnbarkeit, Pulswellengeschwindigkeit und Dimensionen der Aorta bei Kindern und jungen Erwachsenen. Voges, I. ; Pardun, E. ; Hedderich, J. ; HART, C. ; Gabeert, Dominik ; **Pham, M**. ; Andrade, A. C. ; Hansen, T. ; Kramer, H.-H. ; Rickers, C.

5. Jahrestagung der Norddeutschen Gesellschaft für Kinder- und Jugendmedizin (NDGKJ), Kiel, 2012. Herzfehlerspezifische Referenzwerte des rechten Ventrikels beim Hypoplastischen Linksherzsyndrom (HLHS). Hart, C. ; Pardun, E. ; Voges, I. ; Andrade, A. C.; **Pham, M.** ; Hedderich, J. ; Hansen, T. ; Kramer, H.-H. ; Rickers, C.

6. Jahrestagung der Norddeutschen Gesellschaft für Kinder- und Jugendmedizin (NDGKJ), Kiel, 2012. Eingeschränkte Bioelastizität der Aorta und diastolische Dysfunktion bei Patienten nach operativ behandelter Aortenisthmusstenose (CoA) – eine MRT-Studie. Voges, I. ; Jerosch-Herold, M. ; Hart, C. ; Gabbert, D. ; Andrade, A. C. ; **Pham, M**. ; Kramer, H.-H. ; Rickers, C.

7. Jahrestagung der Norddeutschen Gesellschaft für Kinder- und Jugendmedizin (NDGKJ), Kiel, 2012. Die Bedeutung der Magnetresonanztomographie (MRT) für die Differentialdiagnostik kardiovaskulärer Tumore. Voges, I. ; Scheewe, Jens ; Hart, C. ; Andrade, A. C. ; **Pham, M.** ; Hansen, T. ; Kramer, H.-H. ; Rickers, C.

8. Jahrestagung der Norddeutschen Gesellschaft für Kinder- und Jugendmedizin (NDGKJ), Kiel, 2012. Die Bedeutung anatomischer Subgruppen für die regionale und globale Funktion des rechten Ventrikels beim hypoplastischen Linksherz-Syndrom (HLHS). Pardun, E. ; Hart, C. ; Andrade, A. C. ; **Pham, M.** ; Voges, I. ; Scheewe, Jens; Jerosch-Herold, M.; Hansen, T.; Kramer, H.-H. ; Rickers, C.

9. Jahrestagung der Deutschen Gesellschaft für Pädiatrische Kardiologie, Weimar, october 2012. Maladaptive aortic bioelastic properties and diastolic dysfunction in patients with Tetralogy of Fallot (ToF) post surgical repair during long-term follow-up. Andrade AC, Voges I, Jerosch-Herold M, **Pham M**, Hart C, Pardun E, Hansen T, Gabbert D, Kramer H-H, Rickers C.

10. SCMR 16th Annual Scientific Sessions, San Francisco, CA. January 31 - February 3, 2013. New insights in the Fontan circulation: 4-dimensional respiratory- and ECG-triggered phase contrast magnetic resonance imaging. Christopher Hart, Dominik Daniel Gabbert, Inga Voges, Michael Jerosch-Herold, Ana Andrade, **Minh Pham**, Traudel Hansen, Hans-Heiner Kramer, Carsten Rickers. Journal of Cardiovascular Magnetic Resonance 2013, 15(Suppl 1):O38.

11. ESC Congress 2013, **Amsterdam. Poster -** Assessment of myocardial blood flow, viability and diffuse fibrosis in patients after arterial switch and Ross operation with magnetic resonance imaging. **H.M. Pham**, P. Wegner, M. Jerosch-Herold, I. Voges, A.C. Andrade, C. Hart, R. Shah, H.-H. Kramer, C. Rickers. European Heart Journal (2013) 34 (Abstract Supplement), 369-370.

12. ESC Congress 2013, **Amsterdam. Poster -** Patients with tetralogy of Fallot late after sugical repair show subclinical left ventricular systolic and diastolic dysfunction, altered LV geometry and early aortic stiffening. A.C. Andrade, **M. Pham**, I. Voges, M. Jerosch-Herold, R. Shah, C. Hart, P. Wegner, H.-H. Kramer, C. Rickers. European Heart Journal (2013) 34 (Abstract Supplement), 526-527.